

Republic of Iraq  
Ministry of Higher Education  
and Scientific Research  
University of Babylon  
College of Engineering  
Department of Mechanical Engineering



## **Numerical and Experimental Investigation for Air Distribution Index in a Partitioned Room Under Iraqi Climate**

**A thesis submitted to the College of Engineering, University of  
Babylon in partial Fulfillment of the Requirements for the Master  
of Science degree in Engineering/ Mechanical Engineering/ Power**

By  
Shrin Sabah Jasim Flamerz

Supervised by  
Prof. Dr. Alaa Abbas Mahdi

**2022 A.D.**

**1444 A.H.**

بِسْمِ اللَّهِ الرَّحْمَنِ الرَّحِيمِ

(وَاصْبِرْ فَإِنَّ اللَّهَ لَا يُضِيعُ أَجْرَ الْمُحْسِنِينَ)

صدق الله العظيم

(هود - 115)

## **Certification**

I certify that this thesis entitled “**Numerical and Experimental Investigation for Air Distribution Index in a Partitioned Room Under Iraqi Climate**” was prepared by

“Shrin Sabah Jasim”

under my supervision at the University of Babylon as a partial fulfillment of the requirements for the degree of (M.Sc.) in Mechanical Engineering (Power).

Signature

Prof. Dr. Alaa Abbas Mahdi

Department of Mechanical Engineering

College of Engineering

University of Babylon

Data: 25/ 9 / 2022

## **Acknowledgments**

This thesis would not have been possible without the support of our ideal professor; my supervisor  
**(Prof. Dr. Alaa Abbas Mahdi)**.

I deeply appreciate his eagerness to read my numerous revisions and help to make sense of the confusion that permeated this research as well as thanks for his advice.

Furthermore, a special thanks to my committee members, who offered guidance and support.

A very special thanks to the Head of the Mechanical Engineering Department **(Dr. Samer Mohammed)** one who has helped me during the journey of research.

Many generous fellow-professors have scaffolded my effort on this thesis through guidance, encouragement, and moving forward, whom they taught me to be patient, and who listened to me attentively.

**Prof. Dr. Hatem, Prof. Dr. Basim, and Prof. Dr. Essam.**

## **Dedication**

It is with immense gratitude that I acknowledge the individuals who in one way or another contributed and extended their unfailing support, encouragement, and guidance in the preparation and completion of this study.

First and foremost, I would like to extend my deepest appreciation to my thesis adviser (**Prof. Dr. Alaa Abbas Mahdi**) who has a patience, the attitude and character of a genius, with his valuable assistance and encouragement in regard to research. Without his guidance and persistent help this dissertation would not have been possible.

I consider it an honor to work with my study partners, for the memories we had shared and the teamwork in every task and activity were in, we have never failed to cooperate with one another especially in tough and bad times during the last courses, I also thank you.

To my most beloved and supportive parents, **Mom, Dad, and Adam**, for their financial and moral support as well as their unfailing guidance for me to made this far to be able to achieve my dreams and ambition in life.

Lastly, I would like to give my thanks to the absolute one GOD, for giving me strength and courage in times of problems and despair, for the unconditional love and graces he showered upon me, and for always guiding and answering my prayers and needs in making my life full of hope and support.



sincerely

**Anne Shirley**

## **Abstract**

Buildings with ventilation systems have become one of the essential necessities for businesses looking to provide thermal comfort and air quality in order to enhance the level of productivity for employee's performance, especially after the Corona pandemic works became under conditions of social distancing, researchers around the world returned to reconsider their study of the concept of ventilation in the time of the Corona epidemic to know its impact on thermal comfort and air quality.

Therefore, in this research, the effect of placing partitions between the employees of specific office will be studied numerically and experimentally in order to predict the air quality and thermal comfort parameters by adopting mixing ventilation system contains of a side wall air supply, and exhaust air grille in the same wall side under Iraqi climate where the Middle Euphrates, and south regions are hot and dry region in summer.

A thermally insulated office room was chosen as a case for numerical and experimental study and a comparison was made. Besides, two non-thermal insulated office rooms as realistic cases were numerically performed using an accurate and quick simulation software specialized in ventilation systems, each realistic case had different location, dimensions, and different gender, the latter was done according to clothing's types that were used in the simulations.

The efficiency of heat removal and ventilation efficiency were calculated before and after partitioning in every case, in addition to air diffusion index (ADI), and (ADI). Furthermore, thermal comfort parameters (PMV, PPD) and local draft discomfort, the effect of enhancing the partition function through the gap underneath adoption and how it changed the efficiencies and reduce the local draft was studied as well.

According to the findings the mixing ventilation system has the advantage that it provides the occupants with an overall draught sense, due to the slightly gradient of temperature along the occupants' zone.

In addition to gap adoption beside a partition has a significant effect on enhancing the indoor air quality, and thermal comfort, since the ventilation efficiency increased from (0.84) to (0.93) in case of (0.5 of the room's length) with (0.7 of the room's height) for the insulated office room, while in case of non-insulated office room heat removal efficiency has influenced significantly by gap adoption with the partition, since it increased from (0.80) to (0.85). Moreover, the (PPD) values has decreased to such acceptable value from (23.74% to 10.67%) in case of the office room occupied by females, and from (26.4 % to 13.3%) in case of the office room occupied by males.

The study concluded that placing a gap below a partition had a clear role in reducing draft in the region of standing head level and legs level. Furthermore, there is an advantage of using the (AIRPAK3.0.16) software besides the (RNG k- $\epsilon$ ) as turbulence model due to closer results between numerical and experimental approaches, since the higher error which has reached was (3.81%) in case of (10%H) of the gap's height of the partition.

## Table of contents

ABSTRACT		I
Nomenclature and Greek symbols		II
Sub-scripts and Abbreviations		III
<b>Chapter one</b>		
<b>Introduction</b>		
<b>Subject</b>		<b>Page.No.</b>
1	General concept	1
1.1	Mixing ventilation system	1
1.2	Indoor air quality	2
1.3	Thermal comfort	2
1.4	Prediction of mean vote (PMV)	3
1.5	Percentage of perception of dissatisfied (PPD)	4
1.6	Internal partition	5
1.7	Objective of the Present Work	6

<b>Chapter two Literature review</b>		
2.1	Experiment studies	7
2.2	Simulations studies	11
2.3	Experiment and numerical studies	19
2.4	Summary of literature review	24
2.5	Scope of the present work	28
2.6	Motivation of the present work	29
<b>Chapter three</b>		
<b>Mathematical modeling and Numerical Analysis</b>		
3.1	General concept	30
3.2	Governing equations	32
3.2.1	The mass conservation equation	32
3.2.2	Momentum equations	32
3.2.3	Energy conservation equation	33
3.2.4	Turbulence Models	33
3.3	Numerically Simulated Room Types	34

3.3.1	Simulation of a thermally insulated room (CaseI)	34
3.3.2	Non-Insulated Office Room (Case II)	37
3.3.3	Non-Insulated Office Room (Case III)	42
3.4	Generating a Mesh	46
3.4.1	Mesh Independence Study	48
3.5	Theoretical Analysis	50
3.5.1	Isothermal Room cooling load calculation, (Case I)	50
3.5.2	Non-Isothermal Room	51
3.6	Numerical cases setup	53
3.6.1	Working Fluid Properties	53
3.6.2	Boundary Conditions of Momentum	54
3.6.3	Solution Controls	57
3.6.4	Solution initialization and convergence and residuals	58
3.7	Indoor Air Quality	59
3.7.1	Thermal discomfort	60
3.8	Prediction of Thermal comfort parameters	61
3.8.1	PMV and PPD	62
3.8.2	Air distribution index (ADPI), and (ADI)	63

<b>Chapter four Experimental Work</b>		
4.1	Description of the Office Room	68
4.1.1	General description	68
4.1.2	Heat Sources	70
4.1.3	Air distribution system	72
4.1.4	Internal partition	74
4.2	Experimental device	75
4.3	Measurement device	77
4.4	Temperature measurement device	79
4.5	Velocity Of Air Measuring Systems (Thermos-Anemometer Device)	81
4.6	CO <sub>2</sub> Concentration and Humidity Measuring System	83
4.7	Experimental Procedures	84
4.8	Repeatability	86
<b>Chapter Five Results and Discussions</b>		
5.1	Validation	87
5.1.1	Validation (1)	87
5.1.2	Validation (2)	88
5.2	Numerical Results of Insulated Office Room, (case I)	90
5.2.1	Partition's location effect	95
5.2.2	Partition's height effect	98
5.2.3	Partition's gap effect	100
5.2.4	Thermal Comfort Parameters, and Indoor Air Quality	102
5.2.4.i	ADPI and ADI parameters	102
5.2.4.ii	Local thermal comfort	104
5.2.4.iii	PMV and PPD parameters	108
5.3	Experimental Results	113
5.3.1	Average percentage deviation between numerical and experimental results	115
5.4	Numerical results for Non-Thermally Insulated Office Room, (Case II)	118
5.4.1	Locally draught discomfort	121
5.4.2	PPD and PMV	125
5.4.3	Air distribution index (ADI) and ventilation parameter(VP)	129

5.5	Results for Non- Thermally Insulated Office Room, (CaseIII)	130
5.5.1	Local thermal discomfort(draft)	133
5.5.2	Thermal comfort parameters, PMV, and PPD	136
5.5.3	Ventilation parameter and air diffusion index (ADI)	141
<b>Chapter six</b>		
<b>Conclusions and suggestions for future works</b>		
6.1	Conclusions	144
6.2	Suggestions for future works	145
<b>References</b>		146
<b>Appendices</b>		
A	Cooling loads data, for (Case I) Computed by (HAP 4.9)	A-1
A	Cooling loads data, for (Case II) Computed by (HAP 4.9)	A-2
A	Cooling loads data, for (Case III) Computed by (HAP 4.9)	A-3
B	Calibration of Instruments	B
C	Laptop Device, and Windows Specifications	C

## Nomenclature

List of symbols	Description	Unit
A	surface area	$m^2$
$C_p$	specific heat of the air at constant pressure.	kJ/kg.K
$C_{1\varepsilon}, C_{2\varepsilon}$	coefficient in the specific dissipation rate	
DR	daily rang for outlet temperature.	$^{\circ}C$
D	equivalent diameter of panel (4 area/perimeter)	m
F	ratio of chilled ceiling area respect to the floor area	-
G	gravitational acceleration	$m/s^2$
H	convection heat transfer coefficient for inside air	$W/m^2.K$
K	thermal conductivity	
$K_c$	color factors correct	
$k_{i,j,k}$	turbulent kinetic energy at cell (i,j,k)	$m^2/s^2$
M	metabolic heat generation	
P	pressure	N/ $m^2$
V	air flow rate	l/s
Q	cooling load for the heat conduction through the walls and transmitted solar radiation,	W
R	thermal resistance	K/W
S	source term for the rate of thermal energy production	J/kg
T	temperature	$^{\circ}C$
U	total heat transfer coefficient.	$W/m^2.K$
u,v,w	velocity component in x,y, and z-directions	m/s

## Greek symbols

$\rho$	air density	$kg/m^3$
$\Gamma$	diffusion coefficient (diffusivity)	$m^2/s$
$\alpha$	thermal diffusivity	$m^2/s$
$\mu_t$	turbulent viscosity	$N.s/m^2$
S	modulus of the mean rate-of-strain tensor	
$\Delta T$	temperature difference	$^{\circ}C$
$\alpha$	relaxation factor	
$\alpha_k,$ $\alpha_\varepsilon$	coefficient in the specific dissipation rate	

### **Subscripts:**

i,j,k	location of point in a cartesian grid
o	outside
r	radiation
i	inside
s	supply
th	thermal
x	local

### **Abbreviations**

ADPI	Air distribution performance index
ASHRAE	American society for heating, refrigeration, and air conditioning Engineering.
ADI	Air diffusion index
CFD	Computational fluid dynamics
CLTD	Cooling load temperature difference, depend on type of wall.
DV	Displacement ventilation
IAQ	Indoor air quality
LM	Corrector latitude and month
Pr	Prandtl number
RNG	Re-normalization group
SC	Shadow coefficient.
SHG	Solar heat gain.
PMV	Perception of mean vote
PPD	Perception percentage of dissatisfied
VP	Ventilation parameter
PD	Percentage of dissatisfied

# **Chapter One**

## **INTRODUCTION**

## Chapter One

### INTRODUCTION

Since the risk of contracting (COVID) infection was increased in crowded and poorly ventilated settings, improving indoor ventilation reduces the risk of the virus spreading indoors. The process of ventilation involves bringing fresh, outdoor air inside and letting indoor air outside in order to maintain or improve air quality. By controlling the relative humidity and temperature of the indoor air, and carbon dioxide concentrations, the ventilation can affect thermal comfort while also affecting the indoor air quality (IAQ), [1].

There are five different forms of ventilation: natural, mechanical, hybrid, spot, and task-ambient conditioning (TAC). The movement of exterior air through the building's apertures is accomplished by natural forces like wind and thermal buoyancy in natural or conventional ventilation systems. The effectiveness of natural ventilation depends on three things: the climate, people, and buildings,[2]. While the first-time mechanical ventilation was used in 1929, several kinds possessed knowledge, including local exhaust ventilation, piston ventilation, personal ventilation, displacement ventilation, and mixing ventilation, [3]. The latter is most concerned with the present research, which will be explained as follows:

#### **1.1 Mixing Ventilation System:**

In fact, for such approach to work, it is necessary for the supply air and room air to be well mixed by the supplied jet's velocity and buoyancy. The supply air is used to dilute the concentration of contaminants in the room, as shown in Fig. (1-1),[4]. In mixing ventilation system, the air supply is usually done at speed ranging between (2-8) m/s and a temperature of (9 – 40) °C.

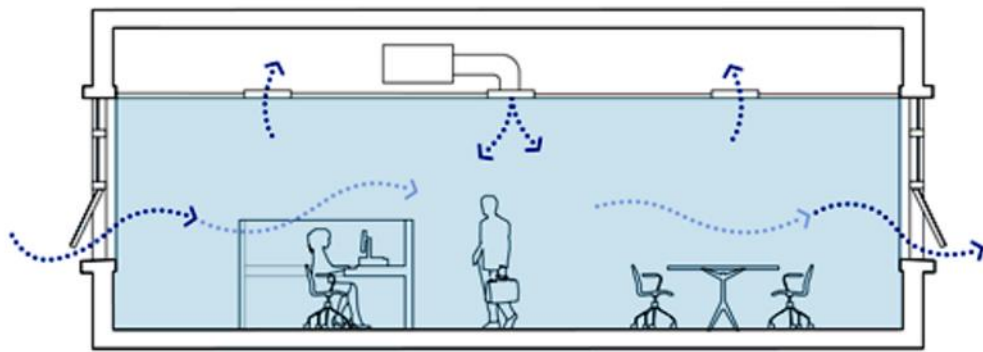


**Fig. (1-1)** mixing ventilation system, [4].

## 1.2 Indoor Air Quality (IAQ):

It is a known fact that individuals in industrialized nations spend over (90%) of their time inside, where they are most exposed to environmental hazards. However, the performance of buildings' interior environmental quality has an impact on the health, mood, and productivity of its occupants [5]. According to the World Health Organization (WHO), hazardous surrounding caused (12.6) million deaths, [6]. The quality of indoor air has a significant influence on the inhabitants' quality of life in both residential and commercial facilities. (IAQ) is a wide term that is affected by several variables such as temperature, relative humidity, air velocity, air flow, occupancy, pollution concentration, noise, and illumination. It's worth noting that the presence of particles, gases, CO<sub>2</sub>, as well as viruses and bacteria cause poor air quality with negative consequences for the occupants, therefore outdoor ventilation and filtration are widely used to improve air quality.

## 1.3 Thermal Comfort:

Human thermal comfort is defined as a state of mind that reflects comfort with one's surroundings, [7]. Heat stress (a decline in the body's ability to cool itself) is caused by high temperatures and humidity. There are numerous strategies for controlling thermal comfort, as needed, replace hot air with cool air as needed, humidify or dehumidify the air, enhance air movement by ventilation

or air conditioning, and limit draught discomfort by diverting ventilation or air movement so that it does not blow directly onto the personnel, e.g., using partitions, [8]. The relationship between thermal comfort, (IAQ), and ventilation is shown in Fig. (1-2).

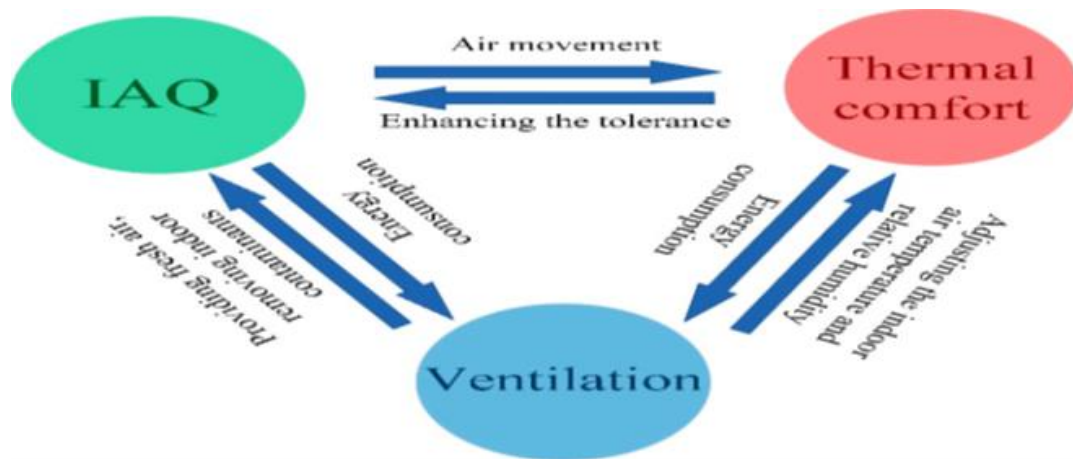


**Fig. (1-2)** ventilation connection between indoor air quality, and thermal comfort, [9].

It's important to manage airflow and air velocity in an occupied zone (space), to ensure proper (IAQ) and thermal comfort, thus a good HVAC should be proper maintained and operated, since (HVAC) can reduce the spread of viruses. These critical building systems not only provide thermal comfort according to (ASHRAE) guidelines, may also improve resistance to infection, so an air conditioning unit need to discharge the airflow, and the direction of the air carefully control, because the goal is to have uniform temperature distribution and avoid air velocity above (40 fpm) or (0.25 m/s). The more the air is blown directly to the occupied area, the more having sensation to draft (unwanted local cooling of the body caused by air movement), the worst the air temperature distribution, [10].

#### **1.4 Prediction of Mean Vote (PMV):**

The Predicted Mean Vote is a famous indication of interior thermal comfort (PMV), forecasts the mean value of a large group of people's votes on a

seven-point thermal sensation scale (-3 cold, -2 cool, -1 slightly chilly, 0 neutral, +1 slightly warm, +2 warm, and +3 hot), [9]. The PMV concept is built on a thermodynamic equilibrium between humans and their surrounding temperature environment. It is assumed that, for the comfort of the people, the quantity of heat created by the body should be balanced by the amount that released to the environment via radiation, convection, and conduction. The PMV index's principal function is used to calculate the average thermal impression score for a group of people which be figured out by four physical elements air temperature, humidity, air velocity, and mean radiant temperature as well as two human characteristics (clothing and activity), [11].

### 1.5 Percentage of Perception of Dissatisfied (PPD):

This is an integral component of thermal comfort evaluation using PMV. It adds to the study by estimating the percentage of occupants that are dissatisfied with the temperature conditions in the investigated space. The association between (PMV) and (PPD) was developed by P.O. Fanger. 1970s, as shown in Fig. (1-3), [12]. The (PPD) index has a minimum value of (5%), indicating that it is not possible to change the settings inside the room to satisfy all inhabitants, [13].

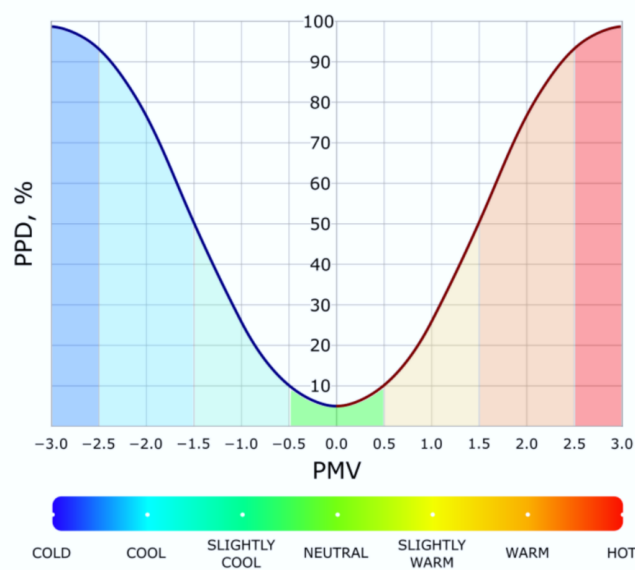


**Fig. (1-3)** Schematic of the link between PMV and PPD, [12].

## **1.6 Internal Partition:**

Building areas in modern office buildings are commonly zoned by installing internal partitioning, which can have a substantial impact on the room air environment,[14]. The thermal sensation and pollutant dispersion in a contemporary building's indoor air-conditioned area are particularly important in a wide range of technical applications. The consequences of contemporary partitions in an air-conditioning area on thermal comfort, air quality, and other aspects, on the other hand, have gotten significantly less attention,[15]. Indoor space partitioning to enable different working zones is not generally addressed during the planning stage of a structure.

Partitions dividing the conditioning area from the corridors, the living room from the bedroom, and the kitchen are rather typical. Similarly, partitions are utilized to regulate the appropriate size of air-conditioning workspace for inhabitants by splitting bigger spaces into smaller compartments, [16]. However, achieving optimum occupant satisfaction in a building with complicated interiors, including walls, is difficult. The partitions become more widespread in modern structures, therefore, the impact of partitions on air flow behavior, thermal comfort, ventilation effectiveness, and indoor air quality requires more investigation, [17] Inappropriate partition placement not only prevents occupants from having optimal movement and spaciousness inside the conditioned area, but it may also cause complications with acoustics and lighting. The choice to install/remove partitions is often made at a later stage of building design, primarily after constructing the duct work mechanism for the HVAC system. In such cases, the installation of a partition significantly modifies airflow behavior and may have a substantial influence on the comfort of the occupants, the image in Fig. (1-4) depicts an idea of such a type of internal partition design, [18] and [19].



**Fig. (1-4)** The interior of an office Building, which can be separated by partition walls, [18].

### **1.7 Objective of the Present Work:**

In the current work numerical and experimental investigations about temperature distribution index in an office room are carried out, by using mixing ventilation system, and partitions under the Iraqi climate (hot and dry climate) with taking an insulated office room as case study.

The main objectives of the thesis are as follows:

- I. Assessing indoor air quality and thermal comfort parameters such as temperature distribution, ( $\text{CO}_2$ ) concentration, local draft discomfort, PMV, PPD, and ADI.
- II. Calculating the heat removal efficiency ( $\epsilon_t$ ) and ventilation efficiency ( $\epsilon_v$ ) for each case study.
- III. Simulating two kinds of non-thermally insulated reality office rooms.

# **Chapter Two**

## **LITERATURE REVIEW**

## Chapter two

## LITERATURE REVIEW

The major goal of the current study's part is to compile all works, and studies at the present time as well as previous studies directly related to the present study. Many experimental and numerical studies have been carried out to verify the flow pattern and air's distribution around and near a person as well as the temperature distribution in the mixing ventilation system, working backwards from the earlier to the most current studies:

**2.1 Experimental Studies**

**Yin, et al., (2009), [20]** investigated the performance of both displacement, and mixing ventilation systems experimentally by using a tested room (5.5 x 4.5 x 2.7) m adopted advanced (HVAC) control system to simulate a single-patient ward; and a four-way overhead diffuser supplied air for the mixing ventilation. Different diffuser mounting locations were permitted in the experimental setup, ceiling position for ceiling diffusers (round ceiling, louvred face, and perforated diffusers) and linear slot diffusers. The ward was outfitted with one bed, cupboards, a television, and medical equipment, contained one patient on the bed and one nurse standing on the patient's right side. (CO<sub>2</sub>) had employed as a tracer gas, and to imitate disease viruses breathing, SF<sub>6</sub> had inserted into a sponge sphere with a diameter of (0.04) m, and the tracer gas was discharged into the patient ward at a very low velocity and at a stable rate. The concentration decays were monitored using in-situ (CO<sub>2</sub>) sensors at (18) sites in the room's inhabited zone. To simulate contaminants breathed out by a patient, a tracer gas (SF<sub>6</sub>). When compared to mixing ventilation, displacement ventilation had generated poorer air quality in the breathing zone if the auxiliary exhaust was positioned at the bottom section of the toilet door. When the exhaust was

moved to the upper half of the wall between the ward and the restroom, displacement ventilation at a lower ventilation rate (4 ACH) gave the same degree of air quality in the breathing zone as mixing ventilation at a greater ventilation rate (6 ACH). The optimum air quality in the breathing zone was given by displacement ventilation with a high exhaust and (6 ACH).

**Karava, et al., (2012), [21]** investigated the possibilities for mixed-mode cooling in buildings with high exposed thermal mass and hybrid ventilation. The study had used a large-scale experimental setup to collect data over a long period of time in an occupied institutional building with motorized façade openings connected with an atrium. Options for pre-cooling thermal mass at night were analyzed, including the using of motorized grilles with adjustable low temperature set points and a fictitious fan with changing speeds. Wind and buoyancy-driven airflow rates, as well as thermal conditions in the heavily glazed atrium area, displayed that the free-cooling provides for a sizable fraction of building's cooling supplies. When the incoming air stream was (12 °C) on average, heat removal from concrete floors was (2-5) times more than when the air stream was (15°C) or (18°C). The results helped advance model-predictive control methods for hybrid ventilation in HVAC systems.

**Tomasia, et al., (2013), [22]** investigated an extensive experiment on thermal comfort and ventilation efficiency in occupied rooms adopted with mixing ventilation and radiant floor systems for heating and cooling conditions, by a full-scale room (4.2 × 4.0 × 2.4) m. The experimental testing room had been setting up in order to simulate a residential room, equipped with a floor heating or cooling mode and a radiant (heating/cooling) wall simulating a window of (8) m<sup>2</sup>, and by mechanical ventilation which was able to provide primary air at various air changes and temperatures. As

supply terminals for residential structures, perforated wall mounted devices located in the middle of the side wall, opposite side of the window (0.15 m below the ceiling), or a circular device placed in the middle of the roof were employed. When fresh air was given from the intake air positioned at the roof, an additional perforated wall mounted unit put on the back wall slightly below the supply device was used as an extract air terminal, as well as an extract air circular device. Air velocity measurements were taken using a variety of hot sphere anemometers. The pollutant removal efficiency had been determined using carbon dioxide (CO<sub>2</sub>) by using a smoke generating system placed in the duct of ventilation air supply at a distance of (1.3) m from the occupant. The study discovered that air change indices and pollutant removal efficacy provided opposite information on ventilation performance in both summer and winter conditions; thus, both must be used to complete the analysis.

**Yin, et al., (2016),[23]** introduced a model air distribution pattern that may be used in ventilation and air-conditioning systems in big buildings, the square column connected ventilation mode. The experiment room was (6.6 x 6.6 x 3.15) m, adopted three ceiling supply air with different velocities (1, 1.5, 2) m/s; the room was covered with fabric curtain in order to visualize the white smoke, under isothermal circumstances, the square column had positioned in the center of the room and measures (1 x1 x 2.5 ) m, on the top of the column, there was an air supply device (2.5 x0.5 x 0.5) m designed to increase outlet homogeneity by adding a partition plane and a perforated plane. The air dispersion parameters of the new ventilation system were examined. The results showed the behavior of square column connected ventilation for a variety of supply air velocities in terms of maximum jet velocity decay, non-dimensional velocity profiles, and jet spreading rate. Square column connected ventilation combines mixing and displacement

ventilation. Airflow from a (20:1) slot outlet can be approximated as a plane wall jet; however, velocity decay and jet diffusion may be faster, beneficial in preventing human draughts in the occupied zone. The (SCAV) mode combines the advantages of standard mixing and displacement ventilation systems, and its air distribution may be employed for ventilation and air-conditioning systems, particularly in big buildings.

**Borowski, et al., (2022),[24]** presented the analysis of (IAQ) as the primary focus in five rooms located on the first and second floors of the building in southern Poland for three weeks. The article had examined the relationship between air quality (temperature, humidity, CO<sub>2</sub>) and thermal comfort. Studying air parameter changes and dynamics, besides the Predicted Mean Vote (PMV) had been studied as well as the Predicted Percentage of Dissatisfied (PPD) guides to determine how satisfied a guest with their room's comfort. Two of the guest rooms studied had (CO<sub>2</sub>) concentrations that briefly exceeded the value of (2000) PPM, which could be uncomfortable for hotel guests. A higher airflow rate had been considered for these spaces' ventilation systems. There were no visible patterns in the measured parameters' dynamic time-dependent variations. This was due to the fact that consumers' tastes differ, and they behave differently. A full study was extremely difficult due to issues such as users possibly opening windows, guests' uncertain presence, and the difficulties of certifying the specific number of users in the room during measurements.

## **2.2. Simulation Studies**

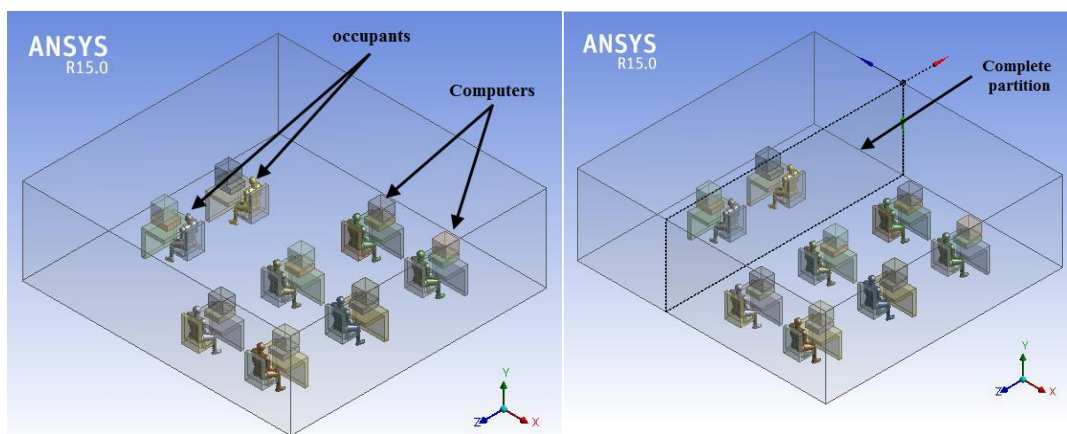
**Cheong, et al., (2003) [25]** conducted a full-scale test in a classroom utilizing objective measurement, a (CFD) modelling approach was used to simulate a number of interior comfort characteristics, counting air-temperature, air velocity, relative humidity, in addition airflow rate. In order

to evaluate the quality of the interior air, the carbon dioxide content during the busiest hour with (100) occupants were also recorded. The outcomes of the (CFD) simulation were within acceptable comfort levels and demonstrated fair agreement with measured empirical data. The results of the simulation were used to calculate thermal comfort indices like (PMV) and (PPD), and then compared to the respondents' own reports on an occupancy survey. The results of both studies showed that the residents were uncomfortable due to the cool air, hence an increase in the thermostat setting had been suggested. To further lessen carbon dioxide accumulation throughout peak occupancy, it had been suggested that a demand control ventilation system replace a variable air volume (VAV) ventilation system.

**Cao, et al., (2011), [26]** looked into how an innovative ventilation approach could safeguard open-plan office workers against the spread of contagious respiratory infections. The fundamental concept was to improve (IAQ), thermal comfort, and energy economy by employing a plane jet diffuser with a high turbulence intensity. In open-plan offices and public spaces, the revolutionary ventilation approach introduced here was able greatly to improve ventilation efficiency, hence reduced the risk of epidemic respiratory disorders and improving air quality in the breathing zone (BZ).

**Ahmed, et al., (2016), [27]** studied how well under-floor air distribution (UFAD) systems functioned to ensure office workers were comfortable. A spacious office with the dimensions (8.4 x 8 x 2.7) m high has been taken into consideration. Internal heat gains were made up of (8) people with (126) W, (8) computers with (120) W, and overhead illumination provided by fluorescent bulbs that had been positioned in the room's ceiling. The air temperature, and relative had supplied at (18 °C), (60%) respectively, with velocity of (1) m/s. Computational fluid dynamics (CFD) simulation

with the commercial (CFD) code (ANSYS 15) was used for the study. In addition to the (RNG  $k-\varepsilon$ ) model equations for turbulence model, the (CFD) modeling techniques also solved the equations of continuity, momentum, energy, and species transport. The governing equations were discretized using a second order upwind scheme, and the pressure-velocity coupling remained handled with the simple procedure. The study looked at how different types of office partitioning affected thermal comfort and the efficiency of the unoccupied space air distribution (UFAD) system, as shown in Fig. (2-1) The third scenario had the lowest  $\text{CO}_2$  values, which were at (586) PPM, or a (2.33) percent drop from case 1's pollutant concentration. The office space's average (PMV) value was raised by the partial partition's existence. (PMV's) average value increased by (8.6) percent on average.



a- Before partitioning

b- After partitioning

Fig. (2-1) configuration of the simulated office unit before and after partitioning.

**Pradip and Thananchai, (2016), [28]** studied the impact of a partition on thermal comfort, indoor air quality (IAQ), energy usage, and perception in an air-conditioned room of a library (38 x 27.3 x 3) m, non-insulated from the left, right, window, and the door, had supplied by (38)

ceiling square diffusers (300 x 300) mm with temperature and relative humidity of (17 °C), (70%) respectively, and (4) exhaust air grills (2.5 x 0.4) m; at Sirindhorn International Institution of Technology and Thammasat University, numerically examined before and after using the indoor partition, by (CFD) software (Solid Work) flow simulations. (35°C) has been recorded as the outside temperature. there was a (400) PPM concentration of carbon dioxide that was distributed evenly to each supply diffuser. The research advised using the predicted mean vote (PMV) of thermal comfort, the concentration of carbon dioxide, the rate of energy consumption in making up air, and an overall perception score for the purpose of assessing effects in a segmented region. According toward the research, the partition reduced the perceived mean vote (PMV), making people feel significantly cooler. The results of the research had showed that the splitter could be used to minimize the cooling supply and so conserve energy. The (CO<sub>2</sub>) concentration was within the acceptable range, but it had been increased in the particular region with resident.

**Hyeunguk, et al., (2017), [29]** investigated the indoor environmental quality as well as the effectiveness of the air conditioning in a partitioned room, the computational domain consisted of two identical spaces with a dimension (4 × 4 × 2.5) m. The two spaces were connected through a door in a partition wall and air could move from one space to the other using two different ventilation systems (mixed and displacement ventilation). For the mixing ventilation case, a wall supply diffuser had placed in each room at ceiling height, whereas the supply diffuser for the displacement ventilation case had installed at floor level, only one section had exhaust in both situations, which was positioned at the ceiling. Through the using of computational fluid dynamics (CFD), (Star-CCM+) simulations, and (RANS) as a turbulence model, by making the model's envelope

adiabatically with the exception of windows and human simulators, outside conditions were eliminated. Based on the typical solar heat gain factors (SHGFs) for southern exposure at (40 N) latitude during cooling seasons, the window emitted (400 W) or (160 W/m<sup>2</sup>) sensible heat flux, and the human simulator emitted (75 W/m<sup>2</sup>) of total heat flux to represent a seated person performing office work like typing or filing (ASHRAE 2009). Supply air temperature were (16°C ), (17 °C) for the mixing, and displacement systems respectively. The temperature distribution between two partitioned rooms, as well as the ventilation efficiency, energy consumption, and individual thermal comfort, are all investigated. The study concluded that the presence of an internal partition has an important effect proceeding the temperature distribution in room, regardless of whether a mixing or displacement ventilation system was used, and that rearranging the air diffuser in more than one location had no significant effect on the air distribution. Besides, the presence of the partition had greatly affected on the age-of-air.

**Awbi, (2017), [30]** gave a brief overview for many mechanical ventilation, and air distribution technologies used for buildings. Evaluation of the ventilation's performance in terms of (IAQ) providing, as well as the ventilation's performance in relations of air distribution, and ventilation's energy effectiveness, were all included in the study. The research relied on the air distribution index, which could take on one of two forms depending on the characteristics of the space being ventilated. The first method was designed for use in situations that were uniform, whereas the second method could be utilized in settings that were either uniform or non-uniform. The study indicated that more recently developed systems might be provide improved indoor air quality while requiring less ventilation energy, as well as demonstrated that the typical displacement ventilation (DV) system operated effectively in general .However, generally recognized that the (DV)

system had limitations in terms of the quantity of cooling that could be given as well as the (DV) jet's penetration depth. After comparing traditional ventilation systems with the unconventional ventilation systems, the study found that the mixing ventilation system gave the best indoor air quality with low energy requirements.

**Al-Assaad, et al., (2017), [31]** demonstrated how well a hybrid system consisting of a mixing ventilation (MV) unit and an individual unit (PV) worked. The computational fluid dynamics (CFD) typical remained used for simulation to locate the optimum airflow frequency. The temperature and velocity fields in a standard office space (2.5 x 2.75 x 2.8) m were simulated using a (3D) CFD model. Average room air temperature was (25 °C), while supply air from individual ventilation was (22 °C). Even though the constant (PV) jet provided more cooling for a specific body area, the technology demonstrated that supplying localized airflow under transient conditions increased thermal comfort. The results of the investigation demonstrated that thermal comfort rose by (15.2 %), at what time the frequency had raised at a constant airflow rate. However, when the fixed frequency with an increase in the airflow rate, the thermal comfort declined and unacceptable with a frequency of (0.3 Hz), but then again it was suitable with a frequency of (0.5 Hz) (0.5 Hz). The thermal comfort went up from (0.79 to 0.91) when the frequency was raised from (0.3 to 0.5) hertz (0.91).

**Liu, et al., (2018), [32]** investigated the influence of internal office partitions affecting pollution dispersion and on-air flow. Different ventilation patterns were used with a room of dimensions (3.7 × 3 × 3) m. This study was conducted numerically using (ANSYS FLUNENT commercial CFD software,). Several turbulence models had been used, the best of which was (RNG-kε). The effect of the distribution of air inlets and

outlets was studied, as well as the effect of pollutant sources and the performance of diffusion in the case that there was a partition inside the office room. It had been concluded that the internal partitions have a greater effect on the ventilation situation in the case that the air supply was from an air diffuser installed on the wall and not in the ceiling. Further, the study concluded that the effectiveness of pollutant removal was better in the case of air supply from the upper part of the wall and the air exiting from the lower part of the wall.

**Villafruela, et al., (2019),[33]** looked at the feasibility of implementing a displacement ventilation approach in airborne infection isolation rooms, with an emphasis on health care worker exposure to pathogens breathed by infected patients. The analysis was mostly based on numerical simulation findings generated with the assistance of a three-dimensional transient numerical model verified using experimental data. A thermal breathing manikin was lying on a bed represented the source patient, while another thermal breathing manikin was standing alongside the bed and facing the patient represented the exposed individual. A radiant wall was an outdoor wall that was exposed to sun radiation. The investigated research of a patient laid on a hospital bed and a health care worker (HCW) stood near to the bed in a typical room was carried out in a (4.5 x 3.3 x 2.8) m test room at Cordoba University. The geometry of the two thermal breathing manikins was the same. Each manikin's total sensible heat released corresponded to a metabolic rate of (1 met) for the (HCW) and (0.7 met) for the patient, or (80) W and (70) W, respectively. The (4.5) m wall opposite the (HCW) had a (500) W external heat gain, indicated that was exposed to sun radiation. The remaining walls, as well as the floor and ceiling, had been repaired. In a typical airborne infection isolation room with three air renewal rates ( $6\text{ h}^{-1}$ ,  $9\text{ h}^{-1}$ , and  $12\text{ h}^{-1}$ ), two exhaust opening positions, and two health care workers

positioned, the air change efficiency index and contaminant removal effectiveness indices, as well as inhalation by the health care worker of contaminants exhaled by the patient, were considered. The findings demonstrated that the radiant wall had a substantial impact on the air flow pattern and pollutant dispersion. The lockup phenomena happened at the standing manikin's inhaling height.

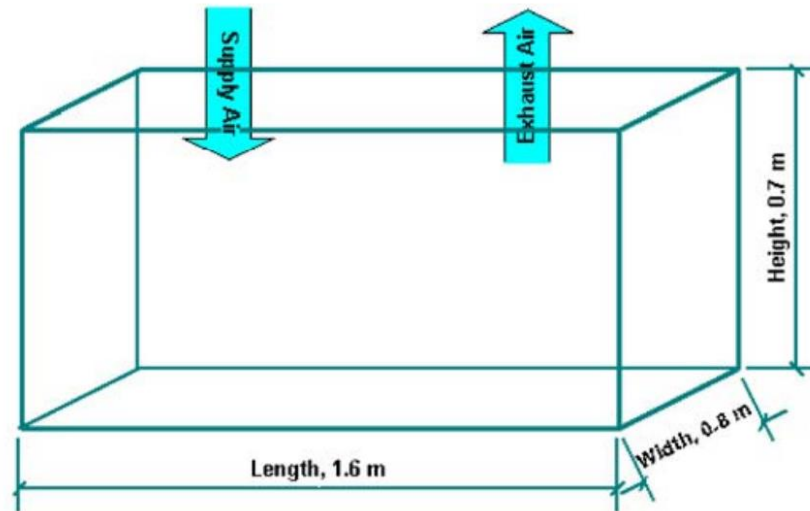
**Roasaeia and Rahaei, (2020), [34]** studied mixed method to predict airflow speed and direction in an office space and to increase airflow homogeneity at the administrative unit level. The office building in Ahvaz was chosen as a case study and field observation site, (an area with a hot semi-humid climate in which it was required to provide abundant cooling using mixed air conditioning systems). The building's office hall was planned and built with partition walls, with dimensions of (54 x 7.60 x 5) m, and the spaces divided by light partition walls with dimensions of (22) m (height) providing autonomous places for each employee's activities. The researchers employed (GAMBIT) and (ANSYS FLUENT) for numerical simulations. The results showed that in addition to the positioning of airflow distributor valves, the height of internal partition walls affects inside airflow, and the appropriate design may make indoor airflow uniform and predictable.

**Kurnitski et al., (2021), [35]** examined the flow characteristics of a typical (ICU) unit computationally. When developing a sanitization and virus-control system for the intensive care unit (ICU) of (5 x 5.5 x 3) m. The (ICU) model included a bed, a table, a chair, a regular-sized fan, and an air conditioner with input and output. The study room assembly was developed in (Solid-works 2016) software and was loaded into (ANSYS FLUENT 2019), and the (RNG  $k-\varepsilon$ ) as a turbulence model, focused on the flow of

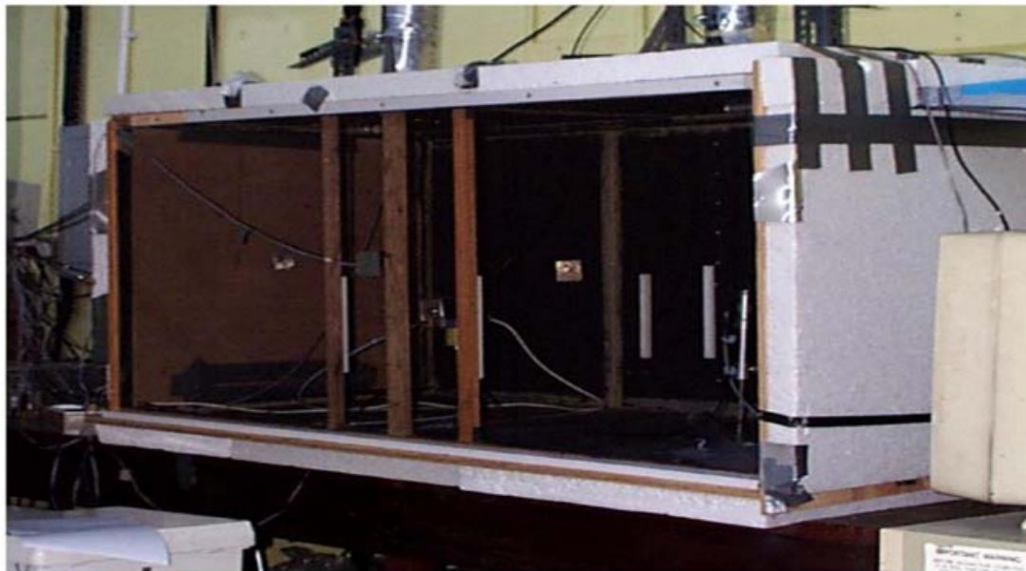
aerosol particles while taking into account both the combined and individual impact of the fan and (AC). Because of the relatively constant flow circulating regions in the area and the significant amount of particle deposition on surfaces, ventilation at a single area was particularly ineffectual at removing particles, even at the maximum rate currently applied.

### **2.3 Experimental and Simulation Studies**

**Lee and Awabi, (2004), [36]**, studied the impact of room division on ventilation and air quality. Small model room dimensions of (1.6 m(L) 0.8m(W) 0.7m(H)), source opening dimensions of (0.9 x 0.9) m, and exhaust grille of the same size were used for the computational and experimental analysis. After experimenting with different ventilation rates, it was found that (50 ACH), (equivalent to a supply air velocity of 1.54 m/s) achieved the necessary ( $Re=9174$ ). Numerical modeling carried out by a CFD simulations of (Vortex-2), with turbulence model (RNG k- $\epsilon$ ). Mixing ventilation from the roof was adopted. A tracer gas was used to anticipate the chambers inside conditions ( $CO_2$ ). The study relied on the location, height of the interior partition, and the gap under it, in addition to the location of the pollutant source. The study carried out under isothermal conditions and concluded that the presence of the gap leads to an increase in the effectiveness of the removal of pollutants. The location of the internal partition had influenced to the inlet and outlet of ventilation air affected the effectiveness of pollutant removal. The study showed that the gap between the partition and the floor has a significant role in improving the environmental conditions inside the room if it does not exceed (10%) of the partition height.



a- Schematic, ventilation scheme



b- Photograph of the model test room

Fig. (2-2) Schematic, ventilation scheme, and photograph of the model test room of the study.

**Alaa, et al., (2016), [37]** studied the effects of the Iraqi climate on indoor air quality through computational, and experimental investigation of air flow diffusion and pollutant circulation, by using (ANSYS FLUENT)

version (3.2.26), with (GAMBIT) and (RNG k- $\epsilon$ ), as a turbulence model, the tested office room dimensions was (4 x 3.5 x .75) m, corresponded to a standard two-person workplace, two computers, and two lights. Office ventilation unit of (had been utilized to limit pollutant distribution and improve the quality of the air workers breathe. Many engineers utilized carbon dioxide (CO<sub>2</sub>) concentration as a proxy for air quality as a means of assessing the performance of a mechanical ventilation system. The rate at which carbon dioxide (CO<sub>2</sub>) is produced by human respiration was therefore considered to be a (CO<sub>2</sub>) source, served as a tracer gas. According to the findings of the study, floor-supply displacement ventilation may be able to improve the quality of the air inside a building since the pollutant concentration in the breathing zone is significantly lower than that of a mixing system. A larger risk of discomfort might be presented in enclosed environments with floor-supply displacement ventilation compared to ordinary mixed ventilation since of significant temperature stratification among the ankle then head levels. The findings suggested that the distribution of contaminants in a mechanically ventilated office environment should be investigated separately for each case.

**Hameed, et al., (2017), [38],** looked at the relationship among indoor air quality (IAQ) besides the performance of three different types of air diffusers using numerical and experimental analysis (three direction-square diffuser, semi-circle diffuser and one direction-square diffuser). This study examined the effects on indoor air quality and air diffuser performance when the location of return air grilles was shifted three times. Three different types of air diffusers were used. In all diffuser designs, air was delivered at velocities between (0.24 and 0.25) m/s and temperatures between (19 °C and 20 °C). All experiments were carried out in a standard office space of (4 x 3.2 x 4) m. Based on the values of air distribution performance index (ADPI)

(66.675%) and effectiveness temperature, the study found that positioning the diffuser of air and the return air grille on the same side wall delivers good thermal comfort and acceptable to the room occupants (1.824). According to the results of the research, the three-directional square diffuser was the most effective design.

**Ammar, et al., (2018), [39]**, used a combination of experimental and numerical methods, they simulated the climate of Iraq in a controlled laboratory setting, studying factors for instance temperature, wind speed, humidity, too the presence of pollutants. The finite volume technique in conjunction with the (SST  $k-\epsilon$ ) as a turbulent model had been used, and according to the findings, the mixing ventilation system was able efficiently remove heat from the internal combustion laboratory at a rate of (85%), and it removed a wide range of pollutants with an efficiency of up to (90%). For instance, in a second scenario at the laboratory of chemical and petroleum products, data showed a boost in comfort of up to (40%) when the supply air terminal diffuser was located on the same side.

**Contrada, et al., (2021), [40]** explored a unique approach for measuring air exchange performance, including natural and mixed mode ventilation for healthy applications and the relationship between air exchange efficiency and airborne virus transmission. The work compared Sandberg's innovative approach with the (ASHRAE 129) mechanical ventilation procedure. The work also analyzed the practical problems and uncertainties of implementing this technique in a new commissioning protocol. At low airflow rates, the (ASHRAE) 129 technique (51.8%) and the novel procedure (47.4%), with an average uncertainty of (7%) were statistically indistinguishable. Results proved the procedure's validity and applicability to natural and mixed-mode ventilation.

**Chi, et al., (2022), [41]** showed that the hydraulically powered ventilation system performed well in driving airflow. The suggested ventilation system was installed in the study building, and its performance in two testing rooms was measured numerically. When planning the building's interior, thermal comfort concerns were considered. The building energy assessment tool estimates that during the plum rain season (March through May) and the summer (July through September), the hydraulic-driven ventilation device (also called a renewable energy provider) and the building space division arrangement increase the building's capacity to reduce energy consumption by (46%) and (43%), respectively (i.e., thermal comfort demander).

**Liu, et, al., (2021), [42]** utilized the Wells-Riley equation with a genuine instance involving a COVID-19 outbreak aboard a long-distance bus to get the quanta value. In a seven-seater cabin dummy, researchers compared displacement and mixing systems through experiments and computer simulations. The study measured the air velocity, temperature, in addition particle distribution (1 m and 5 m) using ultrasonic anemometers and thermocouples. Additional scenarios through varying occurrence source locations were too simulated to ensure these operating conditions were accurately replicated. The risk of infection in airplane cabins might be estimated using polydisperse particles, according to this study. Moreover, (DV) infection risk was lower than (HIV) infection risk at the onset of the pandemic (MV). Passengers' risk of contracting (MV) during the epidemic's middle and late phases could be lowered by wearing masks, brought it down to a level roughly equivalent to that of (DV).

## 2.4 Summary of Previous studies

The tables (2-1, 2-2, and 2-3) present the key finding of the preceding studies.

**Table (2- 1) summary of experimental studies**

Reference	Year	Place of study	Main focus	Main Findings
Yonggao Yin, et al, [20]	2009	Nanjing, China	the spread of contaminants from the patient to the rest of the room, as well as the danger of infection to the nurses	According to the findings, displacement ventilation might or might not improve air quality in the ward, depending on the location of the exhaust in respect to the restroom.
P. Karava et al,[21]	2012	Cambridge (US)	Mixed- mode cooling ways in the occupied buildings.	The findings had been enabled model-predictive control strategies for space conditioning employing hybrid ventilation.
R. Tomasia, et al,[22]	2013	International center for indoor environment of technical University of Denmark	Assessment of the thermal comfort and ventilation efficiency in residential rooms with radiant floor heating and cooling systems.	pollutant removal efficacy and air change indices provided conflicting information on the effectiveness of ventilation, both in summer and in winter conditions. It is important to take into consideration both of them to complete the study.
Haiguo Yin et al,[23]	2016	China	Airflow characteristics of square column attached ventilation investigation.	The SCAV mode combines the advantages of classical mixing with those of displacement ventilation systems, and its air distribution may be employed for ventilation and air-conditioning systems, particularly in big buildings.
Guangyu Cao, et al,[24]	2022	Hotel rooms in southern Poland	Air quality assessments in hotel rooms	The CO <sub>2</sub> contents in two of the studied guests' rooms briefly surpassed the value of 2000 ppm, which might cause discomfort to hotel visitors. It is necessary to consider increasing the amount of ventilation airflow.

**Table (2- 2) summary of Simulation studies**

Reference	Year	Place of study	Software	Main focus	The most important results
Cheong et al[25]	2003	Singapore	ANSYS	Evaluation thermal comfort conditions in theatre	For optimal CO <sub>2</sub> concentration during peak occupancy, suggested to switch from a variable (VAV) ventilation system to a demand control ventilation system.
Cao et al.[26]	2011	Finland	ANSYS	protect office workers from infection by epidemic respiratory diseases in open-plan offices and public spaces	The risk of respiratory illnesses spreading in open-plan offices and public areas was reduced by development design that reduces the combination of supply air and ambient air.
Ahmed M. M. Abouzaid et al, [27].	2016	Cairo	ANSYS	interior partitions' impact on the thermal comfort and indoor air quality (IAQ) level offered by the underfloor air distribution system in a typical office space	The third case had the lowest CO <sub>2</sub> values, which were at (586) PPM, or a (2.33) percent drop from case 1's pollutant concentration. The office space's average (PMV) value was raised by the partial partition's existence. PMV's average value increased by (8.6) percent on average.
Pradip Aryal, et al., [28]	2016	Thammasat University	Solid work	impact of a partition on the occupant's degree of thermal comfort	the splitter might been utilized to reduce cooling demand and so save energy. Although the CO <sub>2</sub> level was higher in the specific area where people lived, it was still below safe limits.
Hyeung uk Ahnl, et al.[29]	2017		(CFD) (Star-CCM+)	IAQ evaluation, energy saving, and diffuser layout on airflow distribution with combined ventilation systems	displacement ventilation had taken less time than mixing ventilation to attain an interior set-point temperature in a partitioned space. When each partitioned space was fed by its own diffuser, the air conditioning time for mixing ventilation was the shortest.
Hazim B Awbi, [30]	2017	UK	ANSYS	Encourage the community the concept of (ADI) on effectiveness assessment	The study found that the mixing ventilation system gave the best indoor air quality with low energy requirements

Al-Asaad et al.,[31]	2017	Beirut Lebanon	ANSYS FLUENT	the performance of an (MV) system combined with a (PV) that delivered a sinusoidal horizontal airflow jet towards the occupant's upper body	The study found that a rise in frequency while maintaining the same airflow rate improves thermal comfort by (15.2) percentage points.
Xiaoping Liu, et al.,[32]	2018	China	ANSYS FLUENT	a numerical simulation of interior airflow and pollutant dispersion under three ventilation patterns to investigate the impact of internal partitions and supply and exhaust opening locations	Different ventilation modes had a significant impact on interior airflow distribution, with the top-supply down-return ventilation mode outperforming the down-supply up-return and flow-supply up-return modes in terms of creating a desired airflow pattern.
Villafruela, et al., [33]	2019	Cordoba University	ANSYS	Evaluation of the suitability of applying the DV strategy in AIRs	It had been discovered that increasing the ventilation rate does not reduce exposure and may, in fact, increase it in some conditions. A radiant wall had a considerable impact on air flow pattern and pollutant dispersion.
Amin Roasaeia and Omid Rahaei, [34]	2020	AHWAZ, Iran	GAMBIT and FLUENT version (6.3)	investigate the influence of internal partition walls, as one of the criteria determining the quality of air flow in office spaces, on a case study in hot, humid, and semi-humid climates	The findings demonstrated that the height of interior partition walls, in addition to the positioning of airflow distributor valves, influences the indoor airflow, and that their uniform and predictable distribution may be achieved by careful design.
Prajapati, et al., [35]	2021	India	Solid work 2016 ANSYS FLUENT 2019	Aerosol transmission of covid-19 particles in an ICU room simulation.	The sick person can spread the disease when under the impact of the fan and AC; tThe results also demonstrated that the aerosol particle flow had a promising use in sterilizing the room.

**Table (2- 3) summary of experimental and numerical studies:**

Reference	Year	Software	Main focus	The most important results
H. Lee and H.B. Awbi, [36]	2004	VORTE X-2	Effect of internal partition on indoor air quality.	the contaminant source location has a little influence on the room air quality and ventilation performance. However, when the test room is partitioned, the contaminant from the source placed in the exhaust zone of the room is removed e effectively.
Alaa Abbas Mahdi et al., [37]	2016	(ANSYS) FLUENT version (3.2.26)	Investigation of air diffusion and contaminant concentration.	The contaminant distribution in a mechanical ventilated office should be separately for each case
Hameed, et al., [38]	2017	AIRPAK	performance of three different types of air diffusers using numerical and experimental analysis	the study found that having the diffuser of air and the return air grille located on the same side wall provides good thermal comfort and is acceptable to the room's occupants (1.824).
Ammar abdulhussien, et al., [39]	2018	ANSYS FLUENT	Temperature distribution, velocity, contaminant concentration, in the air conditioned in the laboratory for Iraqi climate.	The findings demonstrated that the mixed ventilation system can successfully remove a wide range of pollutants (up to 90%) and provide human thermal comfort conditions (up to 85%) through the removal of heat.
Francesca Contrada and et at, [40]	2021	ANSYS	Thermal comfort enhancement with hydraulic-driven ventilation system and space partition layout for building energy savings	the building's energy saving potentials could be increased by 46% and 43%, respectively, due to Hydraulic-driven ventilation equipment (renewable energy supply) with building partition layout
Fang'ai Chi et.al., [41]	2021	ANSYS	measuring the air exchange efficiency index by extending current standardized techniques that were established for mechanical ventilation to natural and mixed-mode ventilation systems.	a slight gap between the air exchange efficiency values calculated using the ASHRAE 129 protocol (51.8%), and the innovative approach (47.4%). the findings substantiated the correctness of the method and demonstrated its viability for use in conjunction with natural and mixed-mode ventilation.

Mingxin Liu, et al, [42]	2022	ANSYS	ventilation, thermal comfort, and COVID-19 infection risk evaluation.	Passengers can protect themselves from contracting MV in the epidemic's later stages by wearing masks, bringing their risk of infection down to about that of DV.
Present work	2022	AIRPAK (3.0.16)	IAQ, thermal comfort assessment in hot and dry climate	Partition adoption has a significant effect on (PPD) value, it helped to reduce the (PPD) value to (5.26%) in case of partition gap's height of (5%) of the room's height.

### 2.5 Scope of the Present Work:

Earlier studies had demonstrated a good indoor air quality by using combined ventilation systems, and by reviewing previous studies, it was discovered that there is an absence of Iraqi research on topics related to providing mixing ventilation systems and partitions to office units in a hot and dry climate. Most previous studies dealt with combined ventilation systems to assess indoor air quality rather than focusing on assessing thermal comfort parameters such as (ADI, PPD, PMV, and locally draught discomfort) by adopting mixing ventilation.

Therefore, the current study will focus on as follows:

- Effect of offices partitioning on air distribution index, by adopting mixing ventilation system under Iraqi climate, numerically and experimentally.
- Assessing thermal comfort parameters such as (local draft, ADI, PMV, and PPD).

## 2.6 Motivation of the Present Work:

The performance of air conditioning is one of the aspects useful in producing workplaces with ideal thermal comfort conditions, and it is always necessary to consider employees' thermal comfort in the office building interior. Meanwhile, one of the most important factors determining the pattern of interior air flow is the presence of internal partition walls. However, studies suggest that in order to increase the ventilation quality in office spaces, the interior air flows must be controlled in a desired manner. The current study tried to investigate the influence of internal partition walls, as one of the criteria influencing the quality of air flow in office spaces adopted mixing ventilation system, on a case study in hot and dry climate. By using a simulation software specialized in ventilation systems that is (AIRPAK 3.0.16), and (RNG-  $k\varepsilon$  ) as a turbulence model.

Through the current investigate, the results will discuss the following questions:

- How well do interior partition walls impact airflow quality and an air conditioner's performance?
- What relation was observed between the interior partition walls and the office's uniform airflow?
- Does the height and placement of interior partition walls in design concept improve the quality of airflow?

# **Chapter Three**

**MATHEMATICAL MODELLING**

**AND**

**NUMERICAL ANALYSIS**

## Chapter Three

## MATHEMATICAL MODELLING AND NUMERICAL ANALYSIS

In order to create and evaluate numerical solutions to issues that occur in other branches of mathematics, such as calculus, linear algebra, or differential equations, numerical analysis is used. In the current study, the parameters (ADPI, ADI, PMV, PPD,  $\varepsilon_v$  and  $\varepsilon_t$ ) were studied numerically and their impact on human comfort and indoor air quality was predicted, as well as the air movement and temperature distribution in the simulated rooms were numerically predicted. Twenty tests were studied numerically as listed in Tables (3-1), (3-2), and (3-3). The numerical simulations were carried out by AIRPAK3.0.16, which is an accurate, quick, and user-friendly design tool that makes it easier to apply cutting-edge airflow modelling technology. This technology is used to the planning and evaluating of ventilation systems. Additionally, the postprocessing features necessary to the ventilation sector allow designers and engineers to have access to a tool that gives the most accurate solution feasible in the shortest period of time compared to other software tools for airflow modeling. Thermal and fluid flow calculations are performed by AIRPAK using the CFD solver FLUENT for computational fluid dynamics. This tool solves complicated geometries by utilizing unstructured. Calculations are speedy and reliable because to the multigrid and segregated solver algorithms.

**Table (3-1)** Description of numerical and experimental study tests (without gap).

Test	Case I	Description	
		partition height	Partition location
1	Numerical and Experimental	0	0
2	Numerical	0.6 H	0.4L
3	Numerical	0.6H	0.5L
4	Numerical	0.6H	0.6L
5	Numerical and Experimental	0.7H	0.5L
6	Numerical	0.8H	0.5L

**Table (3-2)** Numerical, and experimental study tests of gap underneath.

Test	Case I	Description		
		Gap	partition height	Partition site
7	Numerical And	5%H	0.7H	0.5L
8	Experimental	10%H	0.7H	0.5L

**Table (3-3)** Description of numerical study tests (non-insulated office room).

Test	Case II, and III	Description
9, 13	Numerical study	Non insulated office unit before partitioning
10, 14	Numerical study	Non insulated office unit partitioned without a gap.
11, 15	Numerical study	Non insulated office unit partitioned with(5%H) gap.
12, 16	Numerical study	Non insulated office unit partitioned with(10%H) gap.

### 3.2 The Governing Equations

In the current work, according to CFD simulation, the flow was assumed to be steady, Three dimensional, Newtonian, incompressible fluid, without chemical reaction, and turbulent flow, ideal fluid and frictionless.

#### 3.2.1 The mass conservation equation

For the purpose of computing laminar and turbulent flow with heat transfer,) AIRPAK3.0.16) solves the Navier-Stokes equations for mass, momentum, species, and energy transmission. AIRPAK3.0.16 guide, [43].

$$\frac{\partial}{\partial x}(\rho u) + \frac{\partial}{\partial y}(\rho v) + \frac{\partial}{\partial z}(\rho w) = 0 \quad \dots (3.1)$$

#### 3.2.2 Momentum equations

*u. momentum equation:*

$$\begin{aligned} \frac{\partial}{\partial x}(\rho uu) + \frac{\partial}{\partial y}(\rho uv) + \frac{\partial}{\partial z}(\rho uw) &= -\frac{\partial p}{\partial x} + \frac{\partial}{\partial x}\left(\mu \frac{\partial u}{\partial x}\right) + \frac{\partial}{\partial y}\left(\mu \frac{\partial u}{\partial y}\right) + \\ \frac{\partial}{\partial z}\left(\mu \frac{\partial u}{\partial z}\right) + \frac{1}{3} \frac{\partial}{\partial x}\left[\mu \left(\frac{\partial u}{\partial x} + \frac{\partial v}{\partial y} + \frac{\partial w}{\partial z}\right)\right] &+ \frac{\partial}{\partial x}(-\rho \overline{u'u'}) + \frac{\partial}{\partial y}(-\rho \overline{u'v'}) + \\ \frac{\partial}{\partial z}(-\rho \overline{u'w'}) + \rho g_x & \quad \dots (3-2) \end{aligned}$$

*v. momentum equation:*

$$\begin{aligned} \frac{\partial}{\partial x}(\rho uv) + \frac{\partial}{\partial y}(\rho vv) + \frac{\partial}{\partial z}(\rho vw) &= -\frac{\partial p}{\partial y} + \frac{\partial}{\partial x}\left(\mu \frac{\partial v}{\partial x}\right) + \frac{\partial}{\partial y}\left(\mu \frac{\partial v}{\partial y}\right) + \\ \frac{\partial}{\partial z}\left(\mu \frac{\partial v}{\partial z}\right) + \frac{1}{3} \frac{\partial}{\partial y}\left[\mu \left(\frac{\partial u}{\partial x} + \frac{\partial v}{\partial y} + \frac{\partial w}{\partial z}\right)\right] &+ \frac{\partial}{\partial x}(-\rho \overline{u'v'}) + \frac{\partial}{\partial y}(-\rho \overline{v'v'}) + \\ \frac{\partial}{\partial z}(-\rho \overline{v'w'}) + \rho g_y & \quad \dots (3-3) \end{aligned}$$

*w. momentum equation:*

$$\begin{aligned} \frac{\partial}{\partial x}(\rho u w) + \frac{\partial}{\partial y}(\rho v w) + \frac{\partial}{\partial z}(\rho w w) = & -\frac{\partial p}{\partial z} + \frac{\partial}{\partial x}\left(\mu \frac{\partial w}{\partial x}\right) + \frac{\partial}{\partial y}\left(\mu \frac{\partial w}{\partial y}\right) + \\ \frac{\partial}{\partial x}\left(\mu \frac{\partial w}{\partial z}\right) + \frac{1}{3} \frac{\partial}{\partial z}\left[\mu\left(\frac{\partial u}{\partial x} + \frac{\partial v}{\partial y} + \frac{\partial w}{\partial z}\right)\right] + \frac{\partial}{\partial x}(-\rho \overline{u'w'}) + \frac{\partial}{\partial y}(-\rho \overline{v'w'}) + \\ \frac{\partial}{\partial z}(-\rho \overline{w'w'}) + \rho g_z \end{aligned} \quad \dots (3-4)$$

Where the terms  $(\rho \overline{v'w'}, -\rho \overline{w'w'}, \rho \overline{u'v'}, \rho \overline{v'w'}, \rho \overline{u'w'})$  are the turbulent Reynolds shear stress ( $\tau_t$ ) and  $(\rho g_{x,y,z})$  is body force.

### 3.2.3 Energy conservation equation

$$\begin{aligned} \frac{\partial}{\partial x}(\rho u t) + \frac{\partial}{\partial y}(\rho v t) + \frac{\partial}{\partial z}(\rho w t) = & \frac{\partial}{\partial x}\left(\Gamma \frac{\partial t}{\partial x}\right) + \frac{\partial}{\partial y}\left(\Gamma \frac{\partial t}{\partial y}\right) + \frac{\partial}{\partial z}\left(\Gamma \frac{\partial t}{\partial z}\right) + \\ \frac{\partial}{\partial x}(-\rho \overline{u't'}) + \frac{\partial}{\partial y}(-\rho \overline{v't'}) + \frac{\partial}{\partial z}(-\rho \overline{w't'}) + S_t \end{aligned} \quad \dots (3-5)$$

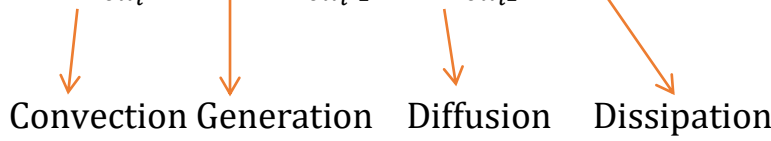
Where  $\Gamma$  is diffusivity, the term  $(S_t)$  is source term and term  $(-\rho \overline{u't'}, -\rho \overline{v't'}$  and  $-\rho \overline{w't'})$  are the turbulent heat fluxes respectively.

### 3.2.4 Turbulence Models

The turbulence models include the (RNG) model, the Spalart-Allmaras model, zero indoor equation, and the zero-equation (mixing-length) model (AIRPAK3.0.16) as listed in Table(3-4). The turbulence model used in the present study is defined as two equation eddy viscosity model. Renormalization Group Method (RNG k-  $\epsilon$ ) was a good choice for users in numerical analysis for a ventilation system. According to Chen, [44], the (RNG k- $\epsilon$ ) model was the best of the eight (K- $\epsilon$ ) models with mixed convection flow. Yakhot, [45] discovered that the (RNG k- $\epsilon$ ) model outperformed all other models examined.

The (RNG k-ε) equations are given by, [46]:

$$(\rho U_i) \frac{\partial k}{\partial x_i} = \mu_t S^2 + \frac{\partial}{\partial x_i} \left[ \alpha_i \mu_{\text{eff}} \frac{\partial k}{\partial x_i} \right] - \rho \epsilon \quad \dots (3-6)$$



Where,  $S \equiv \sqrt{2S_{ij}S_{ij}}$        $S_{ij} = \frac{1}{2} \left( \frac{\partial U_j}{\partial x_i} + \frac{\partial U_i}{\partial x_j} \right)$

Dissipation rate equation:

$$\rho u_i \frac{\partial \epsilon}{\partial x_i} = C_{1\epsilon} \frac{\epsilon}{k} \mu_t S^2 + \frac{\partial}{\partial x_j} \left[ \alpha_\epsilon \mu_{\text{eff}} \frac{\partial \epsilon}{\partial x_j} \right] - C_{2\epsilon} \rho \frac{\epsilon^2}{k} - R \quad \dots (3-7)$$



The values of the model's constants are as follows:  $C_{1\epsilon}=1.42$  and  $C_{2\epsilon}=1.68$ . The above equations were written under steady, incompressible flow without body forces.

**Table (3-4)** Turbulence models.

Case	I	II	III	IV	V
<b>turbulence models</b>	Zero equation	Indoor zero equation	Two-equation	RNG	Splart allmaras

### 3.3 Numerically simulated room types

#### 3.3.1 Simulation of a thermally insulated room

The interactive menu-driven interface of AIRPAK3.0.16 provides access to every function needed to create an AIRPAK3.0.16 model, computes a solution, and evaluates the outcomes. A thermally insulated room was built by AIRPAK3.0.16. The dimensions of the room, mixing ventilation system, and indoor and outdoor air conditions are shown in the

Tables (3-5), and (3-6). Fig. (3-1) to Fig. (3-4) show the insulated office room. Appendix (A-1) shows the cooling loads computed manually.

**Table (3-5)** Dimensions of the room's contents, (3×2.5×2.5) m.

Items	No.	Dimensions of the room and its contents,			Sensible heat [47]
		X(m)	Y(m)	Z(m)	
Persons	2	2.7, 0.3	0 , 0	2 , 0.5	75
PCs	2	0.3	0.3	0.3	60
door	1	1	2	2.5	0
Supply air diffuser	1	0.05	0.1	0.2	0
Exhaust air grille	1	0.05	0.1	0.16	0
lamp	1	Cylinder shape r=0.1 height=0.2			100

**Table (3-6)** Air parameters.

Temp air	Speed inlet air	RH	Flow rate	Turbulent intensity
17 °C	2.5 m/s	50%	43.7 l/s	10%

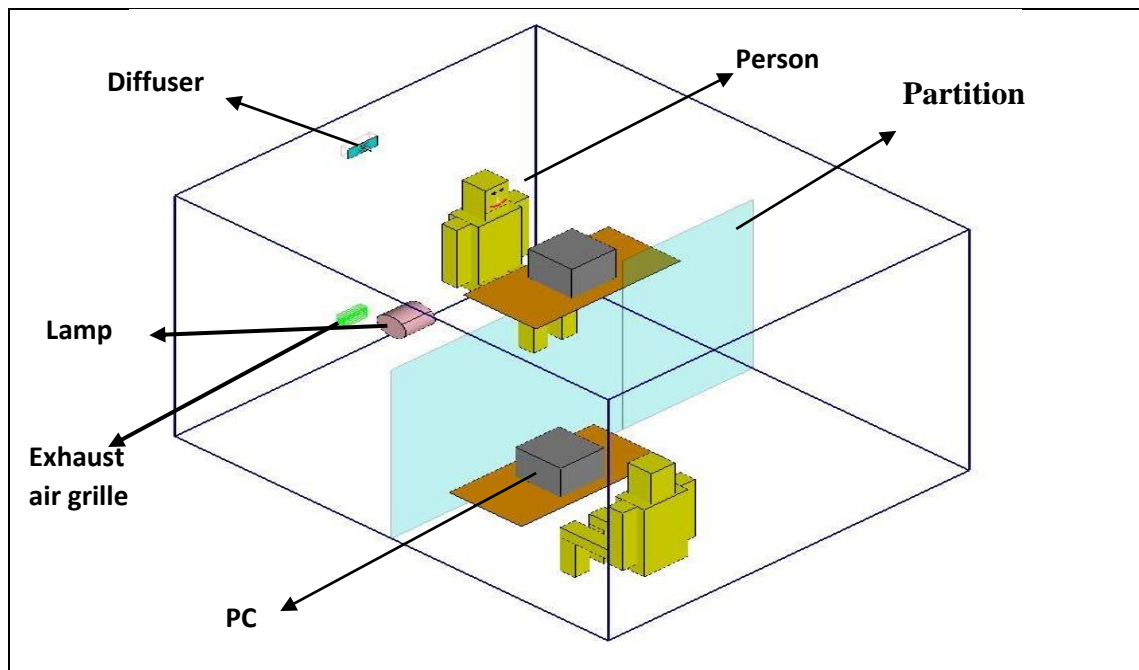


**Fig. (3-1)** ISO view of the thermally insulated office room.

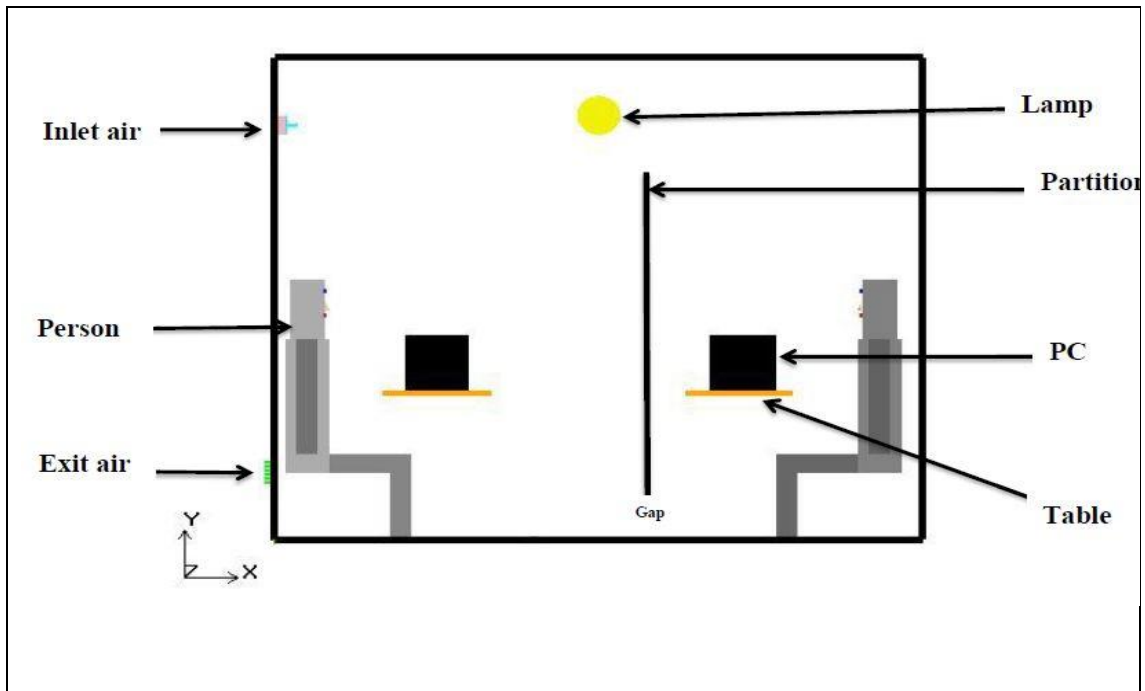


**Fig. (3-2)** Front view of the thermal insulated office room.

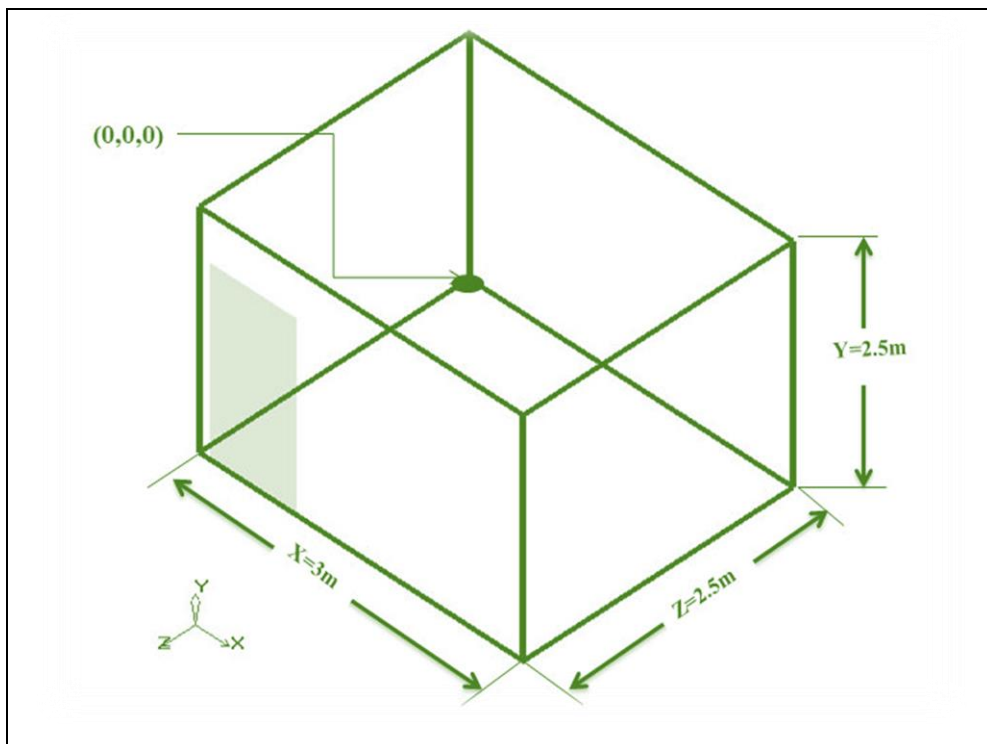


**Fig. (3-3)** Dimensions of the thermally insulated room.

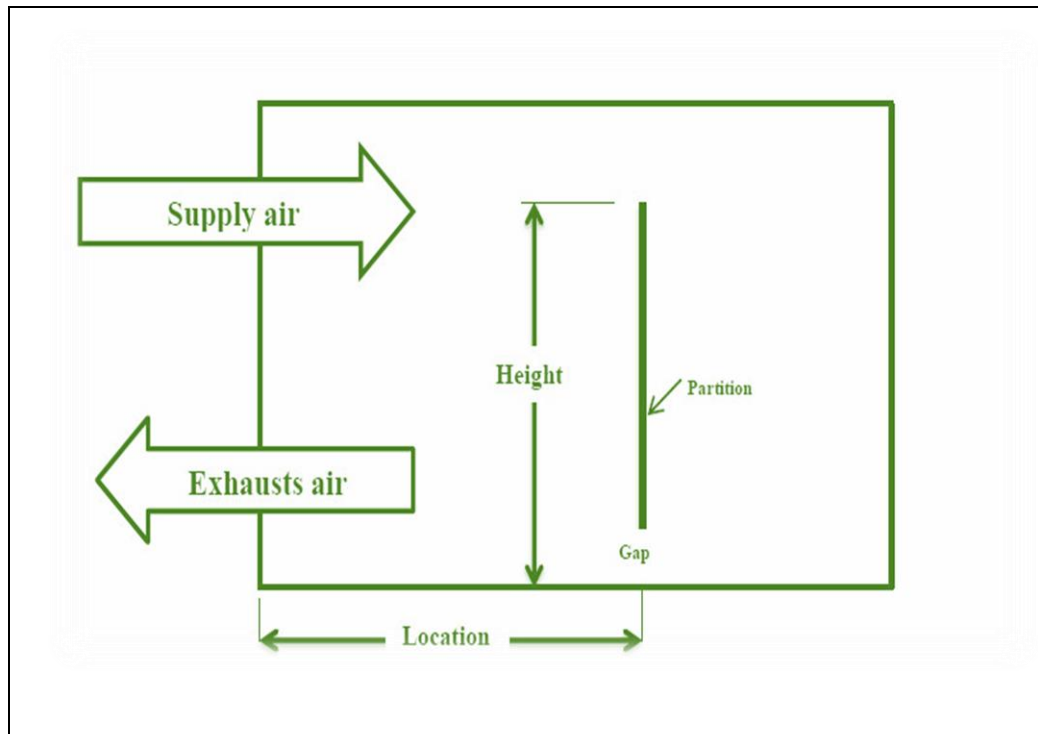


**Fig. (3-4)** Internal partition layout and ventilation scheme.

### 3.3.2 Non-Insulated Office Room (Case II):

A nonthermally isolated actual office room with (6 x 3.75 x 3) m was numerically studied. Using the (AIRPAK3.0.16) software to conduct the simulation by adopting the turbulence model (RNG), after conducting several tests on the rest of the test models. A real room was simulated at University of Babylon, College of Engineering, Department of Mechanical Engineering, where the room contains three persons who perform medium to simple tasks, and the room also contains three (PCs), a refrigerator, in addition to the presence of lighting in the ceiling. The room is not thermally insulated from the northern and southern walls, where the northern wall is exposed to external conditions and has a window, while the southern wall connects the room with the corridor. A mixing ventilation system is also included, glass and wood partitions were simulated inside the room, separating the seated employees, as listed in Table (3-8). Fig. (3-5) shows

the room that is not thermal insulated in the absence of the interior partition, while Figs. (3-6) to (3-9) show the test of the interior partitioning without gaps, where it's at a height of (0.7H) as well as the presence of the gap under the partition with a height (5% H), and (10%H). Appendix(A-2) shows the cooling load calculation, that computed by (HAP 4.9) .

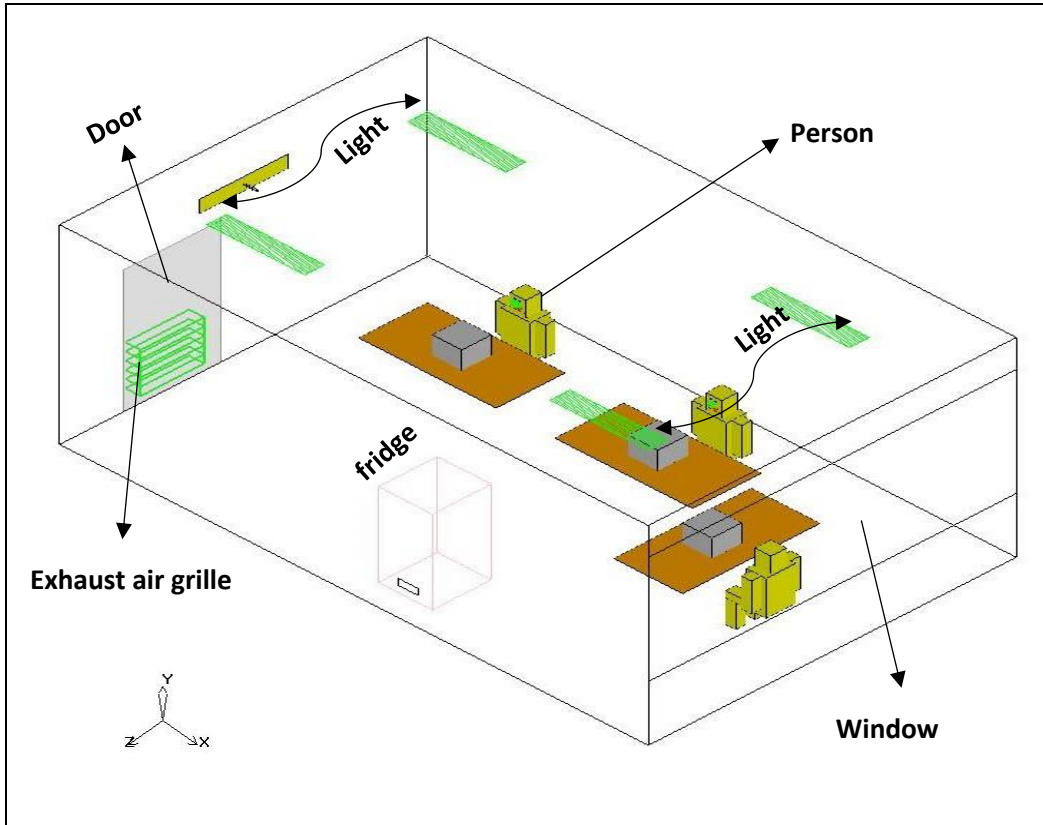
**Table (3-8)** Dimensions of the contents of the room and its sensible heat.

Items	No.	Dimensions (m)			Total Sensible heat (W) [47]
		X(m)	Y(m)	Z(m)	
<b>Person 1</b>	1	5.5	0	2	75
<b>Person 2,3</b>	2	3.7 , 1.7	0 , 0	0.7 , 0.7	75 per person
<b>PC 1</b>	3	0.3	0.3	0.3	60 per Laptop
<b>Table 1,2,3</b>	1	1	0.76	45	-
<b>Window</b>	1	6	1.75	3.75	-
<b>Door</b>	1	0	2.0	0.9	-
<b>Air supply diffuser</b>	1	0.1	0.2	0.9	-
<b>Exhaust air grille</b>	1	0.05	0.65	0.65	-
<b>Lights</b>	4	1	0.05	0.2	100 per light
<b>Refrigerator</b>	1	0.55	1.35	0.6	88

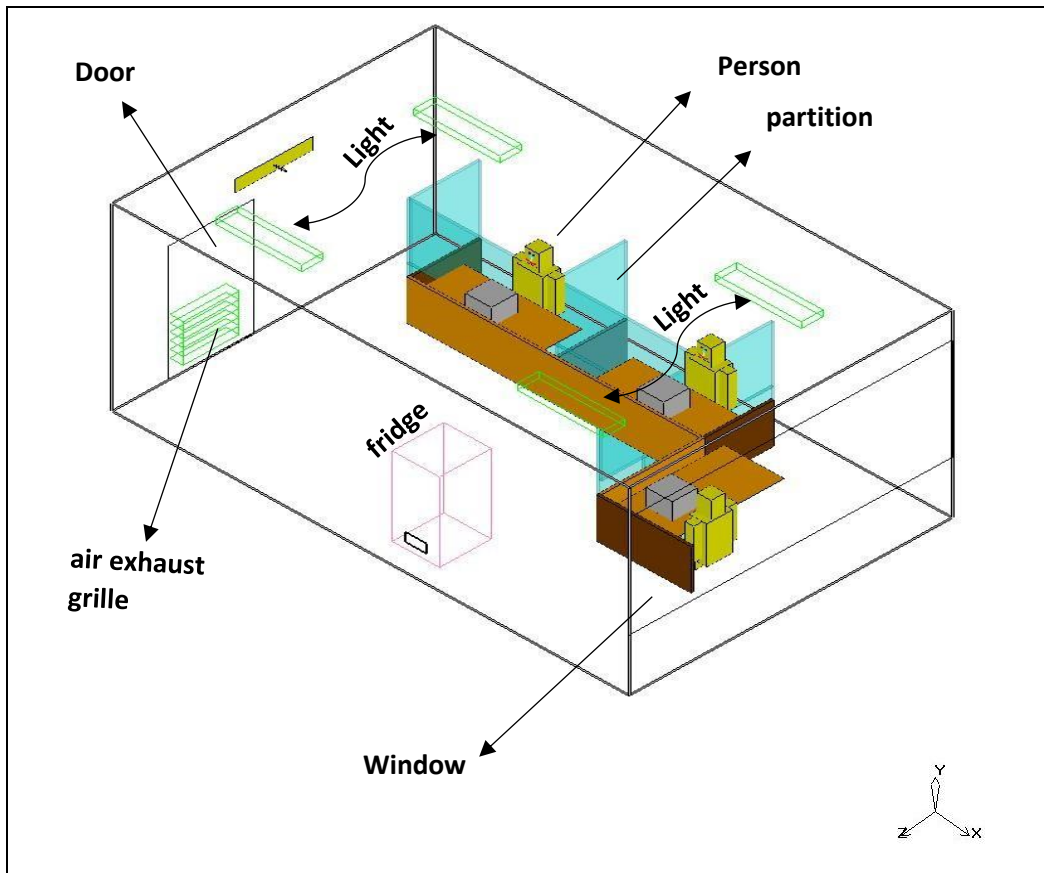
In Iraqi buildings, the walls are mainly formed from multi-materials. The thickness of the wall is (30 cm) and consists of four layers from inside to outside including, (gypsum plaster (2cm), cement plaster (2cm), common brick (24cm) and cement plaster (2cm) as shown in Fig. (3-10). Details of materials and thickness are described in Table (3-9).

**Table (3- 9)** Thermal properties of building materials and their thickness for walls and ceilings, [48].

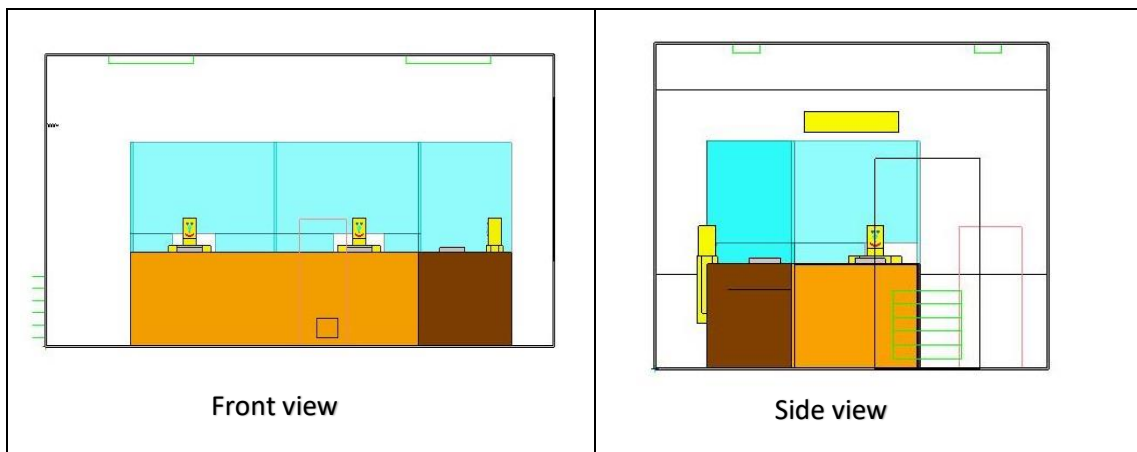
Material	Brick	Gypsum	Cement	Wood	Glass
Thickness(cm)	24	2	2	5	0.6
<b>K</b>	0.69	0.72	1.16	0.28	0.78



**Fig. (3-5)** Non-insulated office room before partitioning.



**Fig. (3-6)** Non-insulated office room after partitioning.



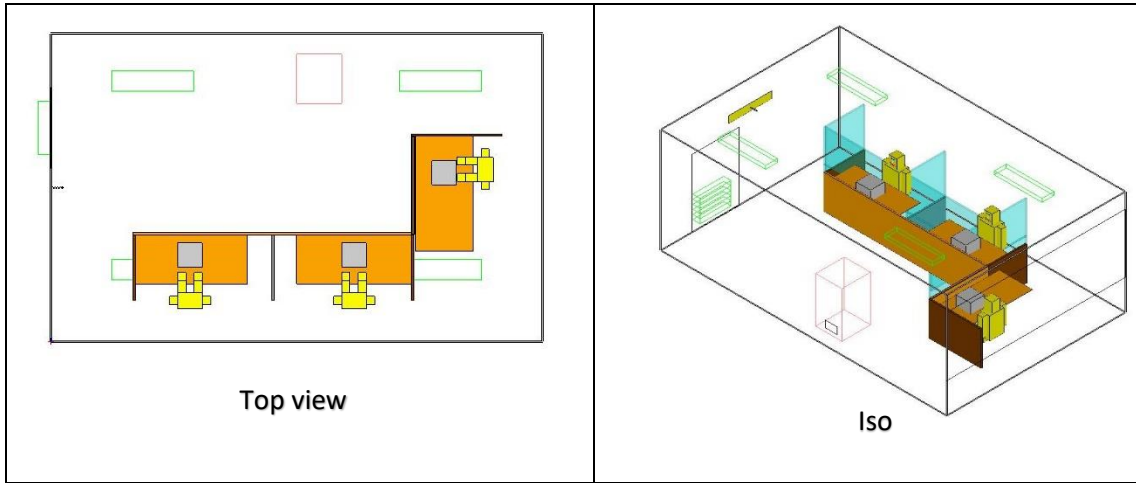


**Fig. (3-7)** Non-insulated office room partitioned without gap underneath.

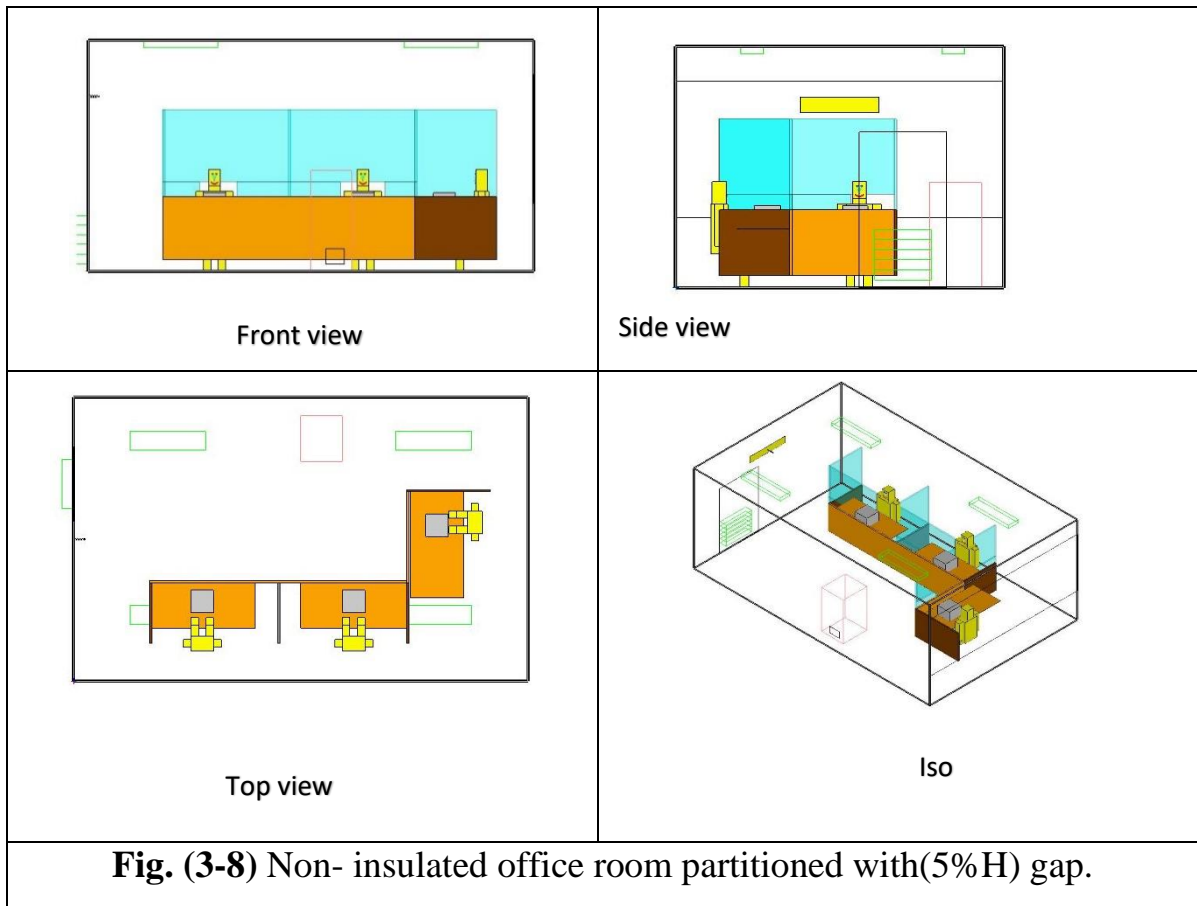


**Fig. (3-8)** Non- insulated office room partitioned with(5%H) gap.



**Fig. (3-9)** Non- insulated office room partitioned (10%H) gap.

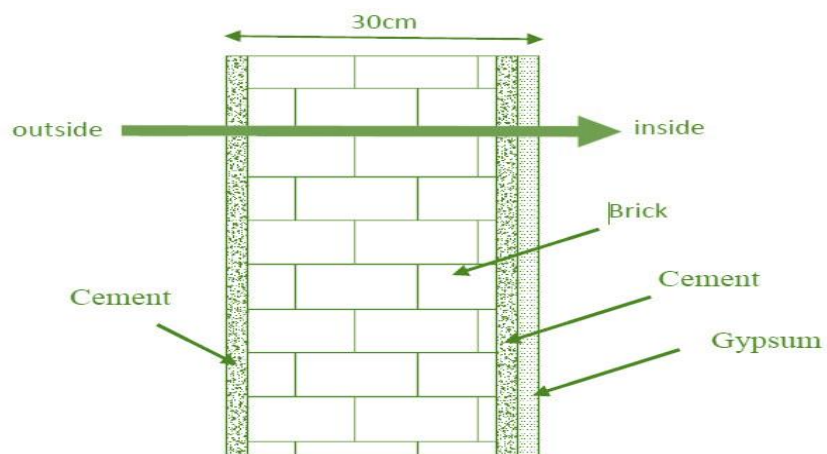
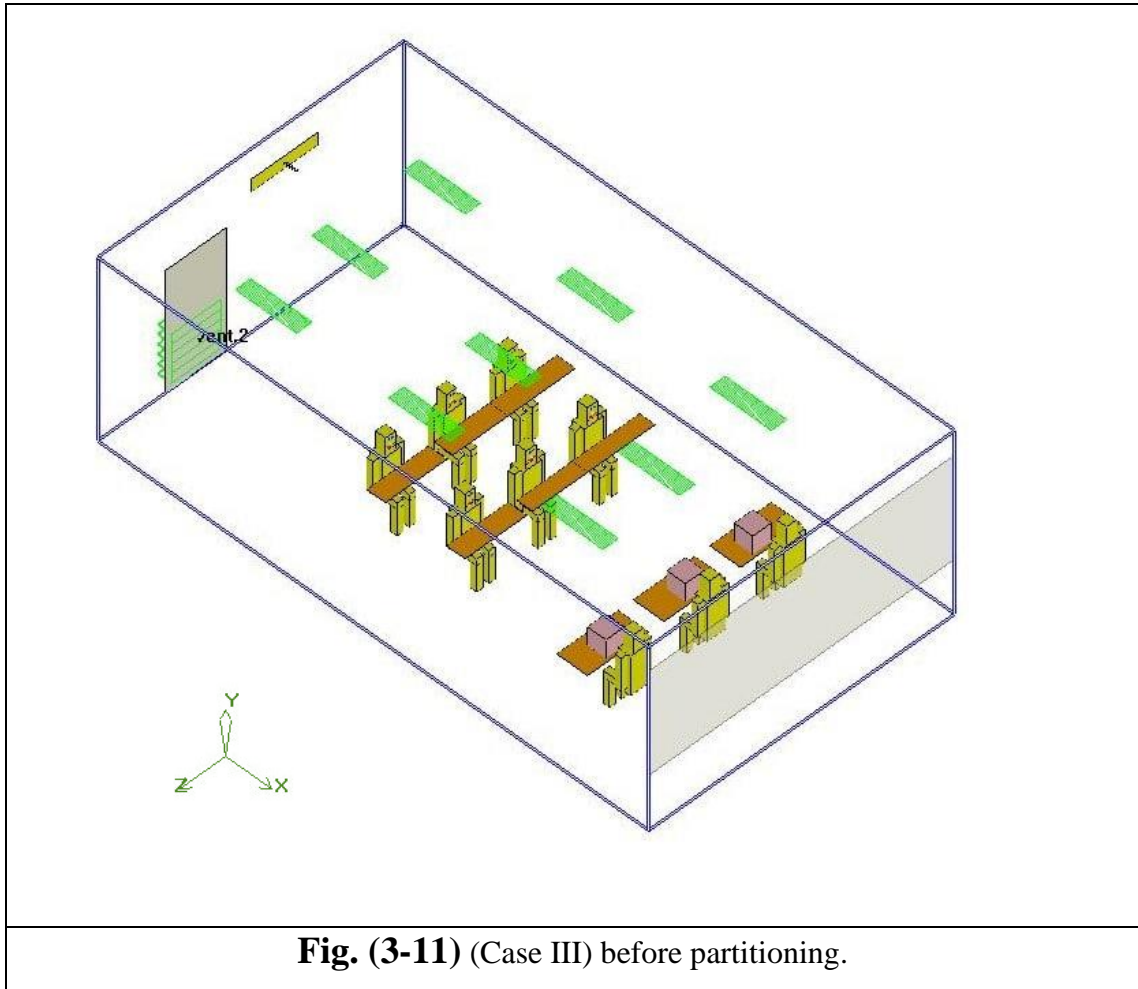


**Fig. (3-10)** Heat transfer through the side walls and their components.

### 3.3.3 Non-Insulated Office Room (Case III):

An exchange and financial transfer office was simulated using (AIRPAK3.0.16) software, where the dimensions of the office are (9×5×3) m as listed in Table (3-10) with walls that are not thermally insulated. Where

the northern wall contains a window which is exposed to external conditions, while the southern wall contains a door that connects the office with a corridor, the western, and eastern walls separate the office from other offices, it is considered thermally insulated as there is no heat flow through them. The office is located in Iraq and contains three employees. Its capacity is (9) persons. An internal partition has been set up separating the banking workers and the customers. The interior is made of glass and wood. As for the banking walls, they are made of building materials approved in Iraqi buildings. The office unit contains lighting and is also ventilated by a mixing ventilation system. Therefore, air comes in through a wall diffuser at the top of the southern wall, then it is drawn through the air outlets at the bottom of the wall, as shown in the Fig. (3-11). The cooling and ventilation loads were calculated for such case study (III) using the (HAP 4.9) program, as shown in Appendix (A-3) and all these values were entered into the (AIRPAK3.0.16) for the purpose of completing the simulation, since the turbulence model (RNG) has applied. By computing the thermal parameters ADPI, ADI, PMV, PPD,  $\varepsilon_t$  and  $\varepsilon_v$ , the study focused on indoor air quality and thermal comfort. The air velocity and temperature distribution were calculated by relying on the occupied zone levels of 0.1, 0.4, 0.8, 1.1, 1.4, and 1.8 meters, as shown in Fig. (3-12).



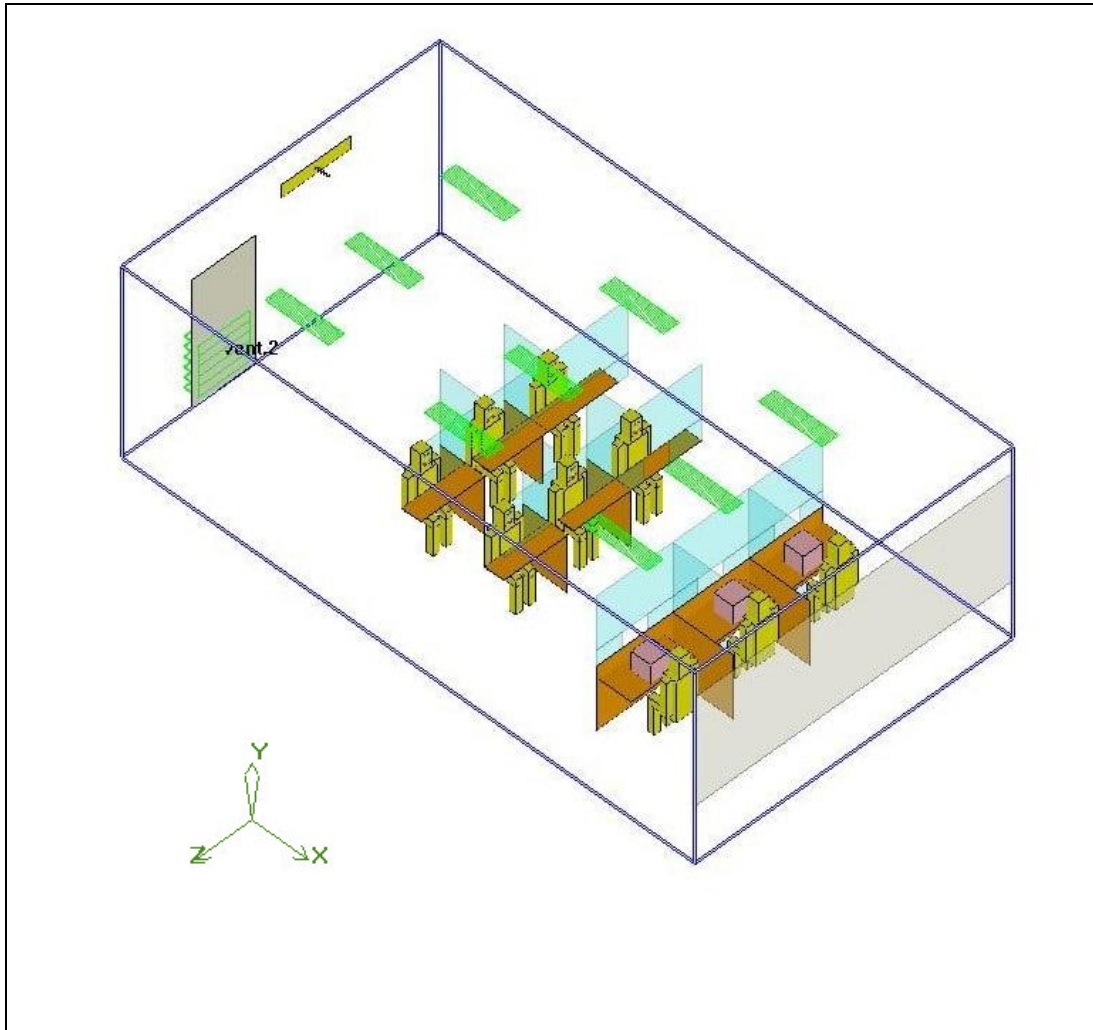


**Fig. (3-12)** (Case III) after partitioning.

**Table (3-10)** Dimensions of (Case III)

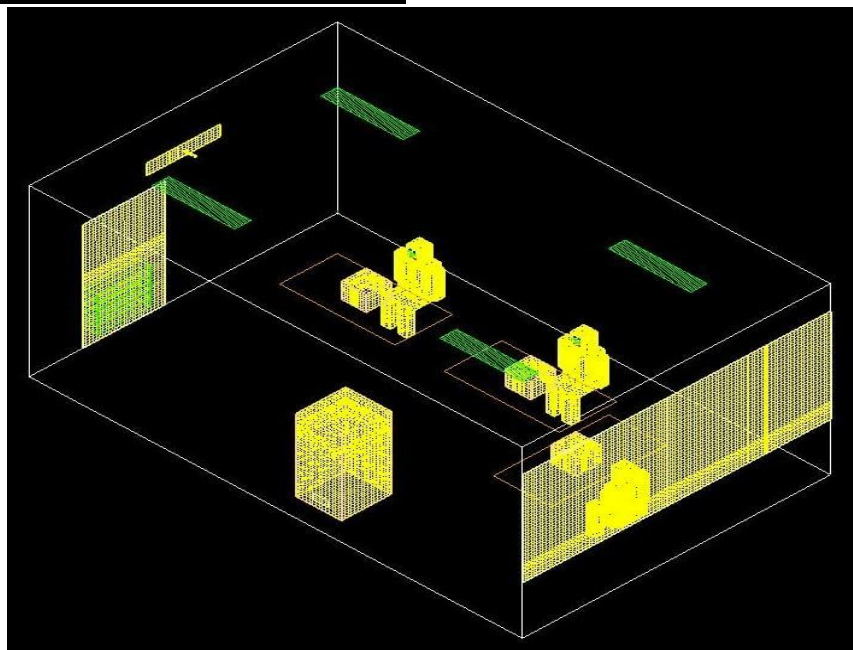
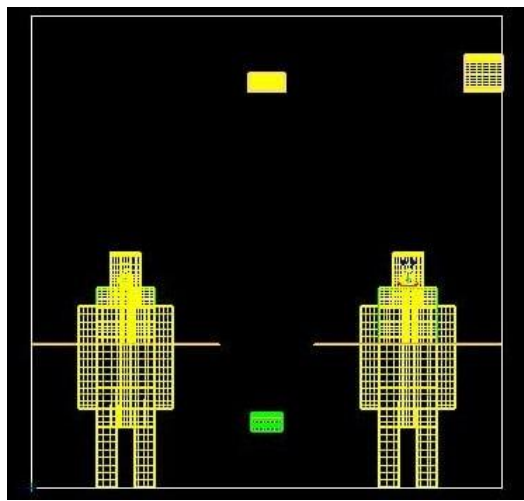
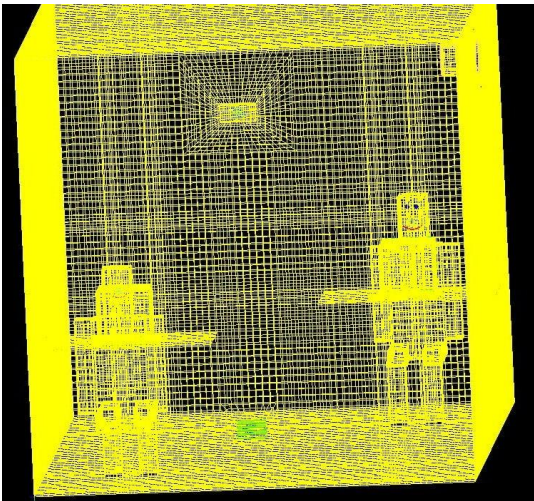
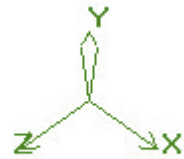
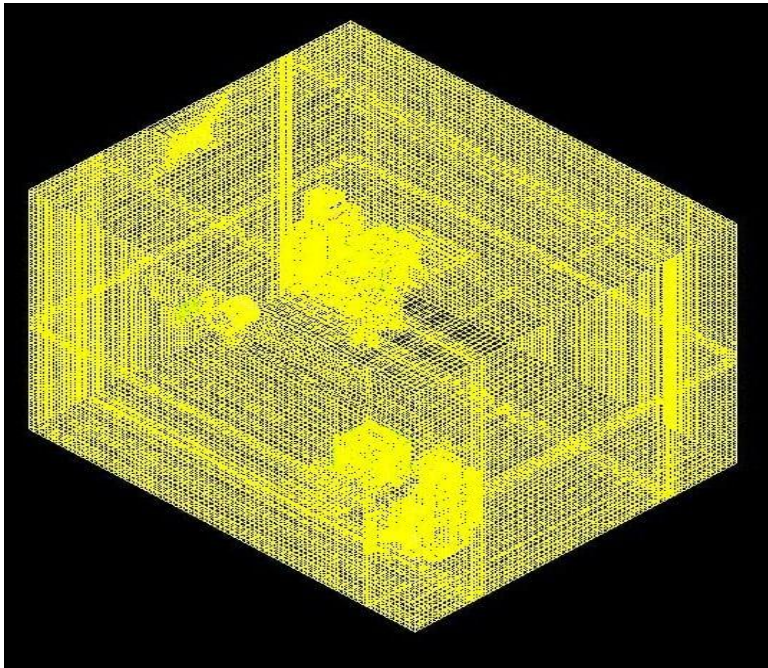
Items	No.	Dimensions of the room and its contents,			Sensible heat, [47]
		X(m)	Y(m)	Z(m)	
<b>Female manager</b>	3	7.5, 7.5, 7.5	0, 0, 0	1.25, 2.5, 3.25	75
<b>Female staff</b>	6	4.5, 4.5, 4.5	0, 0, 0	3.5, 2.5, 1.5	75
<b>(PCs)</b>	3	0.3	0.3	0.3	60
<b>Tables</b>	9	0.5	0.1	1	-
<b>Lights</b>	9	0.75	0.1	0.1	30
<b>Air supply opening</b>	1	0	2.5	0.85	
<b>Air exhaust grill</b>	1	0	0.8	0.8	
<b>Window</b>	1	9	2	5	
<b>door</b>	1	0	2	1	

### 3.4 Mesh generation:

A successful and precise solution requires an excellent computational mesh. The real result can be wrong if the whole mesh is too large. The computational cost could become unaffordable if the total mesh is too small. In conclusion, the mesh quality directly affects the cost and correctness of the solution. The (AIRPAK3.0.16) meshing technique is governed by a set of rules that dictate how each sort of object is to be meshed. To resolve the physics of the solution as optimally as possible, (AIRPAK3.0.16) employs a cocooning technique in which each object is meshed separately, as precisely as your specifications allow, In the current investigation, a strong and super-efficient personal computer specialized in simulation software was employed (Microsoft Surface Book 2), as stated in Appendix (B-2). In each situation, the optimal method for resolving a physics problem depends on the nature of the problem under investigation. In order to account for the heat and velocity gradients that are frequently present close to an object's borders, the mesh elements are smaller close to objects. In contrast, to save computing costs, the wide spaces between objects are meshed with large elements. There are three types of meshes available in (AIRPAK3.0.16) as show in Fig. (3-13)

**Table (3-11)** mesh approach.

<b>Edge line</b>	The edges of space in (x, y, and z dimensions) are meshing with an interval size of (0.04), and the double side ratio is 1. (1.16). As interval size, the edges of the exhaust grill and air supply diffuser are interwoven (0.05).		
<b>Faces</b>	The surfaces meshed as Hexa Cartesian type.		
<b>Volume</b>	Meshed as Hexa Cartesian type for interval size (0.04) in X and Z-direction, 0.04 in Y-direction		
<b>Mesh parameter</b>	Coarse	Mesh unit	meter



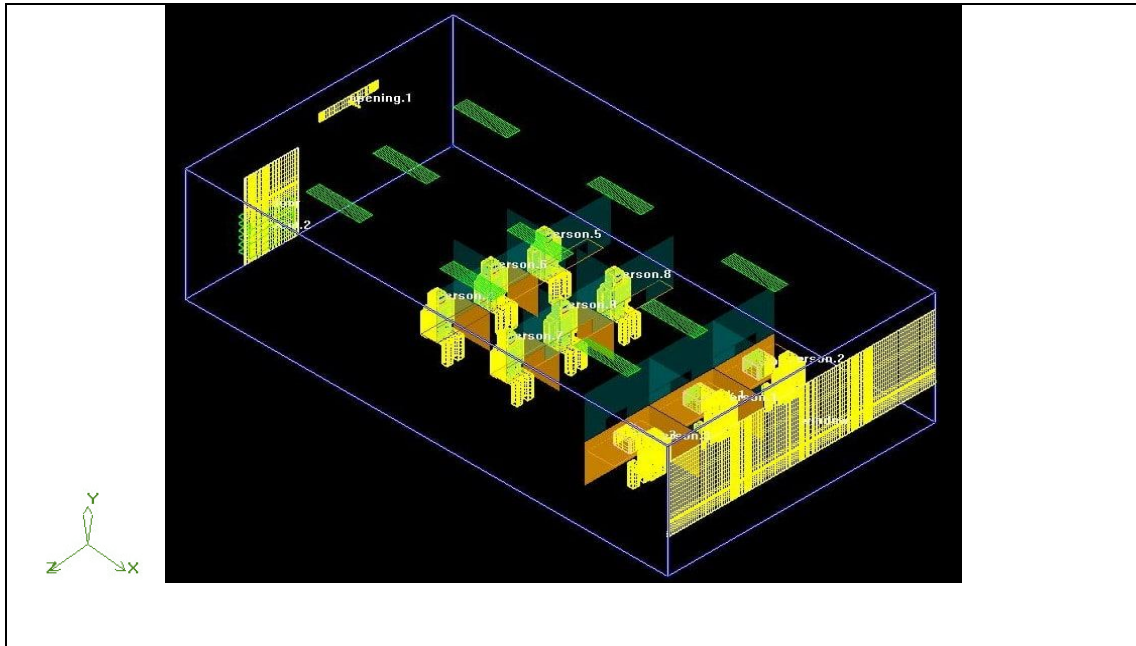
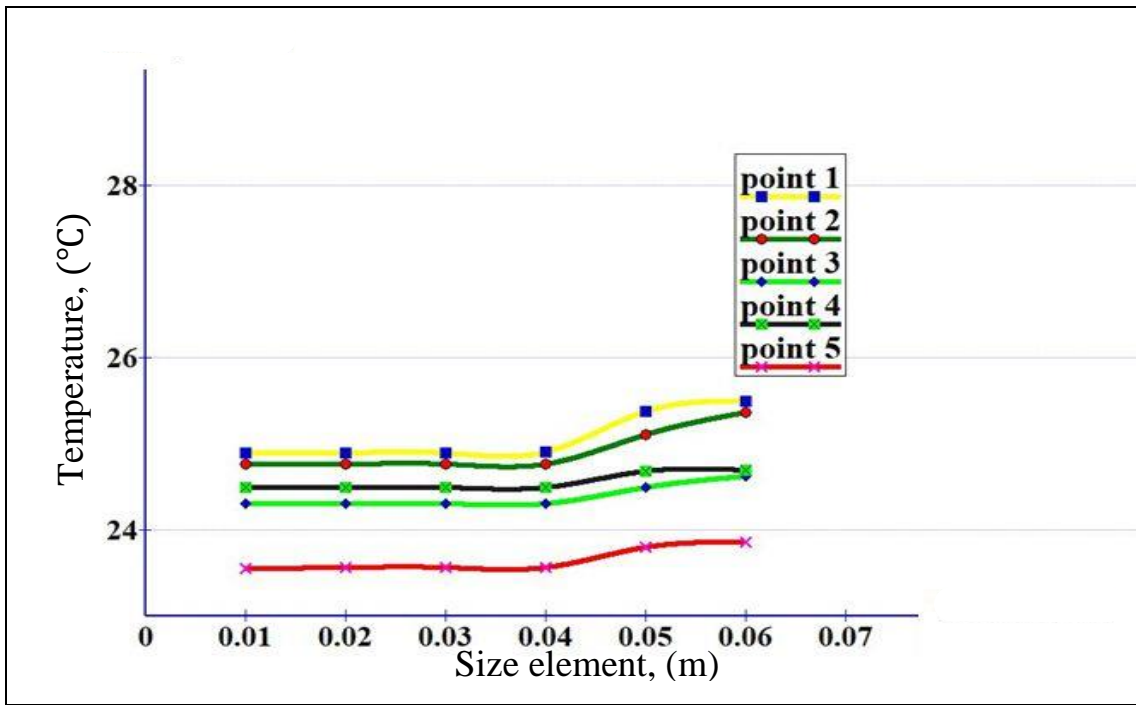


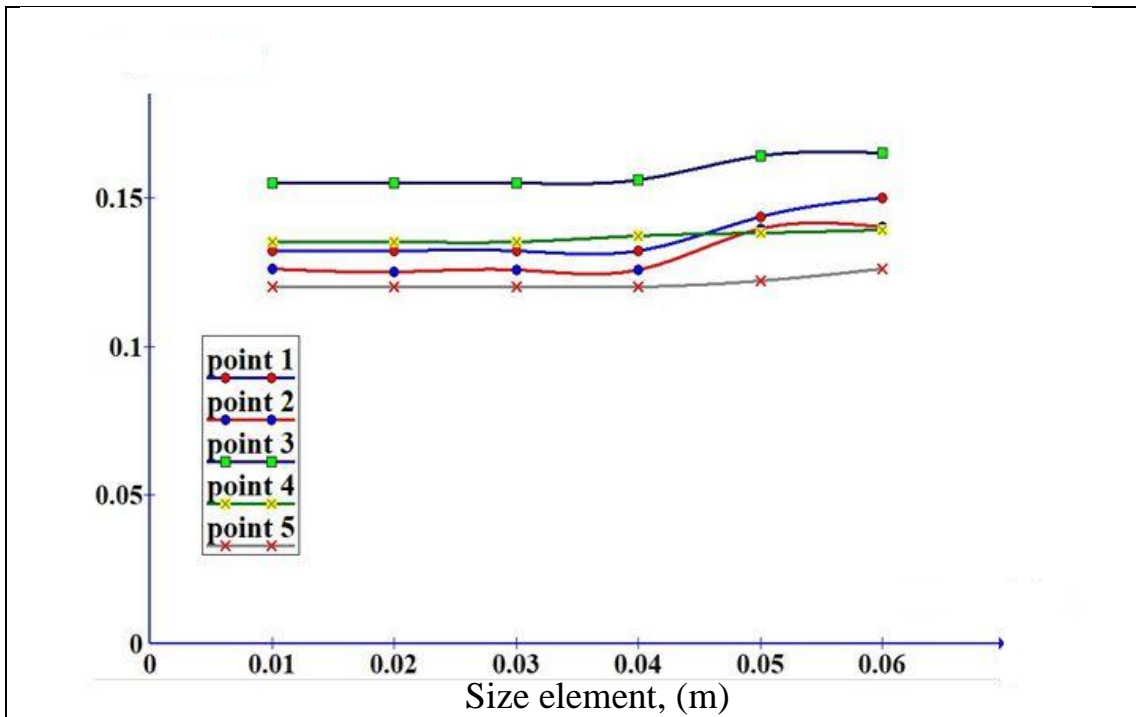
Fig. (3-13) mesh strategy

### 3.4.1 Mesh independence study

Choosing the right mesh in numerical solutions are the most important point to reach the most accurate and best results. Thus, the selection of the current mesh was made after several attempts. (AIRPAK3.0.16) allows to use the mesh types (Hexa unstructured, Hexa Cartesian, Tetra and Mesher HD) that are shown in the table below, where the type (Hexa cartesian) was chosen based on several tests that performed depending on the average room temperature to choose the appropriate mesh which is found that at elements (0.04) and above, the average temperatures inside the room is stabilized. The correctness of choosing the type of network as well as the most appropriate dimensions are verified, depends on each of the five temperatures at five locations  $P_1$  (0.5,0.5,1.25),  $P_2$  (0.5, 1.8, 1.25),  $P_3$  (0.5, 1.1, 1.25),  $P_4$ (0.75, 1.1, 0.5), and  $P_5$  (2.75,1.1, 0.5) since  $P_1$ ,  $P_2$ , and  $P_3$  are in front of the supply and exhaust air grille, while  $P_4$  and  $P_5$  in front of the persons shown in Fig. (3-14) and (3-15).



**Fig. (3-14)** Temperature profiles for five different size elements.



<b>Fig. (3-15) Speed profiles for five different size elements</b>
--

### 3.5 Theoretical Analysis

#### 3.5.1 Isothermal room

To calculate the required airflow rate in the current work, the following are calculated [49],[50].

**1- Heat of ventilation ( $Q_V$ )** sensible heat associated with ventilation air :

$$Q_V = 1.22 \times V_{VENT} \times [T_o - T_i] \quad (W) \quad \dots (3-8)$$

$V_{vent}$ =Ventilation air flow rate,  $T_o$ = Temperature outside the room,

$T_i$  = Temperature inside the room

**2- Heat due to infiltration**

$$Q_V = 1.22 \times V_{inf} \times [T_o - T_i] \quad (W) \quad \dots(3-9)$$

Where:  $V_{inf}$ = Air infiltration rate.,

$$V_{INF} = \frac{N \times V_{volume}}{3600} \quad \dots (3-10)$$

$N$ = Air change per hour

**3- Total heat (heat load) ( $Q$ )** : It is the total heat load of the room contents, (W)

$$Q_{total} = 2Q_{person} + 2Q_{Computer} + Q_{lamp} + Q_V \quad \dots (3-11)$$

**4- Mass flow rate  $\dot{m}$**  : It is calculated by using the following equation, [4]

$$Q_{total} = \dot{m} \times cp \times \Delta T \quad \dots (3-12)$$

Where,  $\Delta T = (T_{room} - T_s)$  is the difference in temperature inside the room and the supply air temperature.

$cp = 1.005$  kJ/kg.K , specific heat of the air at constant pressure.

**5- Air volumetric flow rate  $Q_s$** : It is calculated by using the equations, where the unit of  $Q_s$  is ( $m^3/s$  or  $l/s$ );

$$Q_s = \frac{\dot{m}}{\rho} \quad \dots (3-13)$$

$\dot{m}$  is the mass of airflow rate ( $kg/sec$ ), and  $\rho$  is the density of air ( $kg/m^3$ ).

**6-Area of Diffuser** Calculation of the area of the diffuser (MV ventilation) as follows:

$$A_s = \frac{Q_s}{U_x} \quad \dots (3-14)$$

Where: ( $A_s$ ) is the diffuser's area and ( $U_x$ ) is the speed of the air [ $m/s$ ]

### 3.5.2 Non-Isothermal Room

The equations that are entered to the simulation software in order to perform the numerical simulation and provide the area of the air diffuser, the speed, temperature, and amount of supply air, [49], and [50] are:

$$Q = U \times A \times CLTDc \quad \dots (3-15)$$

$$U = 1/Rth \quad \dots (3-16)$$

$$R_{th} = \frac{1}{h_i} + \frac{x_1}{k_1} + \dots + \frac{1}{h_o} + \frac{x_n}{k_n} \quad \dots (3-17)$$

For walls:

$$CLTDc = (CLTD + LM) \times K_c + (25.5 - T_i) + (T_m - 29.4) \quad \dots (3-18)$$

$$T_m = T_o - DR/2 \quad \dots (3-19)$$

For windows:

$$CLTDc = CLTD + (25.5 - T_i) + (T_m - 29.4) \quad \dots (3-20)$$

The heat is also transferred through the glass windows by radiation and is calculated as follows

$$Q_r = A \times SC \times SHG \times CLF \quad \dots (3-21)$$

The corridor temperature is calculated by the following equation:

$$T_{\text{corridor}} = T_i + \frac{2}{3}(T_o - T_i) \quad \dots (3-22)$$

$$\text{For doors: } Q = U \times A \times \Delta T \quad \dots(3-23)$$

### 3.6 Numerical cases setup

Heat removal effectiveness ( $\varepsilon_t$ ) and contaminant removal effectiveness ( $\varepsilon_c$ ) are defined as a ventilation system's ability to remove heat and pollutants produced inside from a ventilated room as stated by.

$$\varepsilon_t = \frac{T_o - T_i}{T_m - T_i} \quad \dots (3-23)$$

$$\varepsilon_v = \frac{C_o - C_i}{C_m - C_i} \quad \dots (3-24)$$

Where (T) denotes the air temperature ( $^{\circ}\text{C}$ ), (C) is the contaminant concentration in part per million (PPM), and (o, I) and (m) are the outflow, inlet, and mean values in the occupied zone prospectively, Appendix(B-1) shows the efficiencies calculations.

#### 3.6.1 Working fluid properties

It is essential to know the properties of materials in the simulation modeling process due to its great importance in obtaining an accurate and reliable solution, as well as reducing the number of iterations required for convergence, i.e., getting convergence in the shortest possible time. Table (3-11) shows the values of the air properties used in the simulation. Air is the working fluid used in this work, and it is assumed that the flow is three-dimensional, incompressible, steady-state, and turbulent. The properties of air which concerned as species shown in Fig. (3-16).

**Table (3-12)** Properties of air at (24°C), [48].

Parameter	Density (Kg/m <sup>3</sup> )	Thermal Conductivity (W/m.K )	Specific Heat (J/kg.K )	Viscosity (kg/m.s)
<b>Air</b>	1.189	0.0258	1005	1.894*10 <sup>-5</sup>
<b>CO<sub>2</sub></b>	1.78	0.016	871	1.495*10 <sup>-5</sup>

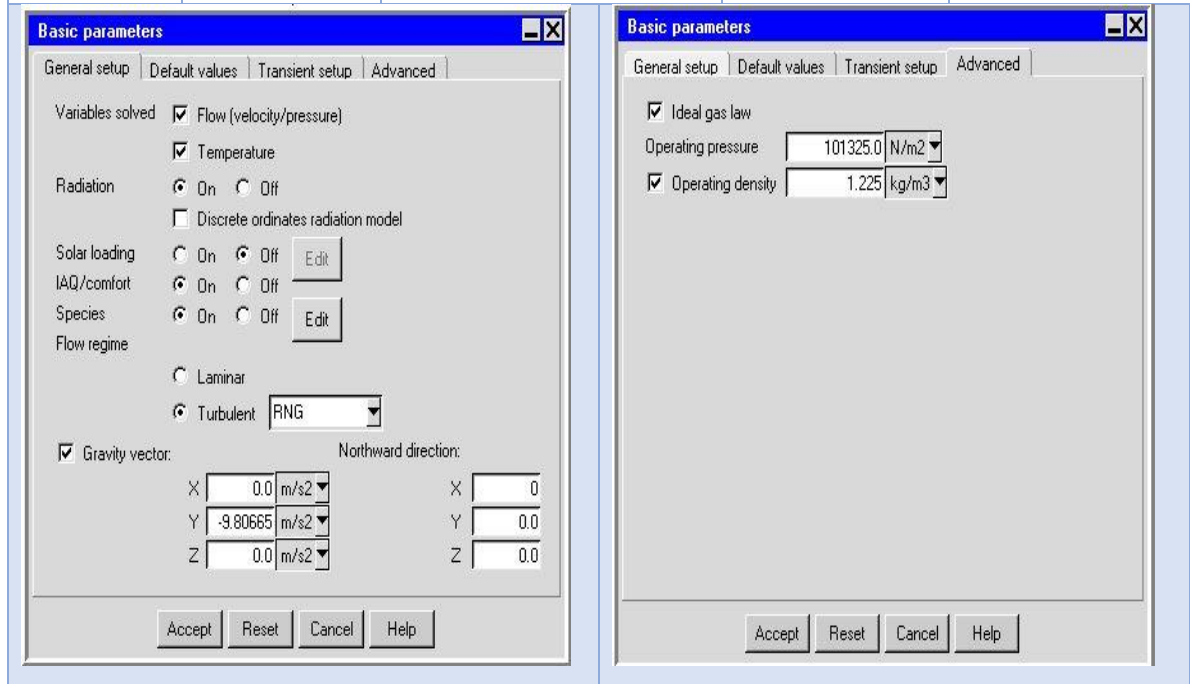


**Fig. (3-16)** Basic parameters by (AIRPAK 3.0.16)

### 3.6.2 Boundary conditions of momentum

Boundary conditions significantly influence a CFD simulation's ability to produce accurate results for a problem solved. In the current study, three different types of wall boundaries, velocity inlets, and outflows are assumed in a (CFD) simulations, these circumstances are listed in Table (3-13) to (3-15). As illustrated in Fig. (3-17), wall and surface limits with heat transfer, temperature, species, convective heat transfer coefficient, radiance input options, and symmetry requirements. Isothermal walls made up the wall boundary. Due to the poor accuracy of the numerical findings, scaled residuals of error for several factors, including speed components,

continuity, and epsilon, must be determined. A specific heat flux or a constant temperature are two different thermal boundary conditions that might apply to external walls. The wall is automatically considered to have zero thickness in both scenarios.

**Table (3-13)** Boundary conditions of momentum.

Part	Type	Condition of momentum	
		Motion of wall	Condition of shear
<b>Persons no. 3</b>	Wall	Stationary	No Slipping
<b>Computer no.2</b>			
<b>floor, Sidewalls, ceil, Tables no.2 and lump no.1</b>			
<b>Supply air diffuser (MV)</b>	Velocity inlet	magnitude, normal to the boundary	
<b>Extract air grill</b>	Pressure outlet	-Gauge Pressure = (0 Pascal), [constant]. - Backflow direction specification method: (normal to boundary).	

**Table (3-14)** Illustrates the insulated office room's boundary conditions (Case I).

Parts condition	Boundary	Equation
<b>Rectangle air supply diffuser</b>	Inlet velocity	$U=U_x$
<b>East, south floor and ceil Walls</b>	No penetration and no slip condition	$U=0$
<b>North and west walls, window and door, sidewalls, ceil and floor</b>	Zero heat flux	$\frac{d_q}{d_x} = \frac{d_q}{d_y} = \frac{d_q}{d_z} = 0$
<b>Exhaust grill</b>	Constant air flow rate	$V_{in}^{\circ} = V_{out}^{\circ}$
<b>Occupants, computers, and lights</b>	Constant heat sources	$q=\text{constant}$

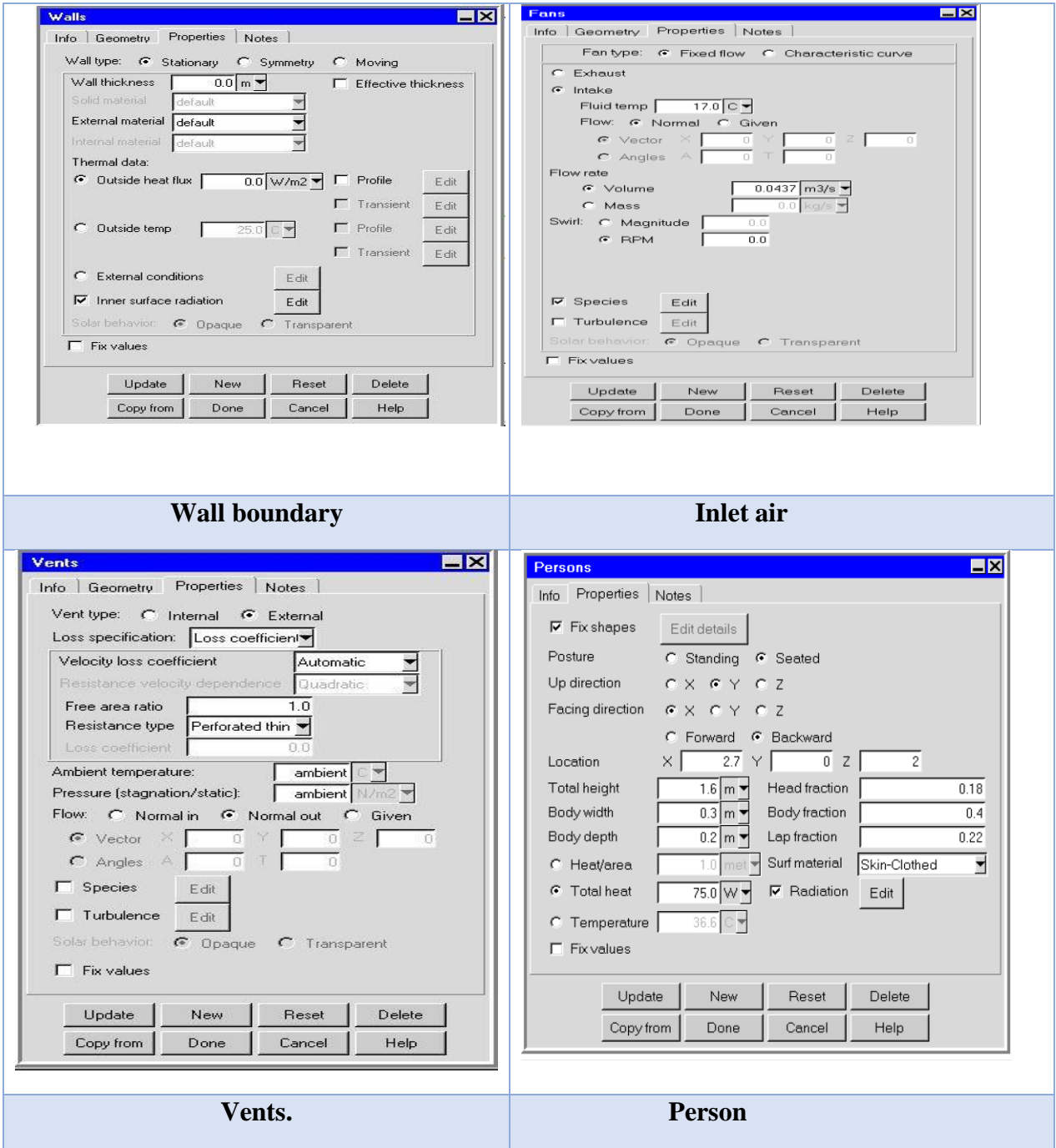


**Fig. (3-17)** Boundary conditions by (AIRPAK3.0.16).

**Table (3-15)** Boundary conditions for non- insulated office rooms (Case), and (Case III).

Parts	Boundary	Equations
<b>Rectangle air supply diffuser</b>	inlet velocity	$\vec{u} = \vec{u}_x$
<b>East, west floor and ceiling Walls</b>	no penetration and no slip condition	$\vec{u} = 0$
<b>North, and south walls, door, and window</b>	constant heat flux	$\frac{d_q}{d_x} = \frac{d_q}{d_y} = \frac{d_q}{d_z} = C$
<b>Side walls, ceiling and floor</b>	Zero heat flux	$\frac{d_q}{d_x} = \frac{d_q}{d_y} = \frac{d_q}{d_z} = 0$
<b>Exhaust air grille</b>	Constant airflow rate	$V_{in}^{\circ} = V_{out}^{\circ}$
<b>Employees, PCS, and lights</b>	Constant heat sources	$q=c$

### 3.6.3 Solution Controls

Advanced solver setup allows selection of higher-order discretization schemes for more accuracy (recommended for test meshes). For the process of solution, the convection terms (momentum, turbulent kinetic energy, turbulent dissipation rate, and energy) are described by using the second-order upwind scheme and pressure as PRESTO (Pressure standard option) is used. A discretization scheme is used for the pressure-velocity coupling, as illustrated in the table (3-16). under-relaxation factors for improving convergence behavior on tougher problems. The step-change must be controlled in the initial variable values because there is nonlinearity in the flow equation to be solved by (AIRPAK3.0.16) By controlling (under-relaxation factors), it is controlled step change. These factors determine the

value of the decrease in the change step for the initial variable values during each iteration. Table (3-16) shows the under-relaxation factors used in the CFD simulation of the current work.

**Table (3-16) Solution methods**

Fluid flow (FLUENT)	Scheme	Pressure	Temperature	Momentum	Turbulent kinetic energy	Turbulent dissipation rate
<b>Solution methods</b>	discretization	Standard			Second-order	

**Table (3- 17) Factors of under-relaxation**

Properties	Under-Relaxation factor	Properties	Under-Relaxation factor
<b>viscosity</b>	1	Pressure	0.3
<b>Momentum</b>	0.7	Turbulent Kinetic Energy	0.5
<b>Temperature</b>	1	H2O	1
<b>Body force</b>	0.1	Turbulent Dissipation Rate	0.5

### 3.6.4 Solution initialization and convergence and residuals

In any iterative numerical solution, initial default variable values are necessary to start the iteration process. So, on, consequently, there must be an initial value that is assumed to be the default guess to begin the solution. Model initialization is also an essential factor for the rapid convergence of solutions. Sometimes the running program needs a long time, and it may be very long, sometimes the convergence never occurs, and the reason for this is due to the weakness of the assumed initial values. numerical forms of governing equations (momentum, energy, etc.) are satisfied within a

specified tolerance (convergence criteria). solution no longer changes with more iterations. It is impossible to get ultra-accurate solutions while solving a problem numerically. Therefore, it is vital to establish the level of residual error that is considered acceptable for continuity, velocities, and energy equations. These limits of residual error scaled are listed in table (3-17). Until the solutions, depicted in Fig. (3-19), were stable, simulations were repeated to a degree of approximation ( $10^{-3}$ ).

**Table (3-18)** residual error.

Equation	Residual error	Equation	Residual error
Continuity	$1 \times 10^{-3}$	H <sub>2</sub> O	$1 \times 10^{-3}$
X-velocity	$1 \times 10^{-3}$	K	$1 \times 10^{-3}$
Y- velocity	$1 \times 10^{-3}$	E	$1 \times 10^{-3}$
Z- velocity	$1 \times 10^{-3}$	Energy	$1 \times 10^{-6}$

### 3.7 Indoor Air Quality:

Poor indoor air quality is practically associated with the term "sick building syndrome." The absence of fresh air and inadequate ventilation systems in these buildings are significant contributing factors. There are many other forms of contaminants in indoor air, in addition to those that are brought into a building by ventilation air and are produced externally and come from sources such boiler flues, process output, exhaust from buildings' ventilation systems, and automobile emissions. Fanger discovered a relationship between the ventilation rate in ( $L s^{-1} \text{olf}^{-1}$ ) and the proportion of dissatisfied (PD) as shown in Fig. (3-19), [51], is calculated for each case study as stated in Appendix(B-3).

$$PD = 395e^{(-1.83\dot{v}^{0.25})} \quad \dots(3-25)$$

PD: is the percentage dissatisfied

$\dot{v}$ : is the rate of the outdoor air flow for 1 (olf). in ( $1 \text{ s}^{-1} \text{ olf}^{-1}$ ).

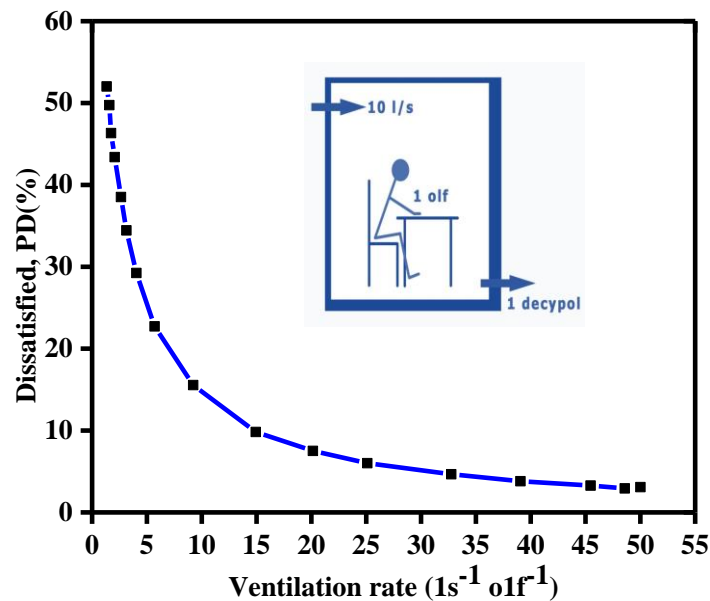


**Fig. (3- 19)** Ventilation rate as a function of the percentage of dissatisfaction for one (olf), [51].

**Table (3-19)** (Olf) values based on different things people do, [52].

Activity	No. of Olfs
Sedentary person (1met)	1
Active person (4 met)	5
Very active person (6 met)	11
Smoker person	25

### 3.7.1 Thermal Discomfort:

The unwelcome local cooling of the human body that is generated by movements of the air is referred to as draught, [53], [54]; It ranks among the most common complaints in warm or cooled buildings as well as in moving vehicles. The few early research on the impact of draught focused mostly on mean air speed, [55]. (SHRAE-55), and in winter (0.15 m/s) and

summer (0.25 m/s) are the maximum mean air speeds established by ISO 7730. A draught chart was created that shows the proportion of subjects that are unsatisfied with draughts in ventilated environments using Equ. (3-26).

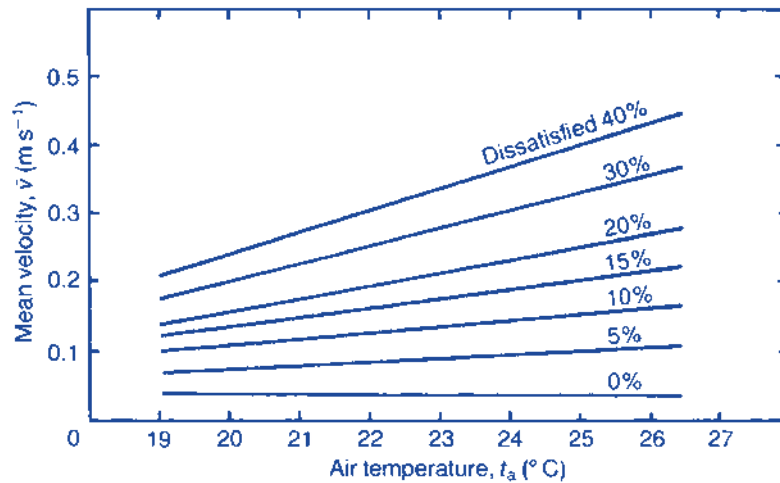


**Figure (3-20)** Draught chart for inactive individuals wearing standard indoor clothes,[56].

$$PD = 13800 \left[ \left( \frac{\bar{v}-0.04}{T_m-13.7} + 0.293 \right)^2 - 8.57 \times 10^{-4} \right] \quad \dots (3-26)$$

Where  $\bar{v}$ : is mean velocity of the air room in (m/s)

$T_m$ : is mean air temperature in (°C).

### 3.8 Predictions of Thermal Comfort Parameters:

#### 3.8.1 PMV and PPD:

Fanger has developed a simpler technique that is supported by extensive testing on human subjects in highly controlled environments and is predicated on a physical study of how the body exchanges heat with the environment. Estimated mean vote (PMV) for a person in thermal balance with their surroundings is calculated using the thermal comfort equation is appropriate. If the body isn't in equilibrium, it will need more physiological

effort to activate the effector mechanism needed to raise the skin's temperature and create a new thermal equilibrium. (Fanger) hypothesized that this strain is connected to the heat feeling at a particular activity level. By using the heat balance equation and his own experimental data, he determined an estimate for the intensity of feeling at different levels of activity. Fanger has established a temperature sensation index that is based on a seven-point psychophysical scale; Fanger found a correlation between the expected mean vote and the proportion of persons who were unhappy with the thermal environment. Plotted against PMV, this ratio is known as the anticipated percentage unsatisfied, see Fig. (3-21).

$$PPD = 5 + 20.97|PMV|^{1.79} \quad \dots(3-27).$$

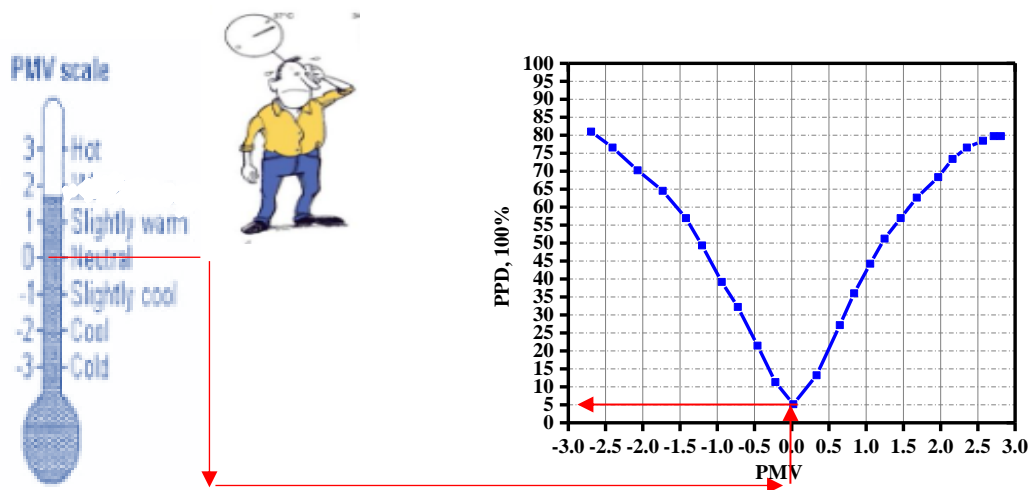


**Fig. (3-21)** Relationship between (PMV), and (PPD).

The type of clothes used for the simulation of employees were entered according to the gender in each case study (Case II) and (Case III) as shown in Table (3-20), and Table (3-21).

**Table (3-20)** Clo value for (Case II)

Clothes	CLO value
Singlet	0.04
Under wear, panties	0.03
T- shirt	0.09
Trousers (normal)	0.25
Socks	0.02
Shoes (thin soled)	0.02
Total	0.45

**Table (3-21)** CLO value for (Case III)

Clothes	CLO value
Singlet	0.04
Panties, and bra	0.03
Sweater	0.28
Light skirt (summer)	0.15
Nylon stocking	0.03
Shoes (thin soled)	0.02
Total	0.55

### 3.8.2 Air distribution index (ADPI) and (ADI):

Is the percentage of the occupied zone that falls within an acceptable speed and temperature range. This is found by calculating the effective draft temperature (EDT), which is the difference in air temperature and air speed. Thermal comfort studies were used to determine the (ADPI) equation's cooling thresholds and boundaries. Thus, there is an implied connection between ADPI and thermal comfort, [57]. (ADPI) was created primarily to combine ventilation with air distribution in order to provide a consistent air environment. 80 percent signifies that 20% of the total occupied space does not fall within the equation bounds as the majority does, whereas 100% ADPI results from a perfect mixing situation. As a result, a greater ADPI number indicates a higher level of mixing in the space.

$$\theta = (t_x - t_c) - 8(V_x - 0.15) \quad \dots (3.28)$$

Here:

$\theta$  : Temperature of effective draft (K)

$t_x$  = The dry-bulb temperature of the local air stream ( $^{\circ}\text{C}$ )

$t_c$  = Average (set-point) room dry-bulb temperature of a room ( $^{\circ}\text{C}$ )

$V_x$  = Centerline speed of the local airflow (m/s)

$$\text{ADP I} = (N_{\theta} * \emptyset / N) \times 100\% \quad \dots (3.29)$$

Where:

$\theta$  = Temperature of effective draft

$N_{\theta}$  = The number of measured points in the inhabited space "falls between  $-1.5 << +1\text{K}$

$N$  = Total number of points that were measured in the space "

The overall ventilation efficiency for pollutants as well as temperature, together with (PD) and (PPD), have indeed been combined to give latest figures for air quality and thermal comfort:

$$N_c = \frac{\varepsilon_c}{PD} \quad \dots (3-30)$$

$$N_t = \frac{\varepsilon_T}{PPD} \quad \dots (3-31)$$

in which ( $N_c$ ) and ( $N_t$ ) are air distribution factors for air quality and thermal comfort, [59]. Equations (3-30 and (3-31) provide formulas for PPD and PD, correspondingly. An effective ventilation system is the kind that achieves the highest possible values of ( $N_c$ ) and ( $N_t$ ).

The two factors can be merged into a single factor that measures an air distribution system's 'global' performance in producing indoor air quality and thermal comfort. Since (ADPI) is not really an indoor thermal index and has no correlation to (ACE, PMV, or PPD), which are often used as thermal comfort standards in the industry, [58]

$(N_c)$  And  $(N_t)$  can be merged in at minimum two ways to yield what Awbi and Gan, [30], referred to as a Ventilation Parameter (VP) or Air Distribution Index (ADI).

$$VP = \frac{N_c}{N_t} \quad \dots (3-32)$$

when:

(VP = 1.0) shows the presence of a balance in the distribution of pollutants and heat in the ventilated space.

(VP < 1) indicates that the efficacy for pollutants is significantly lower than that for temperature

(VP > 1) indicates the reverse.

But a (VP=1) is inadequate to guarantee that the ventilation system adequately distributes pollutants and heat.

Another criterion is used when both  $(N_c)$  and  $(N_t)$  are large.

$$ADI = \sqrt{N_c N_t} \quad \dots (3-33)$$

If a ventilation system is to be constructed with acceptable (PD) and (PPD) values of (10%), a decent air distribution system would have an (ADI) of (10).

# **Chapter Four**

## **EXPERIMENTAL WORK**

## Chapter Four

### EXPERIMENTAL WORK

This chapter describes number of practical experiments were carried out in an insulated room, which is located in one of the engineering workshop's gables at the University of Babylon. In practical experiments, readings were taken in May and June 2022. (Iraq climate in Hilla city). The actual purpose of the experimental investigation is to show how an interior partition affects the air quality and thermal comfort in an office unit. A variety of parameters were investigated and measured, air movement, temperature distribution, and carbon dioxide concentration, within the insulated office room were predicted. The results obtained under steady state; ASHRAE climate design conditions were adopted to determine the necessary information as listed in Table (4-1), [60].

**Table (4- 1)** Outdoor data for Iraq climate in summer, [60].

Experimental location	DMT, (°C)	(RH), %	DR, (°C)	Altitude (m)	Latitude N	Longitude E
Babylon	47.1	14	15.4	35	32.46	44.42

#### 4.1 Description of the Office Room

##### 4.1.1 General description

The tested room made of insulated material (sandwich panel,  $K=0.14\text{W/m.k}$ ), [61] for ceiling and walls, with dimensions of  $(3 \times 2.5 \times 2.5)\text{m}$ . The room contains two thermal manikins, in addition, two PCs were simulated in front of each manikin. Via boxes containing heat sources are used to simulate the dimensions of the (PC) and the heat emitted by it is (60 W). Furthermore, the room was illuminated by using lamp of (100W) and installed on the top western wall. A mixing ventilation system

comprised of a rectangular cross-sectional diffuser is used to supplied air in one direction. The diffuser was indeed installed on the north wall of the office room, just below the ceiling. Fig. (4-1), (4-2) show a simulation domain, the reality setup of the office room. The contents of the room and their locations are dimensioned in the Table (4-2).

**Table (4- 2)** Room configuration.

Item	Location (m)						Sensible heat(W) [47]
	Start(m)			End(m)			
	X	Y	Z	$\Delta X$	$\Delta Y$	$\Delta Z$	
<b>Office unit</b>	0	0	0	3	2.5	2.5	
<b>Rectangular Diffuser</b>	0	2.1	1.15	0.1	2.2	1.35	
<b>Exhaust grille</b>	0	0.3	1.17	0	0.4	1.33	
<b>Manikin no.1</b>	0.15	0	0.3	0.35	1.1	0.7	75
<b>Manikin no.2</b>	2.65	0	1.8	2.85	1.1	2.2	75
<b>PC_no.1</b>	0.6	0.76	0.35	0.9	1.06	0.65	60
<b>PC_no.2</b>	2.1	0.76	1.85	2.4	1.06	2.15	60
<b>lamp</b>	1.45	2.4	2.3	1.55	2.45	2.5	100
<b>PC table 1</b>	0.5	0.76	0	1	0	1	
<b>PC table 2</b>	2	0.76	1.5	2.5	0	2.5	

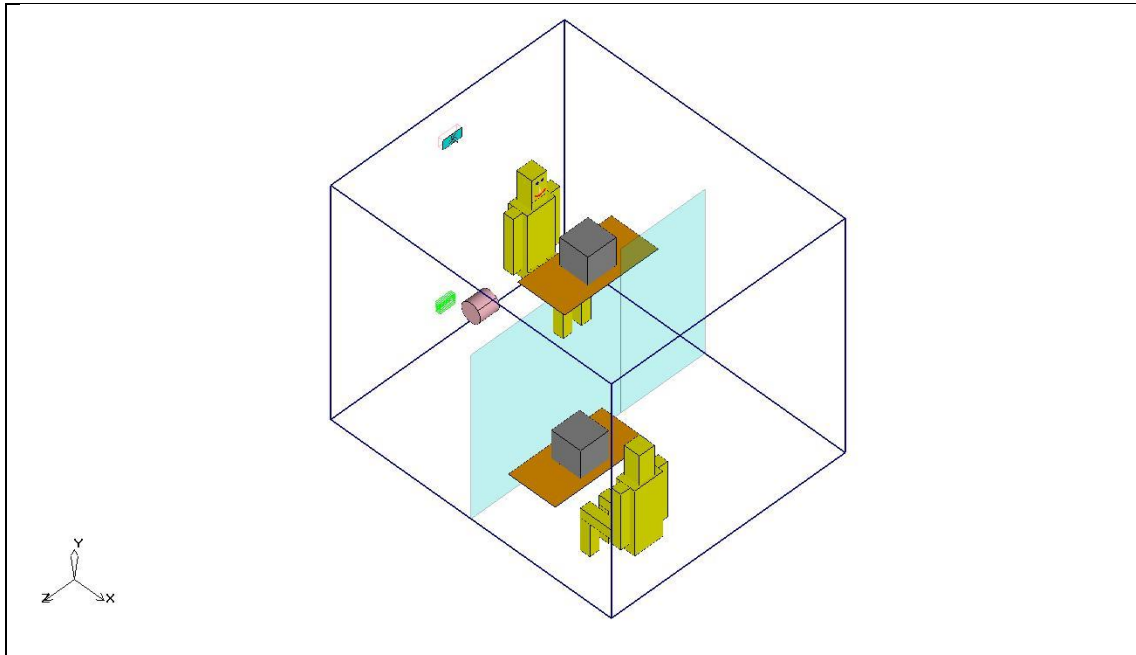


**Fig. (4- 1)** Simulation domain for the tested office room.

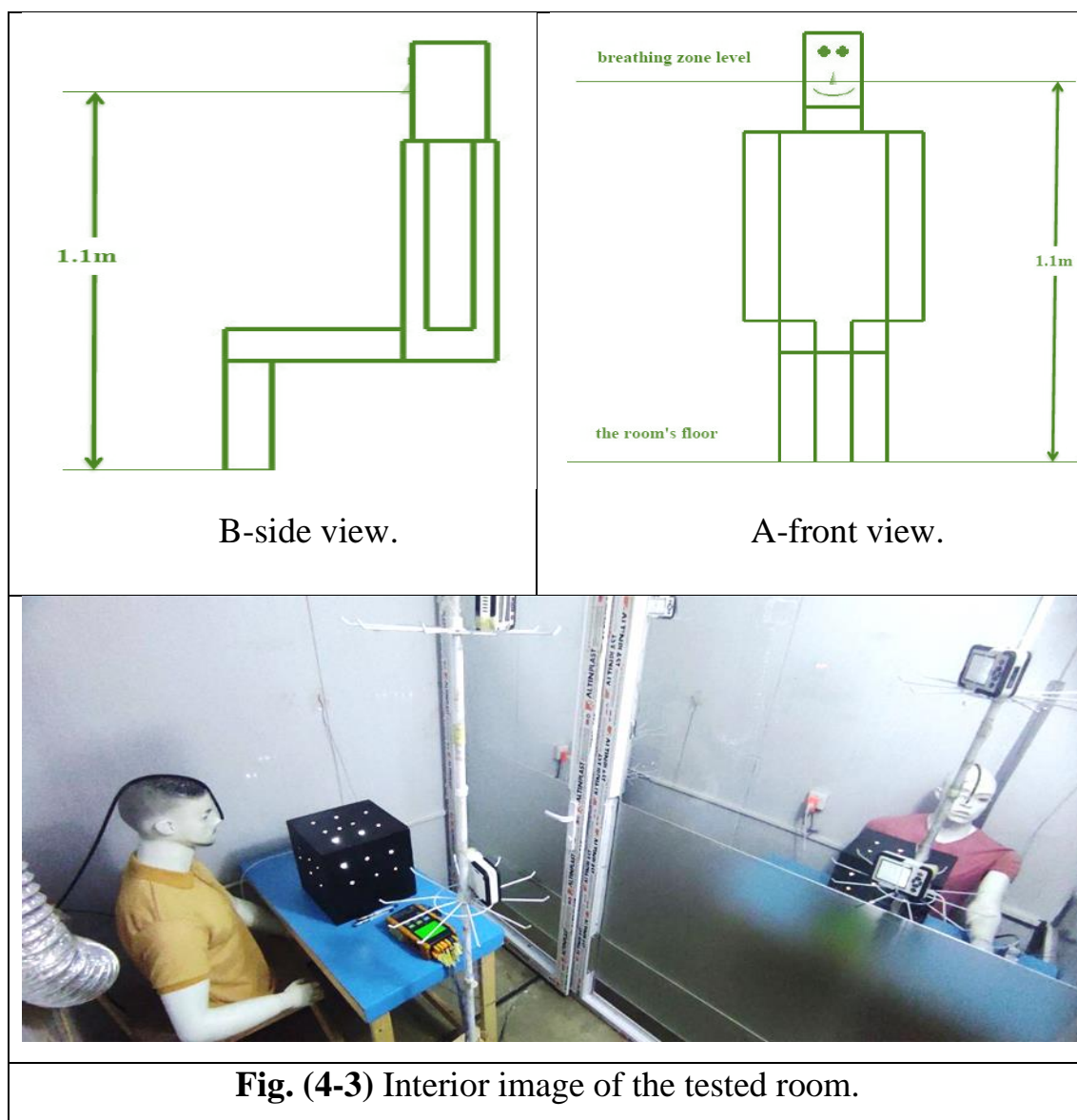


**Fig. (4- 2)** An exterior image of the test office room setup.

#### 4.1.2 Heat Sources

The heat sources in the test room include thermal manikins, (PCs), and an electrical lamp, all of which create sensible heat in a way that mimics reality. The heat sources inside the room are explained further below.

**1- Thermal Manikin:** The tested room contains two thermal seated manikins at breathing level(1.1m),[62], that simulate the human body in terms of temperature, height, and lateral and cross-sectional areas, an electric lamp was placed inside each thermal manikin to generate heat of approximately (75 W), [3] and [4].as shown in Fig. (4-3).



**2- Personal Computer:** Two personal computers are simulated using two wooden boxes with several holes in the same dimensions and the same sensible heat of the real computer by placing an electric lamp inside these boxes so as to generate heat about (60W) from each box in front of each manikin, as shown in Fig. (4 - 4).

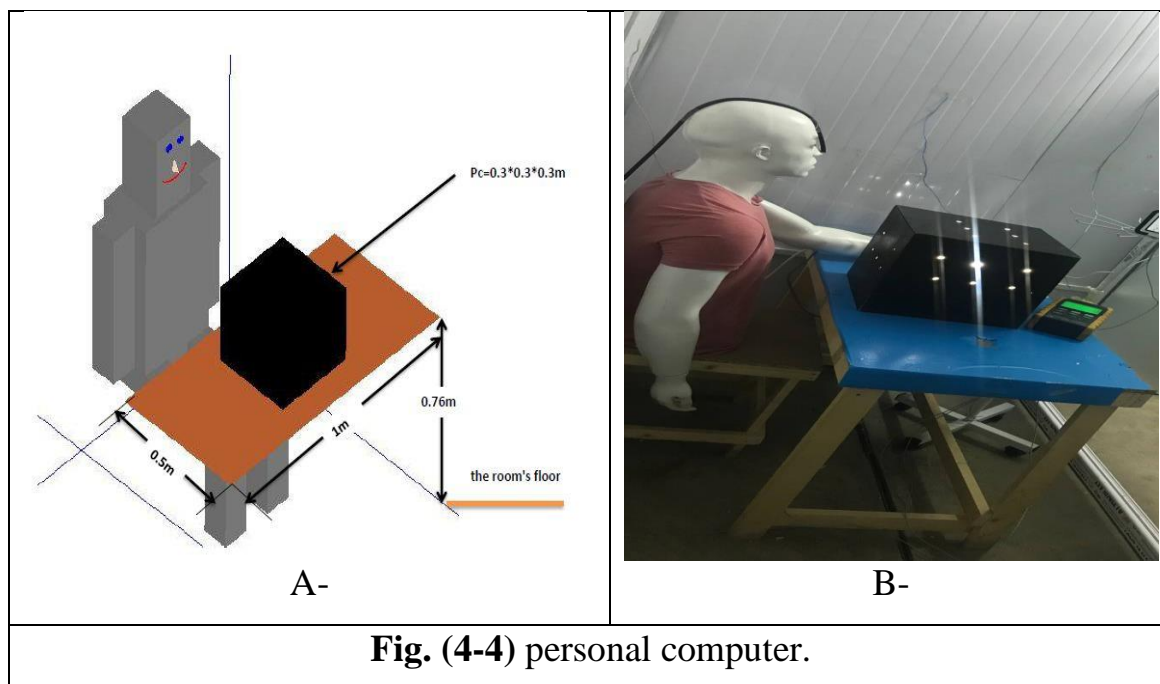


**Fig. (4-4)** personal computer.

3- **The Electric Lamp:** is one of the heat sources inside the tested office room, where an overhead electrical lamp (100W) was placed on middle of the western wall for lighting purposes.

#### 4.1.3 Air distribution system

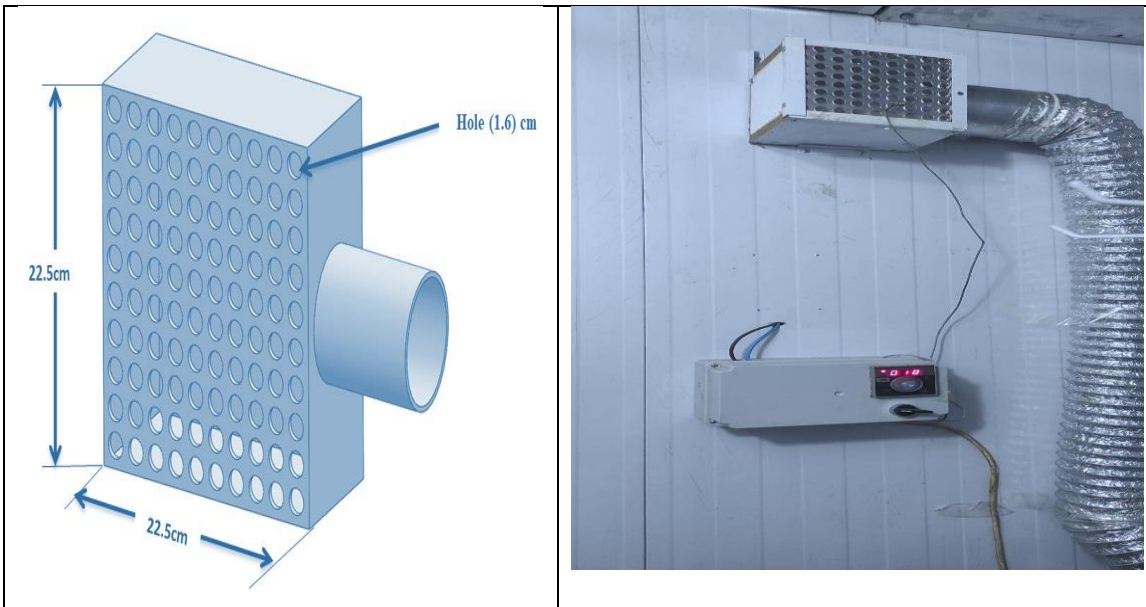
A mixing ventilation system was used to ventilate the thermally insulated office room. This system consists of an air diffuser that distributes air at different speeds and in only one direction. The diffuser has a rectangular cross-sectional area and dimensions of (20 cm x 10 cm). It is installed beneath the ceiling in the center of the north wall at a distance of (30cm). The supplying diffuser is constructed of aluminum with a thickness of (4 mm). This (MV) diffuser has small circular holes made by (Computer Numerically Controlled machine), (CNC) the number of holes is (100) distributed symmetrically, and the diameter of each hole is (1.6) cm.

Fig. (4-5) depicts the dimensions and geometric design of the air diffuser. The air is expelled from the room via an exhaust grille (16 × 10) cm below the diffuser and on the north wall, about (30cm) from the floor. Where

the air inlet and outlet are in the same direction. The ventilation system used is regarded by the ability to use a wide range of temperatures as well as the ability to change the air speed depending on the type of the experiment. As illustrated in Fig. (4-6), an air conditioner unit with a cooling capacity of (2Ton, 7.03371 KW) delivers air to the air diffuser via a connecting aluminum flexible hose that connects the air diffuser to the cooling system.



**Fig. (4-5)** side view shot showing the connection of the flexible hose to the air-condition



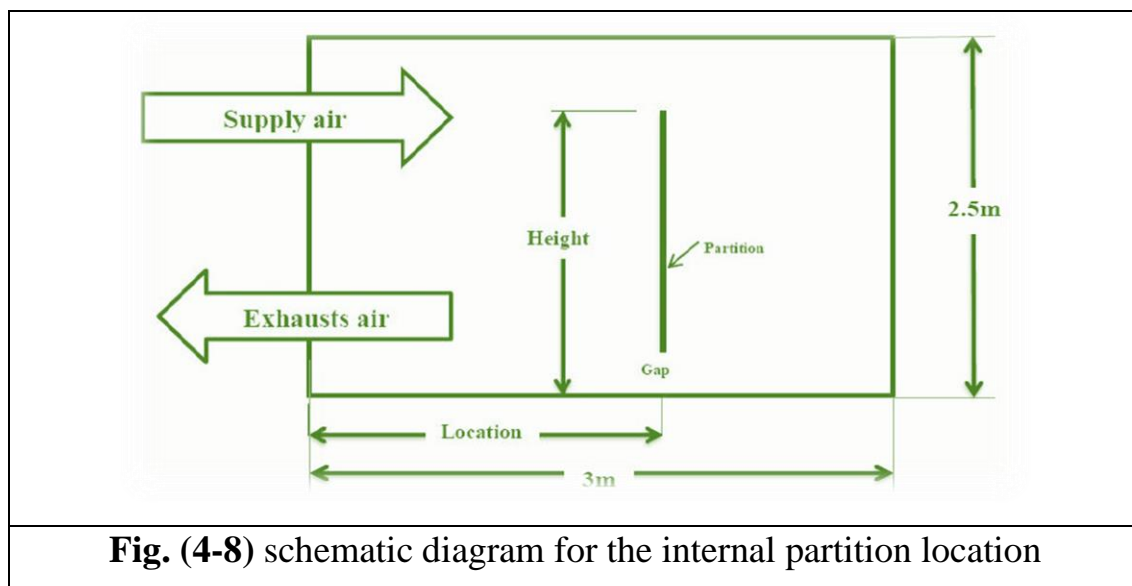
**Fig. (4-6)** Geometrical design of the rectangular air diffuser and its setup.

#### 4.1.4 Internal partition

The insulated tested room was divided into two sections, using an internal partition made of glass framed by (PVC), the location, the height and gap underneath are chosen to place according to the best results that had obtained theoretically; as shown in the Fig. (4-7). The impact of interior partition presence on indoor air quality (IAQ), thermal comfort, temperature distribution and air movement are studied, as well as the effect of the presence of the internal partition on the distribution and spread of pollutants within the two sections. A comparison was made between the concentration of pollutants in the room before and after using the interior partition, as shown in Fig. (4-8).



**Fig. (4-7)** glass partition framed with PVC



## 4.2 Experimental study

In all the experimental cases of the study as show in Fig. (4-9), The air is delivered at a rate of (2.5) m/s and supplied at a temperature of (17°C). The laboratory experiments are conducted on the cases shown in the Table (4-3), (24 °C and 1 bar), where all these experiments are conducted and the steady state results are approved. Different measuring devices are used to take the required readings. Also, the conditions were read before the test and standards were made for the devices used to ensure correct results. The experiment is conducted with and without the use of the internal partition. The source of the pollutants was placed in one space in the room and the concentration of pollutants inside the room is calculated and the effect of using the interior partition on that. where the effect of the presence of the interior was verified by finding the effectiveness of removing contaminants inside the room, where CO<sub>2</sub> is used as a contaminant to calculate the ventilation efficiency.

**Table (4-3)** description of Experimental study cases (with gap and without gap)

Test	Case study	Description		
		Gap	partition height	Partition site
1	Numerical and Experimental		0	0
5	Numerical and Experimental		0.7H	0.5L
7	Numerical and	5%H	0.7H	0.5L
8	Experimental	10%H	0.7H	0.5L

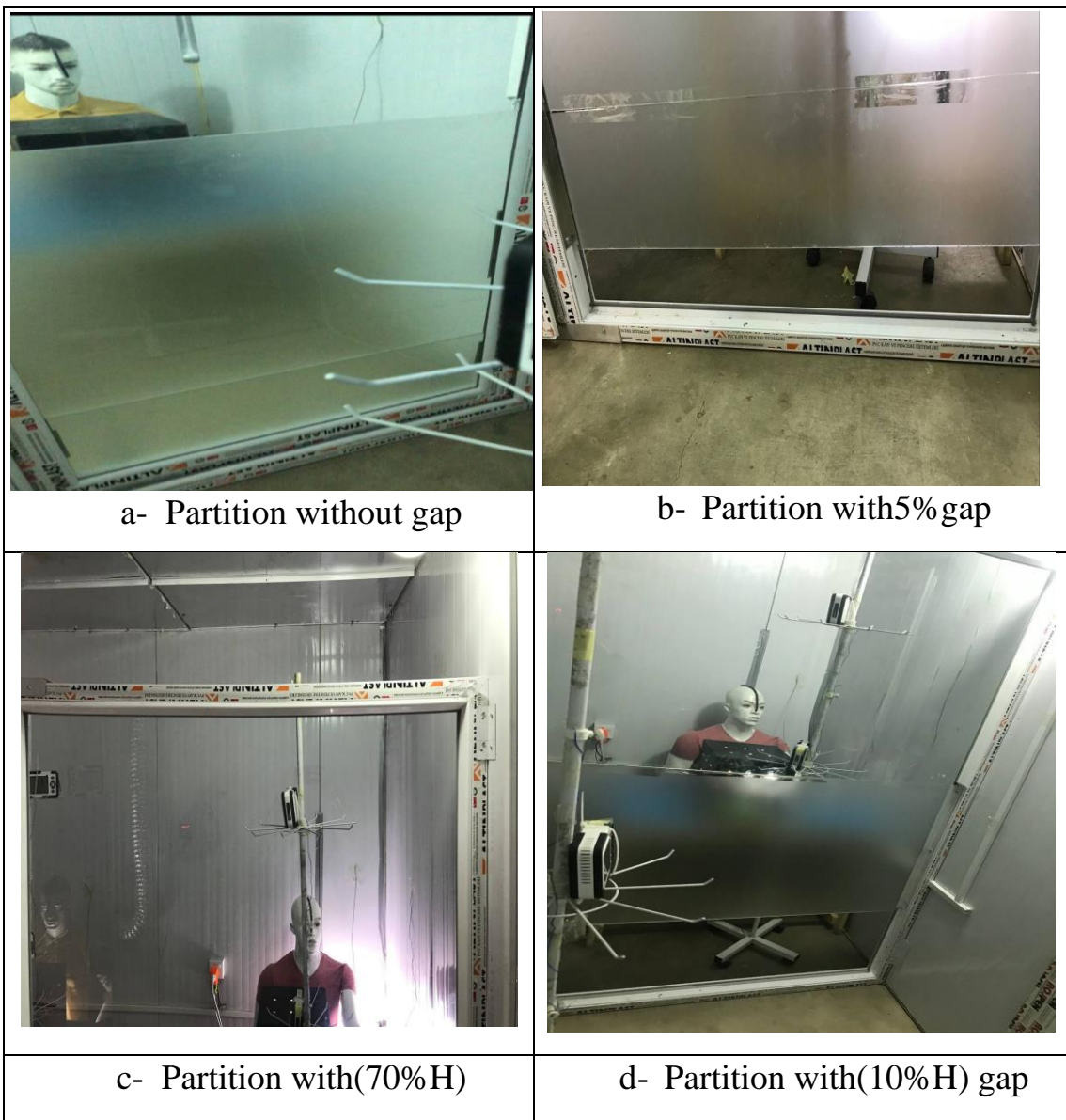


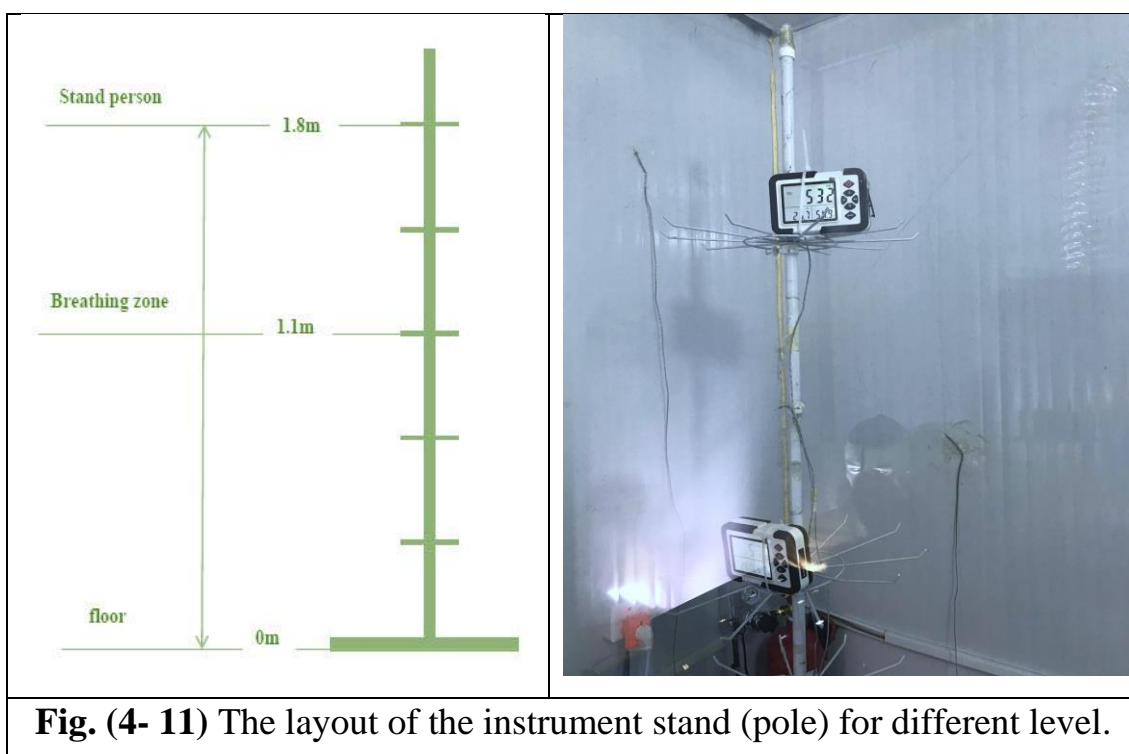
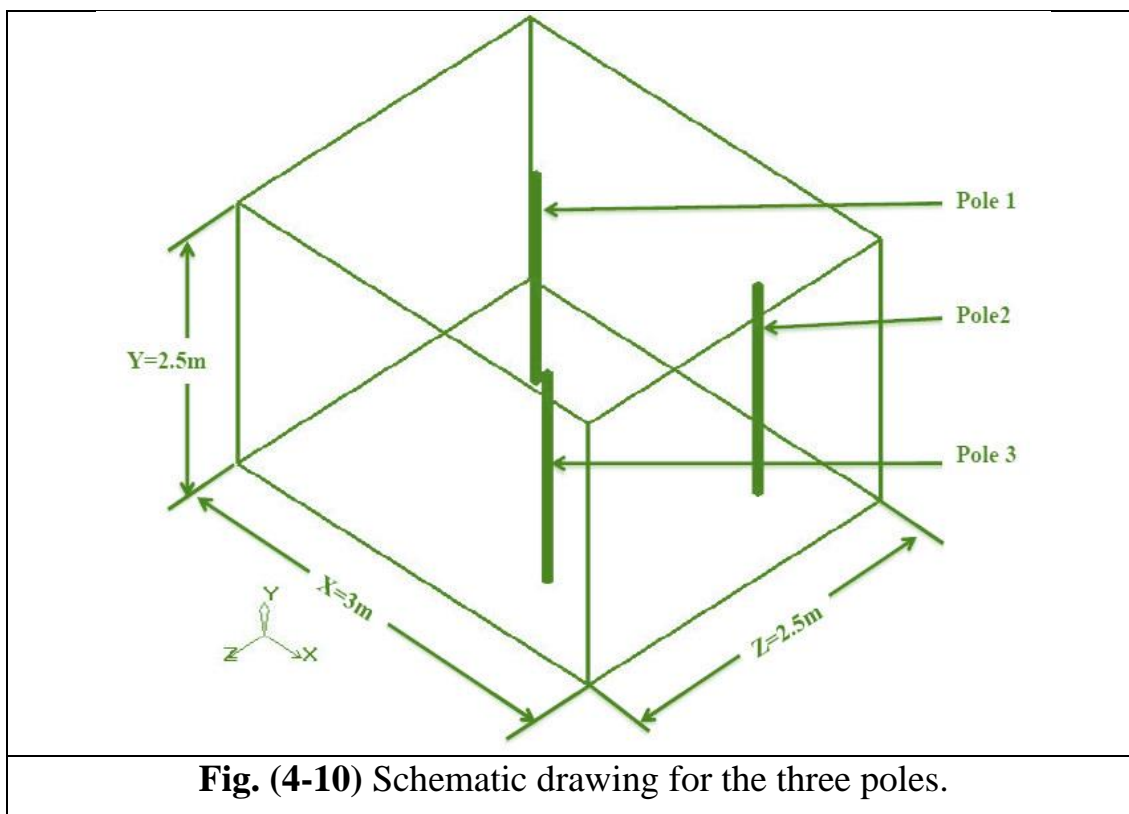
**Fig. (4-9)** cases of partitioning form

### 4.3 Measurement Devices

In practical experiments, different types of measurement devices are used, to measure temperature and air speed, as well as to measure the relative humidity and carbon dioxide concentration inside the office room. The measuring devices are divided into three main systems:

- 1) Air and walls surface temperature measurement system.
- 2) CO<sub>2</sub> concentration and relative humidity measurement system.
- 3) Air supply velocity measurement system.

Various devices are fixed by poles that are distributed inside the room within the occupied zone. These devices are placed to measure temperature, humidity, and pollutant concentrations at different altitudes. These poles are divided into heights from (0 to 1.8) m. Thus, different measuring devices can be installed at heights (0.1,0.4,0.8,1.1,1.4,1.8 m) from the room's floor, where the height of (1.1) m is the breathing level for the seated person, while the height of (1.8) m is for the standing head level. The first pole is utilized to record parameters at (x=1.25, y=0, z=0.5) m from the zero-source point, the second pole at (x=2, y=0, z=0.5) m, and the third pole at (x=1.75, y=0, z=2) m from the zero-source point. as show in Fig. (4-10), and (4-11).



#### 4.4 Temperature Measuring System

Such type of device (temperature recorder (BTM-4208SD)) was used to measure the temperatures inside the room, two devices were used. The

thermocouple wires (type- k) are connected to the temperature recorders (BTM-4208SD) via their ports; each one has (12) channels, as show in Fig. (4-12). The number of thermocouples in use was (24) thermocouples which are placed on each pole, with heights from (0 to 1.8) m, and on each wall. The walls temperatures of the room are measured by placing two thermocouples on each wall and calculating the mean temperature for them. These thermocouples were placed at a height of (1.25) m above the room's floor The measured temperatures are stored in a (RAM) and then read by a computer. These data recorded with time and can be loaded on excel software. Temperatures are measured by thermocouples with mean time of (5 min). These devices have been calibrated as shown in the table (4-4).

**Table (4-4)** Properties of temperature recorder device

Type K thermometer range	sampling time range	Resolution	Accuracy
-100 to 1300 °C.	1 to 3600 seconds	0.1°C/1°C	0.4%

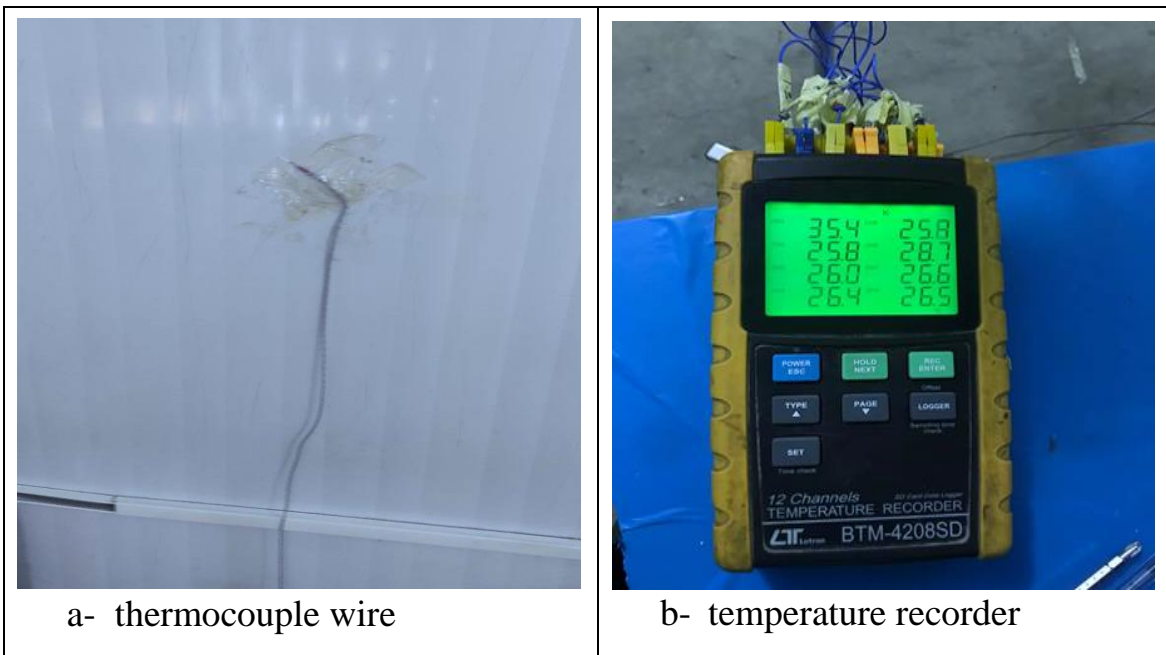


**(Thermocouple wires, type K, calibration)**



**(Temperature recorder calibration)**

Photos above show that the thermocouple wire was calibrated using a special calibrator device, and in the same way the temperature recorders ere calibrated.



a- thermocouple wire

b- temperature recorder

**Fig. (4- 12) Temperature recorder equipment, and thermocouple wire**

#### 4.5 Velocity of Air Measuring Systems (Thermos-Anemometer Device)

The supply air speed and temperature were measured using (thermos-anemometer 8901). Where the air temperature and speed are measured upon entering the room by placing (thermos-anemometer 8901) in front of the air diffuser. This device consists of two parts, the first part is the body of the device, which contains a screen that shows temperature readings and air speed that are sensed by the other part, which is a fan that is placed in the airway to measure both its speed and temperature, as shown in the Fig. (4-13). The table (4-5) listed the properties of the anemometer (YK.2005AH) used in this experiment, and the calibration stated at Appendix(c).



**Table (4- 5)** the thermos anemometer sensor properties

<b>Equipment</b>	<b>Range</b>
<b>Range of Velocity measurement</b>	0 – 30 m/s
<b>Accuracy of Velocity</b>	(±2%)
<b>Resolution of velocity of air</b>	(0.01m/s)
<b>Range of temperature</b>	-10 to +60°C
<b>Accuracy of temperature</b>	± 0.6°C
<b>Resolution of temperature</b>	0.1°C
<b>Resolution of Relative humidity</b>	0.1%RH

#### 4.6. CO<sub>2</sub> Concentration and Humidity Measuring System

This system is based on a set of (CO<sub>2</sub> and relative humidity data logger devices) as shown in Figure (4-14). The features of the devices are provided in the table (4-6) below. Each device came with special software that allowed all recorded data to be transferred to the computer via USB connection; organized as a table in (Excel). The time interval between readings might be set. Appendix (c) contains the certificate of conformity. Six devices were installed in different locations of the tested room, where the first device was placed when the air entered at the diffuse, the second below it at breathing level, both of them were on the (pole1); while the third, fourth devices were placed on the (pole2),(pole3), at (1.1),(1.8); in front each manikin to log the carbon dioxide concentration, relative humidity in the occupied zone as shown in Fig. (4-15).

**Table (4-6)** Properties of CO<sub>2</sub> and relative humidity data logger devices

Carbon Dioxide reading	Range	0-9999 (ppm)
	Accuracy	±5 (ppm)
	response time	30 sec
Humidity reading	Range	0- 99.9%
	Accuracy	±2%

**Fig. (4-14)** CO<sub>2</sub> and relative humidity data logger device.

## 4.7 Experimental Procedures

The most important experimental steps that are taken can be summarized in the following steps:

- 1- Dividing the room into two spaces by an internal partition. Where an internal partition made of glass framed by PVC was used, and placed in the middle of the room, in such a way similar to the theoretical designing.
- 2- Measuring air temperatures and knowing the temperature distribution within the occupied zone at three poles and at different altitudes (0.1, 0.4, 0.8, 1.1, 1.4, and 1.8) m.
- 3- Placing a source of pollutants inside the room by using carbon dioxide bottle, connected with flowmeter regulator and two oxygen tubing each one to the manikin's nose, making them exhale ( $\text{CO}_2$ ) gas in specific quantity and time, then calculating the percentage of pollutants in each room section before and after partitioning.
- 4- The relative humidity is measured at the steady-state condition at six points in the occupied zone, before and after partitioning.
- 5- Measuring the concentration of carbon dioxide gas before and after partitioning, when entering the air and at the exit and in the occupied zone for the purpose of calculating the ventilation efficiency.
- 6- Calculating the temperatures when entering the air and at the exit, as well as calculating the average temperature inside the occupied zone for the purpose of measuring the effectiveness of heat removal.

## 1.8 Repeatability

Every researcher who conducted an experiment and got certain results must pose the question, "Can it be done again?", repeatability is an indicator of how often the response is to be "yes.". Determined by doing the same experiment several times and statistically analyzing the

findings. Some statisticians argue that standard deviation and repeatability are equivalent. The following equations had used, as listed in Appendix (D)

$$T = \bar{T} + u\bar{T}(P\%) \quad \dots (4-1)$$

T: True value

$\bar{T}$  = mean value

$u_{\bar{T}}$  : *un certainty*

$(P_T)$  = probability

$$\bar{T} = \left( \frac{T_1 + T_2 + T_3}{3} \right) \quad \dots(4-2)$$

$$\frac{\partial T}{\partial T_1} = \frac{\partial T}{\partial T_2} = \frac{\partial T}{\partial T_3} = \frac{\partial T}{\partial T_4}$$

$$u_{\bar{T}} \left[ \left( \frac{\partial T}{\partial T_1} * \delta_T \right)^2 + \left( \frac{\partial T}{\partial T_2} * \delta_T \right)^2 + \left( \frac{\partial T}{\partial T_3} * \delta_T \right)^2 \right] \quad \dots(4-3)$$

$$K = 1.87 (N - 1)^{0.4} + 1 \quad \dots(4-4)$$

K: reasonable

N: number of measurements

$$W_T = \left( \frac{\text{Max.value} - \text{Min.value}}{N * K} \right) \quad \dots(4-5)$$

$$P_T = \frac{1}{N(2 * W_T)} \quad \dots(4-6)$$

N: number of measurements

# **Chapter Five**

## **RESULTS AND DISCUSSION**

## Chapter Five

### RESULTS AND DISCUSSION

This chapter presents the whole results of both numerical and experimental cases of the insulated room, and non-thermally insulated office rooms cases under Iraqi climate. A comparison between the insulated office room (case I) with non-insulated office room (case II) is made this chapter focuses on the acceptable values discussions for indoor air quality and thermal comfort parameters within the rooms before and after partitioning. (CFD) simulation allows to study the thermal comfort parameters such as (ADPI, PMV, PPD, and ADI), besides temperature distribution, and mean air velocity. The numerical and experimental results for case(I) are compared within the occupant zone for different levels begin with (0.1) to (1.8) meters in terms of temperature distribution, CO<sub>2</sub> concentration, with respect to heat removal efficiency, and ventilation efficiency.

#### 5.1 Validations :

##### 5.1.1 Validation(1):

To check the reliability of the AIRPAK(3.0.16) software, whether its valid in mixing ventilation systems design, a validation was conducted with another numerical study. The examined cell office, depicted in Fig. (5-1), was built in Oslo to the Norwegian passive house standard. The chamber was (4.2 x 2.25 × 2.7) meters and the window was (1.7 m by 2 m). A modeling of the sitting passenger using a cylindrical (1.1) meter-tall and (0.6) meter-diameter dummy. Additionally, a computer, a table, and lights were present. Placing a radial supply diffuser on the ceiling, the case was simulated using by (Star-CCM+), with the standard (k-ε) turbulence model, The mesh grid was designed to have a (y+) constantly lower than the value at the centre of the room and elements with a closet distance of (0.05) cm to the diffuser surface up to (7 x 5) cm, the supply temperature was (24°C), and the airflow

rate was(49.4 l/s). The comparison has done based on the temperatures results corresponding to each height levels, which are (0.1, 1.1, 1.7, 2.2, 2.5). Percentage avverage error gave acceptable value ( $\mp 2.63$ ), as shown in Fig.(5-2).

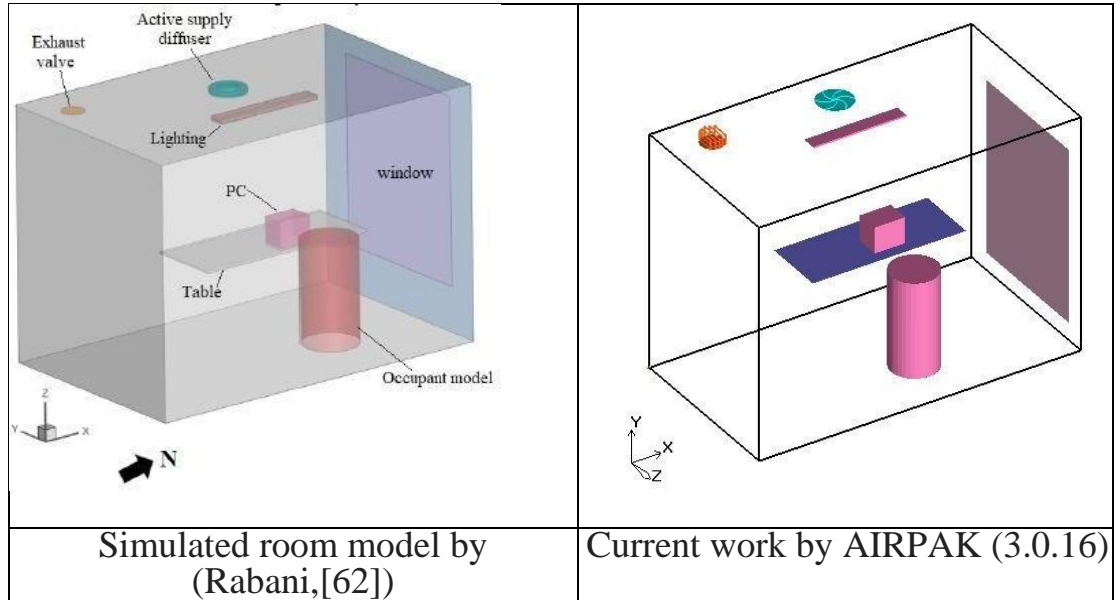


**Fig. (5-1)** Simulated office cell validation.

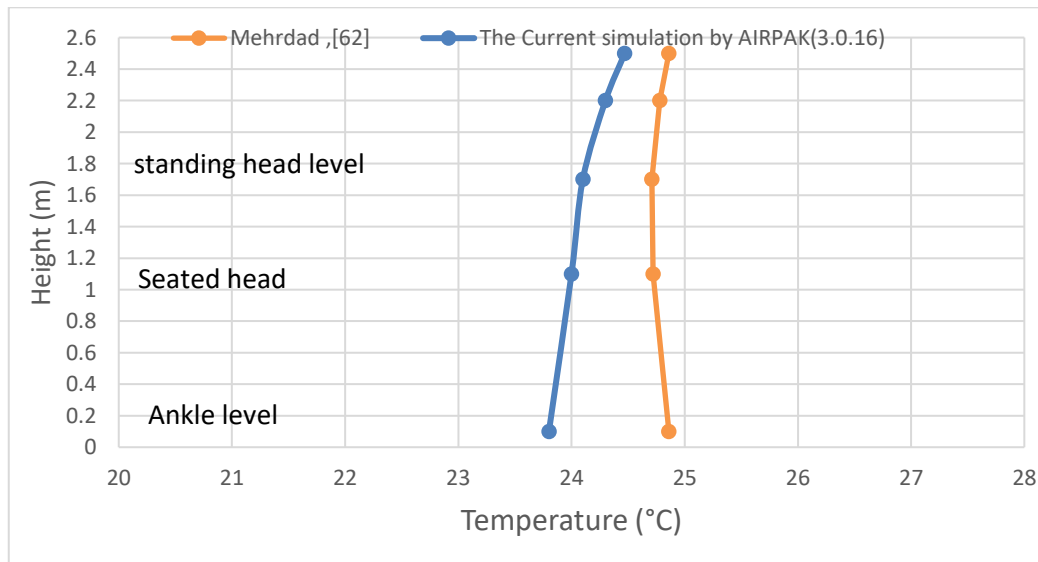


**Fig. (5-2)** Comparison between AIRPAK(3.0.16) results, and Mehrdad,[62]

**5.1.2 Validation(2):**

The experimental work of Zahraa’s research has used to validate AIRPAK(3.0.16), using the turnulent mdel (RNG k-ε).The simulation findings were compared with the results of the Zahraa’s experimental study,

as shown in the Fig. (5-3) a non-isothermal office space was used for the experiment to simulate a displacement and mixing ventilation system. The test chamber's inside measurements were (4 x 3.5 x 3.75) metres, which is equal to a normal two-person workplace, two PCs, two televisions, and has two lights. According to the Iraqi construction code, the chamber walls for this office were made up of many layers (gypsum, cement plaster, and common brick). The air conditioning system was turned on until the testing rooms reached Zahra's working temperature limit of (23°C). Comparison had done between the current results of (AIRPAK3.0.16), with the corresponding results, according to temperatures findings with each height levels (0.4,0.8,1.1,1.8), percentage error which has got, was acceptable ( $\pm 4.5$ ), as shown in Fig. (5-4).

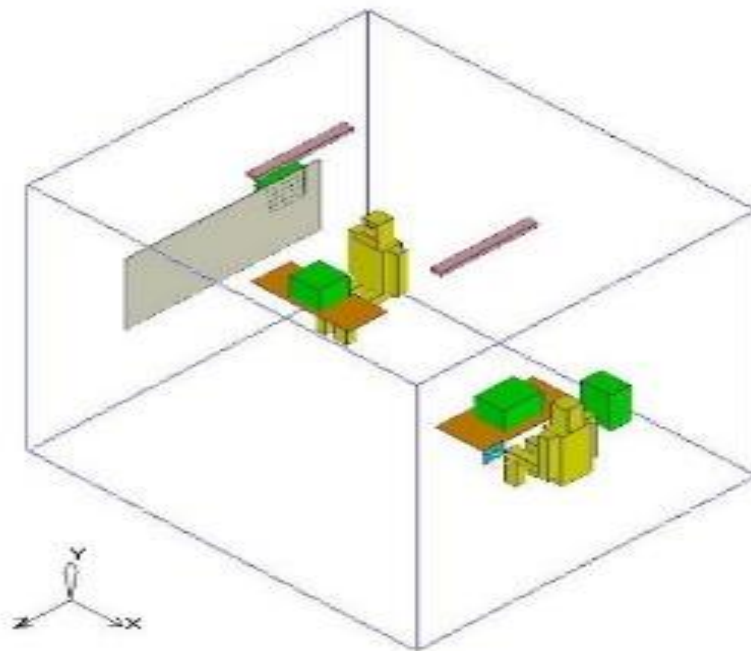


**Fig. (5-3)** AIRPAK(3.0.16) simulation.

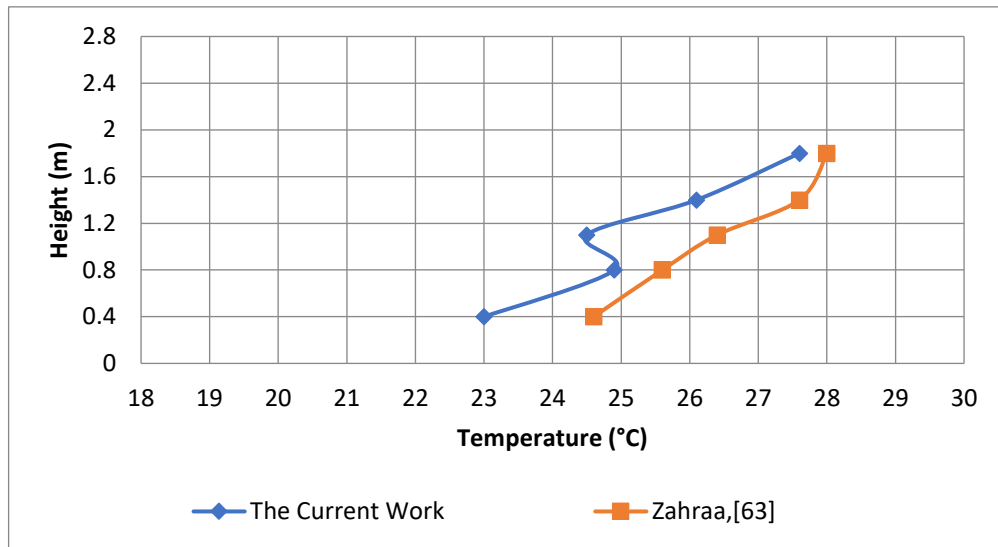


**Fig. (5-4)** comparison between the AIRPAK(3.0.16) results, and Zahraa,[63].

## 5.2 Numerical Results of the Insulated Office Room, (Case I):

The (AIRPAK3.0.16) software, was used for modeling the tested thermally insulated room, after completing all the cooling load calculations, and designing each of the air diffuser and air exhaust grille; besides that choosing the suitable setting location for the manikins within the occupied zone; moreover a contaminate source of ( $\text{CO}_2$ ), has simulated on each manikin's nose just to investigate the indoor air quality and thermal comfort before and after setting up a partition, as showing in Fig. (5-5), present the insulated tested room adopted mixing ventilation system without a partition.

The air temperature enters from the diffuser was designed to be ( $17^\circ\text{C}$ ), until it reaches to ( $22.9^\circ\text{C}$ ) at the end of the room as shown in subplot(a) of the Fig. (5-6). Which represents the (Z-plane of the room's center).

Because of heat transferring between the room's air and the heat sources, the temperature reaches uniformly to the manikins so as their (PC), besides, around the overhead lamp, as shown in subplot (b) to (d) of the Fig. (5-6). As is known heat is a form of energy that is transferred between two

bodies or zones in different temperatures, the main reason for temperature distribution is the density variation resulting from the buoyancy force, which in turn causes the fluid to move; in such a phenomenon lead to a natural circulation which is known as the ability of a fluid in a system to circulates continuously with gravity and provable changes in heat energy.

An obvious characteristic of mixing ventilation is the delivery of air at high velocity beyond the occupied zone. Air leaving the room is drawn in and mixed with the supplied air as a result of the increased pressure caused by the fast-moving air. Air velocity is high during the first cycle of the airflow, but it gradually decreases as a larger percentage of the air in the room is mixed. Cold air naturally slides according to buoyancy force, but air driven upward by the force created by the diffuser opposes this natural motion, keeping cold air circulating around the cold zone; one such phenomenon is known as opposing mixed convection.

An appropriately sized system, such as an office room, guarantees that the supplied air volume is adequately mixed with the air in the room before it reaches the inhabited zone, and that the air velocity rate has decreased to the required level, which varies based on the room types. The subplots (a) to (c) of the Fig. (5-7) showing the air speed distribution and streamlines at the entrance level of the z-plane contour, the fresh cool air from the diffuser mixes by the heated midair within the area. Because the (exhaust grill) is so much less in area than the air supply area, the air exits the room at a faster rate than it entered, as indicated in the subplot(b).

The diffuser is located (0.3) meters off the floor. At a height of (0.3) m above the floor, the air is released into the space. opposite wall is struck by the air that has released from the diffuser. After a tiny bit of the reverse flow hits the opposing wall and flows downward, a larger component of the flow is exhausted, and the remaining portion turns upwards toward the ceiling; the

movement that results causes a circulation zone to be generated in the Centre of the area. Due to the cold air's larger density than warmer air, it converts downward, swirls in a clockwise direction, and rotates close to the objects. When the air terminal device is on the same side as the exhaust grille, the air velocity is often more even.

Ventilation is the process of bringing outside air into enclosed structures like buildings, to be able to maintain satisfactory indoor air quality, this is accomplished by removing polluted air from the building and lowering contaminants with fresh air, and a proper ventilation is likely to provide additional protection against the spread of a (COVID) pandemic where the latest spreads through droplets and comes out when the infected person coughs, sneezes, speaks, or even breathes, so these drops tend to fall and may be transmitted to longer periods, so a person can become infected when drops are on the mouth, nose, and/or eyes membranes.

The current study looked at the best techniques to partition or divide an office area by a thin wall of glass partition due to its flexibility, light weight, and simple in construction, while considering human thermal comfort criteria, represented by (PMV, PPD) besides the indoor air quality criteria represented by (ADPI, ADI), ventilation performance under hot and dry climate.

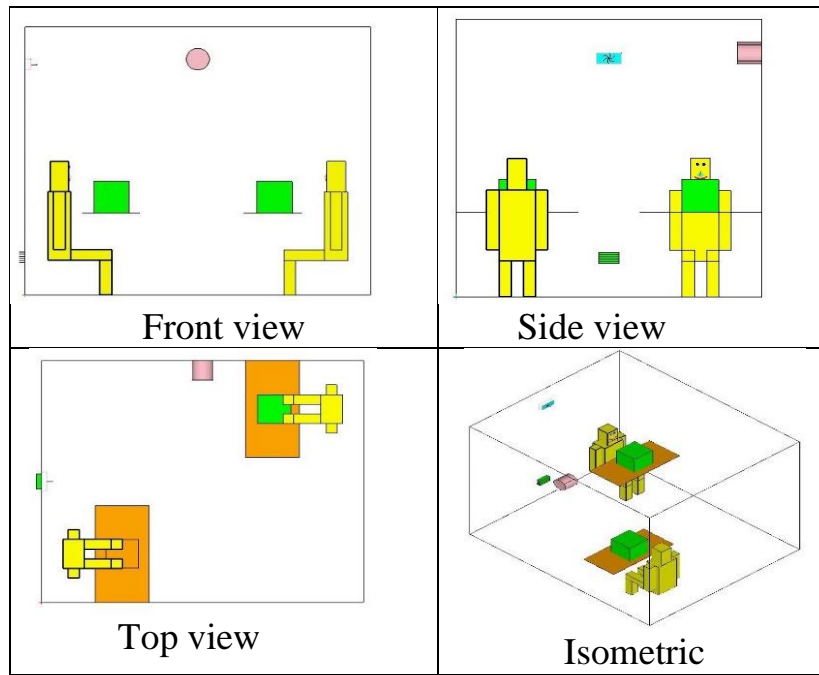
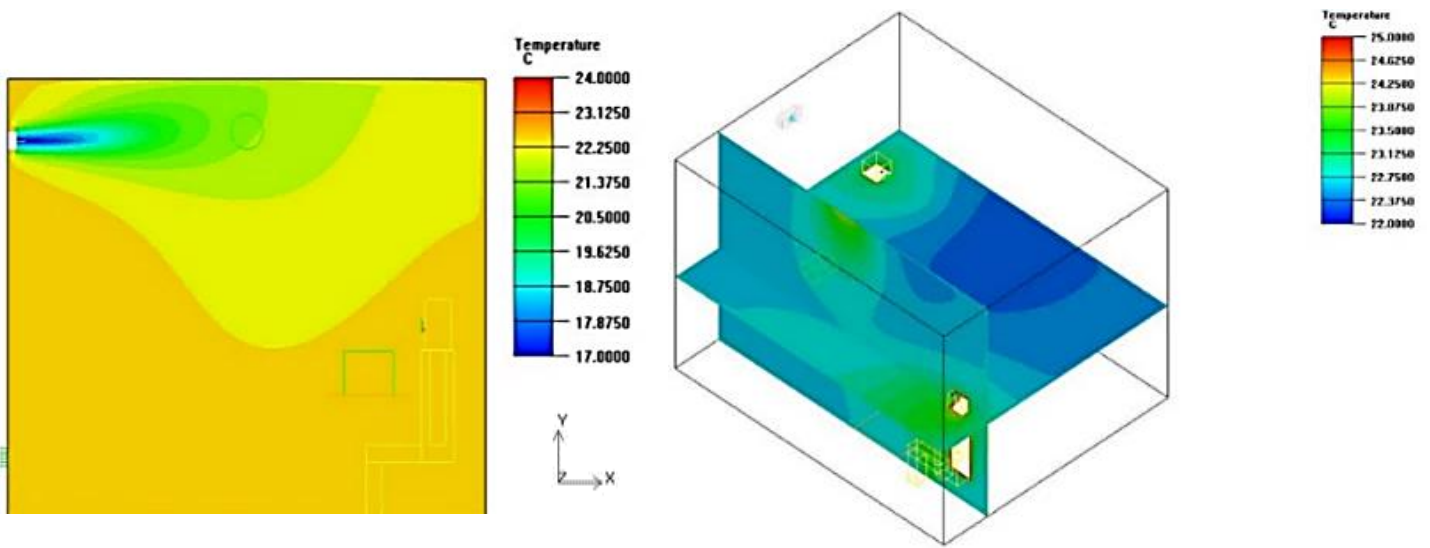
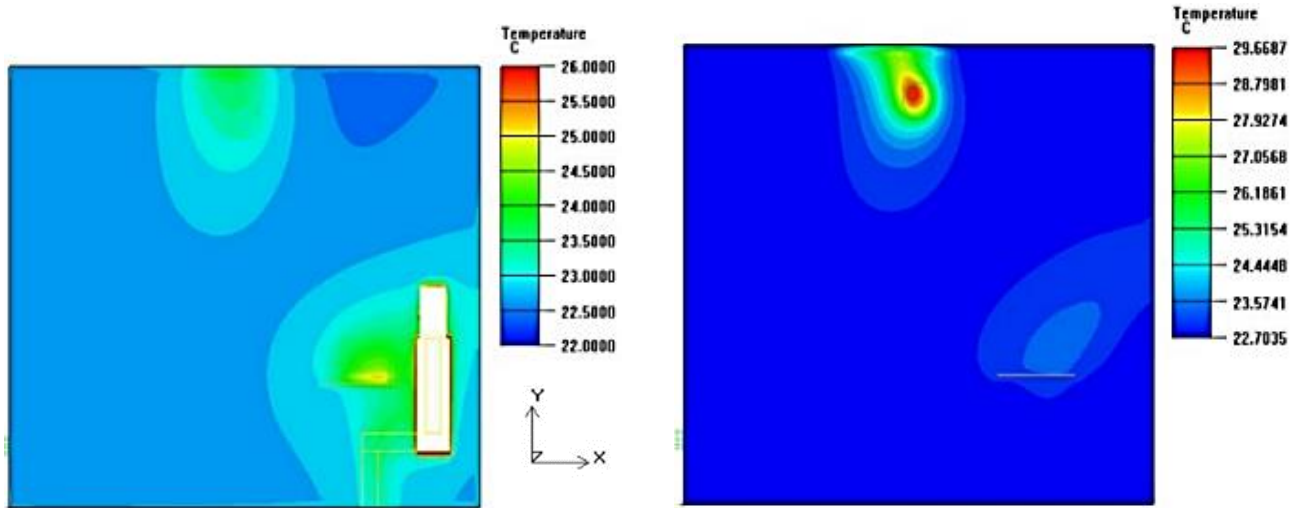


**Fig. (5-5)** Insulated office room full scale.

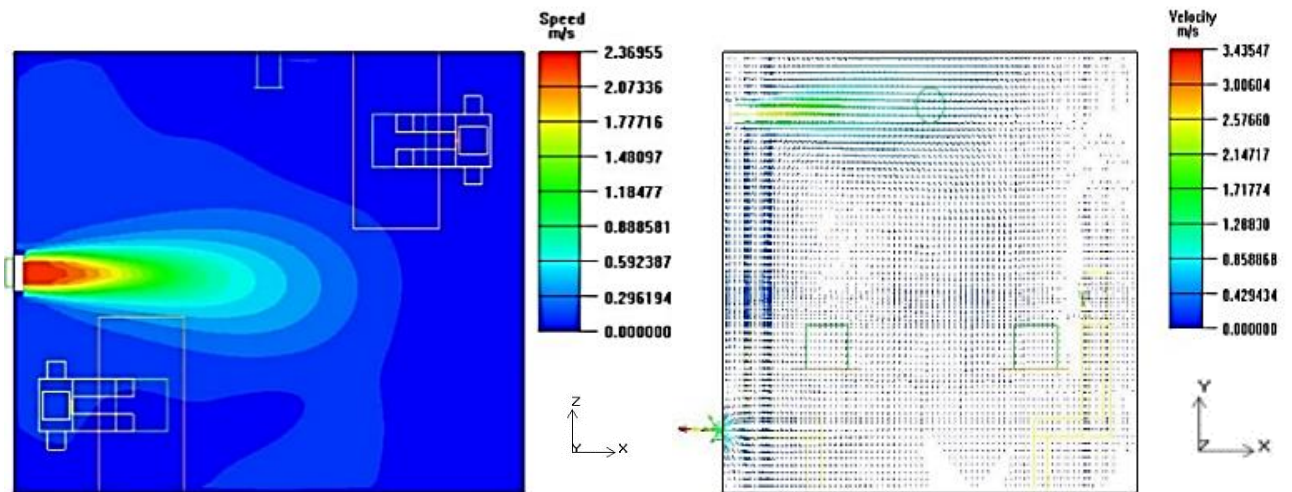


a- Z-plane of the room's center      b- cut planes along the two manikins



c – temperature around the manikin    d- temperature around the lamp

**Fig. (5-6)** Contours of temperature distribution within the office room for test (1).



a- Air speed contour

b- air speed vector

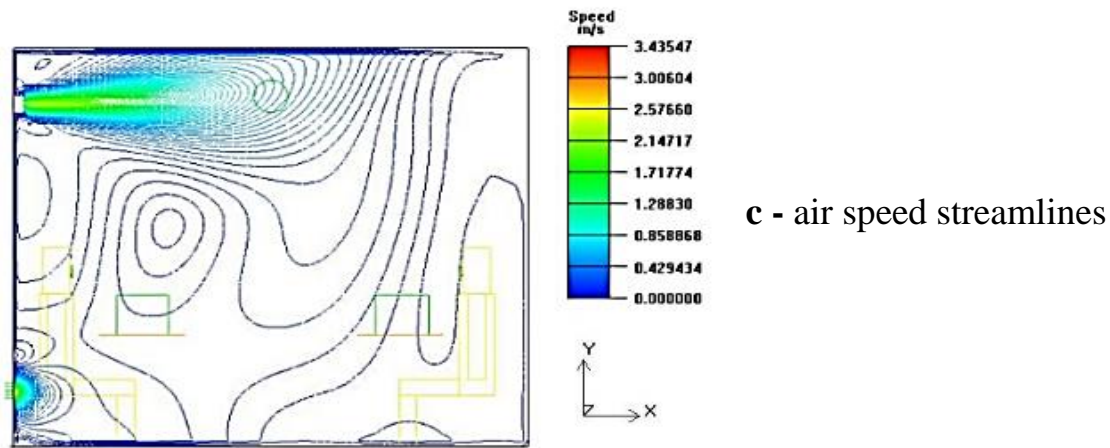


**Fig. (5-7) Contours of the air speed distribution, and streamlines for test(1).**

### 5.2.1 Partition's location effect

The goal of evaluating the partition placement is to enhance room air quality. The partition was shifted from (40% to 50% and 60%) of room's length from the northern supplying wall towards the southern wall, as illustrated in Fig. (5-8), three locations examined by shifting the partition away from the supply zone, and that's what leads to increase the volume of supply zone that is more polluted than the opposite side. Consequently, it can be conducted that shifting the partition away from the supply zone towards the opposite zone enhanced the heat removal efficiency in the tested room. The Fig. (5-10), explain the result of moving the partition location in case of heat removal efficiency and contaminant removal efficiency.

In the Fig. (5-9), the temperatures inside the room are shown at (1.25) Z-plane level, fresh and cold air enters the room with (17°C) and highest point of temperature that reached is (23.9°C) at the roof in test (3) of (50%L), basically this range is within the comfort level in an occupied zone. In the test (2) of adopting (40%L) as shown in the subplot (a) found that the temperatures in the breathing zone on a heights (1.1-1.8) meters are not uniform, that's because of unsuitable partition positioning, since the part of

the room which contain an exhausted opening draws the air consumes, which is higher in temperature as compared to the air temperature in the opposite side to the diffuser, which is slightly cooler and this could give an explanation for the potential inconvenience of the occupants in both sections; while in test of (50%L) air temperatures started to be more uniform from the previous scenario as illustrated in the sub plot (b), the suitable location of the partition in the middle of the room helped distribute the air temperature more regularly than before in each part of the room , and as shown the temperatures inside the room moderated more than previous case, as it reached closer to the standard conditions, where the location of the partition was more appropriate, and the air temperature was able to distribute and reaches the section containing exhaust opening to allow the consumed air to exit and not to stay in one area as before.

Last but not least the sub plot(c) shows temperature distribution in the test (4) of (60%L) inside the room; Here cool air diffusion expanded more in the area of the beginning of the room at the site of air entry and exit, ending with the partition edge, noticed behind less air temperatures at the breathing zone at a heights of (1.1-1.8) meters according to the second sitting person, this may cause the person feels uncomfortable in such section, since the function of the partition location is targeted in place guarantees for everyone feeling in thermally comfortable, besides giving a good prediction of temperature distribution.

The partition in such location may obscures the fresh air, and possible to cause delay in reaching to the next side for the exhaust opening, especially if more height scenarios has been examined. In short, it's worth noting that the further away shifting the partition location, the lower the indicators of good air distribution, partition location reaches its peak in the test (3) of (50%L) according to efficiencies that have been calculated.

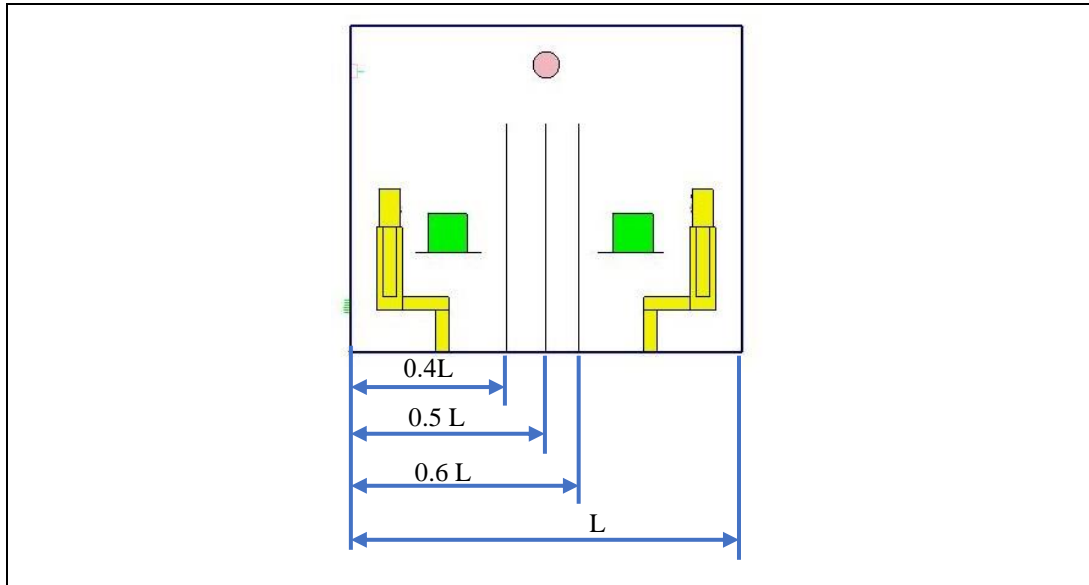


**Fig. (5-8)** Partition's location scenarios.

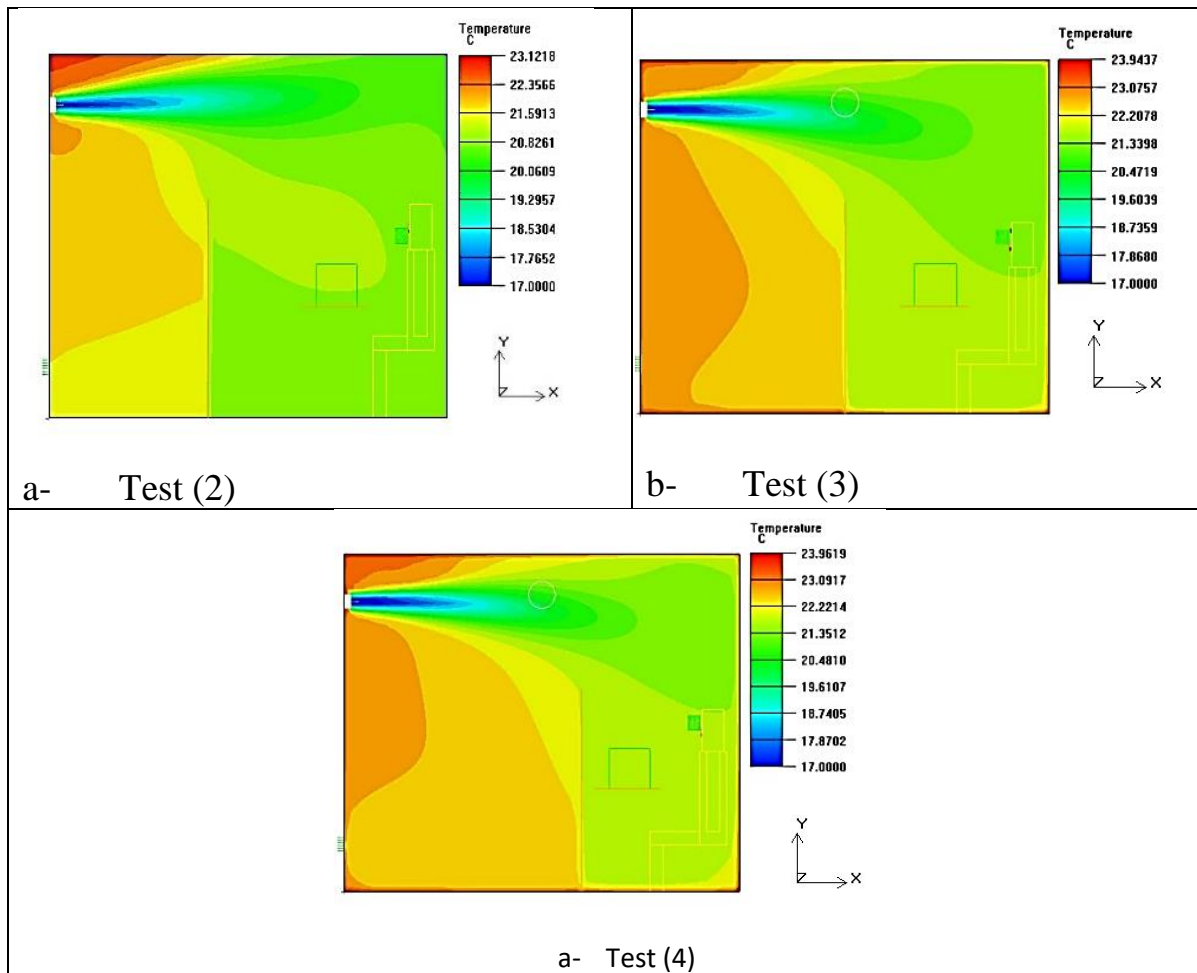


**Fig. (5-9)** contours of partition's location scenarios.

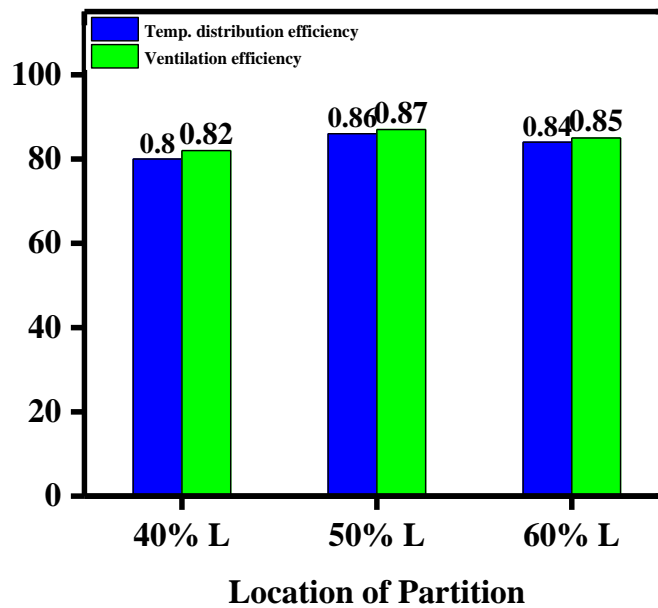


**Fig. (5-10)** Heat removal, and ventilation efficiencies.

### 5.2.2 Partition's height effect:

Another parameter that was investigated was the height of the partition; three heights were chosen (60 %, 70 %, and 80 % of the room's height); The partition was positioned at (50%) of the room's length without gap, it was clear from the result in subplot (a) in Fig. (5-11) that increasing the height of the partition decreases ventilation efficiency, due to the increase in size of the stagnant zone on the opposite side to the supply zone with increasing partition height. as well as the effectiveness of pollutant removal.

The height of the partition has a significant effect in distributing temperature, especially when it became the optimal choice for its location in (50%L) of the room's length, the higher the partition, the higher the temperature within occupied zone. Its crystal clear from Fig. (5-11) the temperature reaches to (23.07°C), (24°C), and (24.26°C) at sub plot (a), (b), and (c) respectively. And certainly, the greatest temperature is at the ceiling, however, the concern is the levels of breathing zones both in sitting and

standing planes which are presented by (1.1), (1.8) meters respectively. Fortunately, these temperatures were within the acceptable range of comfort zone (roughly 21°C-26°C) in summer when adopted mixing ventilation according to (ASHRAE 2013).

The height to be chosen is the height that allows a good distribution of air throughout the room, taking into consideration the stagnant zones, especially the opposite section to the air inlet diffuser, besides, that the air doesn't directly hit the partition, but that the air reaches to the end of the southern wall of the room and then is distributed throughout the room. Furthermore, taken in consideration the role of the proper height of the partition as additional protection to prevent the spread of (COVID) epidemic especially from the transmission of the exhaled polluted air emitted from the seated employees, relying in both heat removal, and ventilation efficiencies, as illustrated in Fig. (5-12).

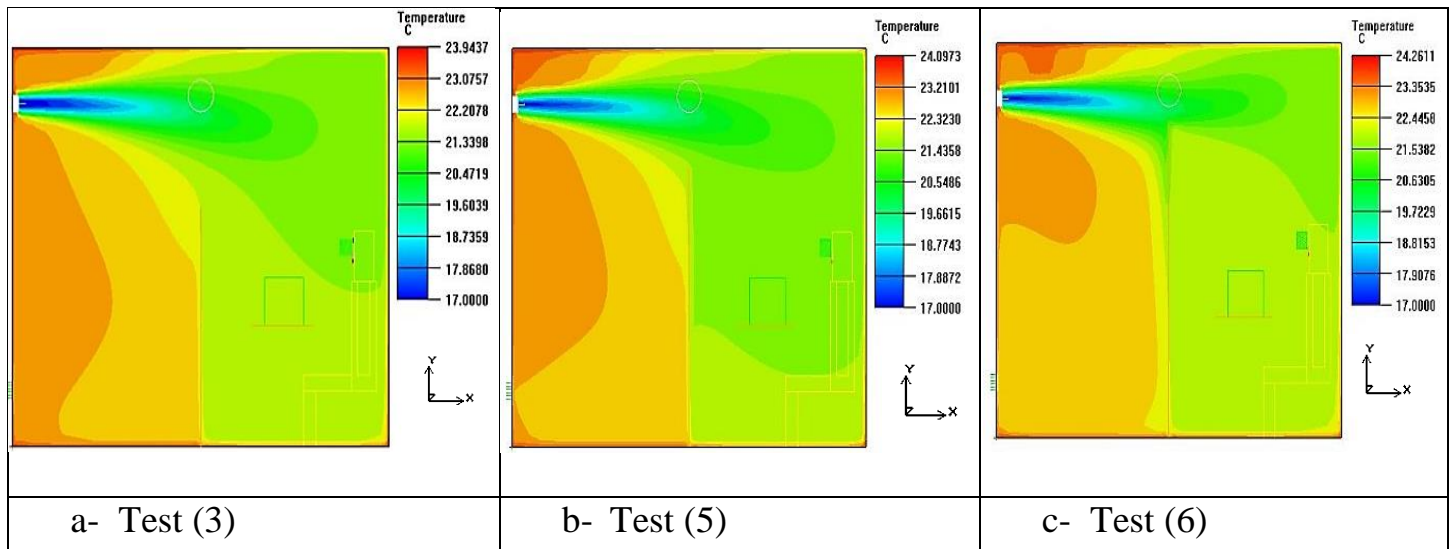


**Fig. (5-11)** Contours of partition's height scenarios.

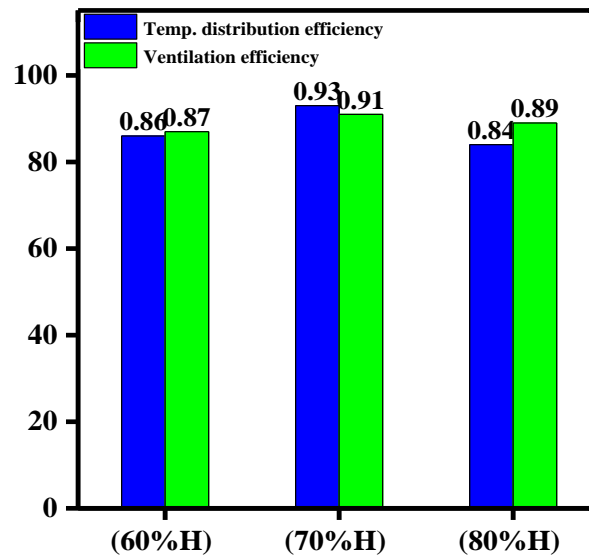


**Fig. (5-12)** Heat removal, and ventilation efficiencies.

### 5.2.3 Gap underneath effect:

A gapless partition effectively isolates the contaminated at the second part of the room from the exhaust opening and causes pollutant backflow over the partition to the supply section, which consequently lowers both heat removal efficiency and the ventilation efficiency in the room. so, the gap underneath was also examined to find if there will be obvious effect on the room air quality (IAQ), two tests (5%,10% of the room's height) were studied after the partition positioned at (50%L, 70%H). By increasing the gap under the partition there will be increasing in recirculation around the partition, in the test (7) of (5%H) the supplied air is allowed to flow through below the partition, and in turns creates air recirculation around the partition by reduces the backward airflow just over the partition. While in the test (8) of (10% of room's height gap), provides broader area for the supply airflow to flow beneath, resulting in an unbalanced airflow between both foreword flow, and backward directions (over the partition).

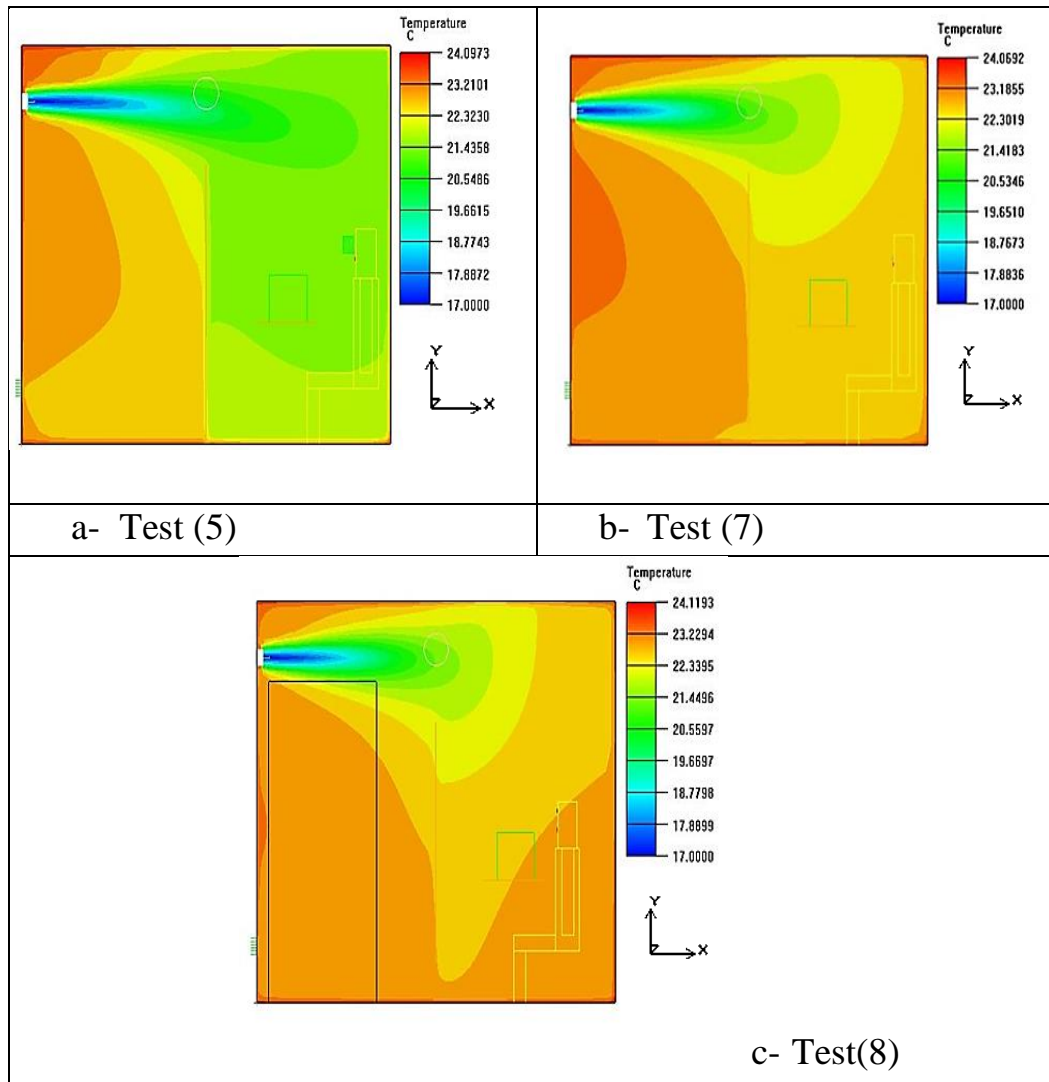


**Fig. (5-13) Contours of office room partitioned with a gap adoption scenario.**

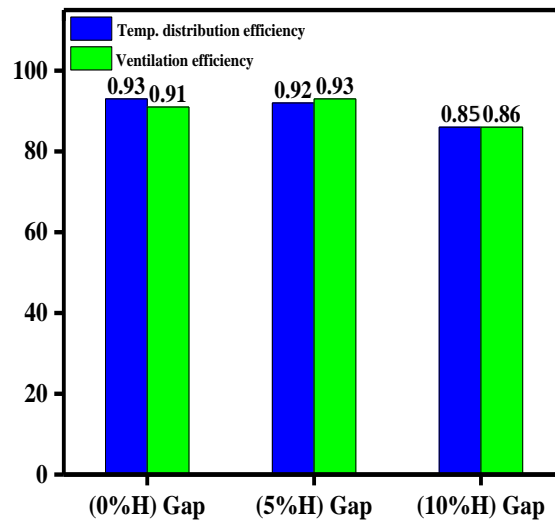


**Fig. (5-14)** Heat removal, and ventilation efficiencies depending on gap's height.

#### 5.2.4 Thermal Comfort and Indoor Air Quality:

##### 5.2.4.i ADPI and ADI parameters:

Air distribution system performance within an office room can be measured in terms of (ADPI). which is a criterion used to assess the performance of an air distribution system within a given office. Its value is heavily influenced by various factors, including room dimensions, air distribution layout of air inlets and outlets, room loads, and air register throw speed and distance. The majority of air distribution systems are designed to reach an (ADPI) of 80% or above (ASHRAE Fundamentals, 2001).

Fig. (5- 15), subplot in (a) shows the relation between the partition gap's height, tests (5,7,8) and (ADPI) which calculated by (AIRPAK 3.0.16) software program, it's found that increasing the gap height leads to increasing the (ADPI) value until it peaks at test (7) of (5%) of room height then its returns in reduction at test(8) of gap (10%) of the room's height. Thermal comfort studies were used to determine the (ADPI) equation's

cooling thresholds and boundaries. Thus, there is an implied connection between (ADPI) and thermal comfort. (ADPI was created primarily to combine ventilation with air distribution in order to provide a consistent air environment. (80) percent signifies that (20%) of the total occupied space does not fall within the equation bounds as the majority does, whereas (100% ADPI) results from a perfect mixing situation. As a result, a greater ADPI number indicates a higher level of mixing in the office room.

The ability of an air distribution system to remove impurities from the ventilated space figures out its efficacy. It ignores the most important room aspects, such as health comfort and air purity; another issue with this strategy is the difficulty in determining an appropriate (ADPI) level for comfort. For example, the (ADPI) concept lacks information on these two properties and hence cannot determine the real quality of an air distribution system. As is well known, a good ventilation system achieves a good thermal satisfaction and quality of air in the inhabited zone. Despite large values of ( $\epsilon_c$ ) and ( $\epsilon_T$ ) indicate to contaminant removal and good heat distribution, such variables, alone cannot provide a reliable indication of thermal comfort and air quality in the inhabited zone. One technique is to mix ( $\epsilon_c$ ) with a subjective factor indicating to indoor air quality perceptions and ( $\epsilon_T$ ) with a parameter denoting thermal perception. The Fanger's Percentage of (PD) for air quality, and the Prediction percentage of dissatisfied (PPD) for the thermal environment will be appropriate criteria to utilize. These parameters, and their equations were discussed in Chapter (3), section (3.10). The ADI does not suffer from the same paradox as the (VP) since it reflects the square root of the products of ( $N_t$ ) and ( $N_c$ ), and a high (ADI) value also indicates a high value of both ( $N_t$ ) and ( $N_c$ ).

An effect of changing gap's height of the partition on the value of (ADI) has shown in subplot (b) in Fig. (5-15), where it found that the greatest value

can be obtained in the case of (5%H) gap's height in the office room, which reached to (7.05), then it's being to fall down when additional increase the gap's height. Since (ADI) is a metric to calculate uniformity of room air; the ventilation system which constructed with acceptable (PD) and (PPD) values close to (10%), will have an (ADI) close to (10). Indoor air quality and thermal comfort characteristics for the well-insulated office space were tabulated and displayed in Table (5-1).

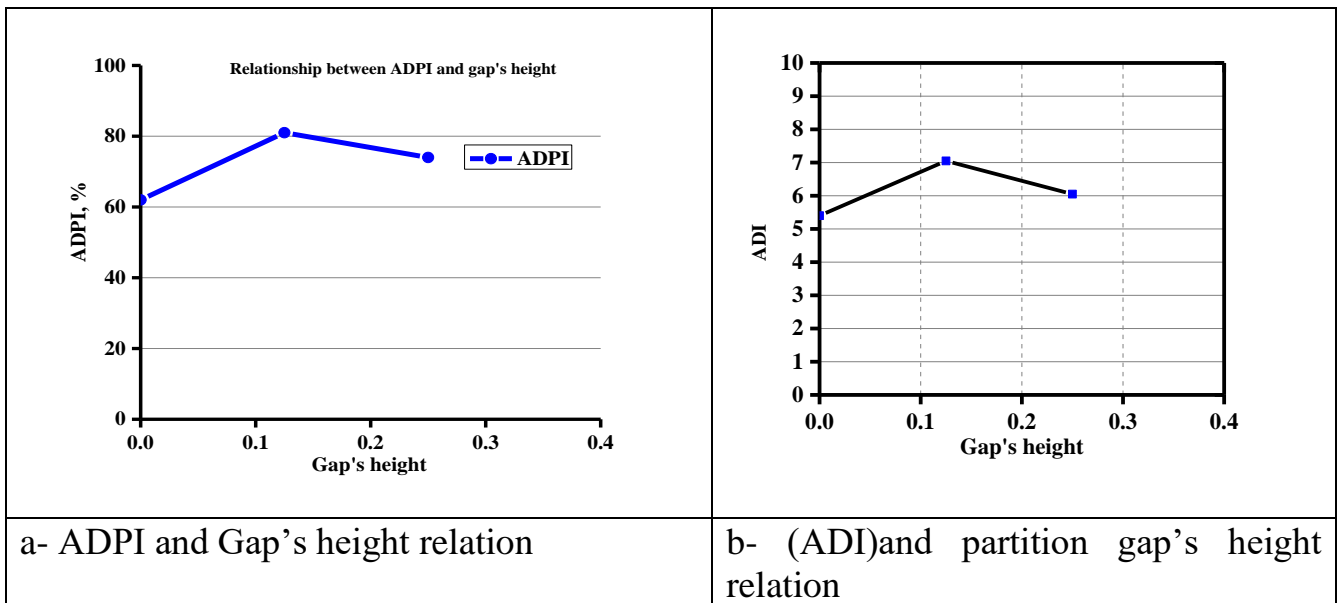


**Fig. (5-15)** Gap's height effect with (ADPI, ADI)

**Table (5-1)** The numerical characteristics of internal temperature regulation and air quality.

Tests	$\epsilon_T$	$\epsilon_c$	$N_t$	$N_c$	VP	ADI
<b>Test (5)</b>	0.86	0.84	8.95	3.28	0.36	5.4
<b>Test(7)</b>	0.92	0.93	13.73	3.63	0.27	7.05
<b>Test(8)</b>	0.84	0.86	12	3.36	0.28	6.34

**5.2.4.ii Local thermal comfort:**

In certain circumstances, the movement of air can be pleasant and reassuring, but in other circumstances, it can be unwelcomed and cause discomfort. Local draft causes cooling effect to the skin by convection,

which is dependent on the temperature difference between the air and the skin. This undesirable air movement is known as a "draft," which is one of the factor effects on the thermal comfort. It is most noticeable when the entire body's thermal sense is chilly.

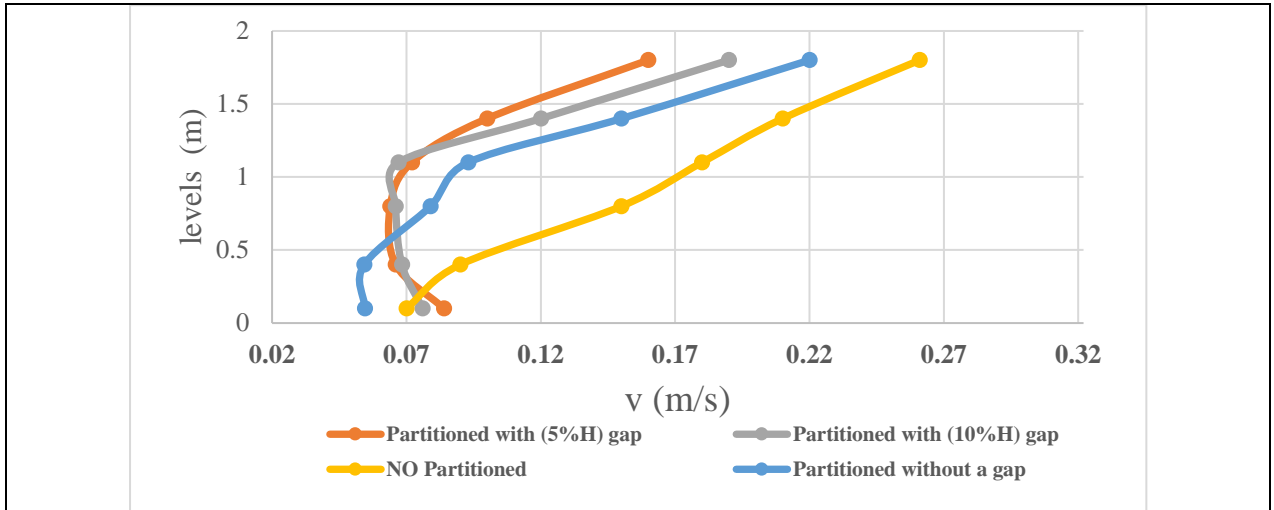
People are more likely to feel a draught on uncovered body parts, such as their hair at head level, neck at chest level, and legs at ankle level. However, this experience also depends on the air speed, air temperature, activity, and clothes; As a result of high air velocity (more than 0.2 m/s) and an operational temperature lower than (23 °C), occupants may be subject to local draft (ASHRAE 2013). Present study checked such an undesirable issue; by examining the amount of air speed for the most important six levels inside the room, starting from the level of the head, which is close to the high-speed air entry opening in accordance with the ventilation system type.

The investigation was conducted once in the case of the room without a partition, and a second when there is a partition without a gap, third and fourth when there is a gap about (5%H, 10%H) of the room's height respectively. Before the partitioning that was done for this study, the average air temperature ranges were as follows: (22.6°C) at the neck, (22.7-22.8) at the middle of the body, and (22.8 - 22.7) at the bottoms of the feet; the system design has adopted mixing ventilation before partitioning in the present work. People who are wearing appropriate indoor footwear are advised by ISO Standard 7730 to maintain a light floor temperature range of 19–26 degrees Celsius.

It is important to keep in mind that the head close is less possible to have temperature fluctuations and more likely to have local draft as a result of its higher velocity (0.261m/s), as compared with the chest level (0.21 – 0.18) m/s, as showing in subplot(a) of the Fig. (5-16).

It is worth mentioning from the findings that the mixing ventilation system has the advantage that it provides the occupants with an overall draught sense, however, through the findings, it was found that the highest values for all cases, were at the head level (1.8), due to its rounding near the high-speed air entry diffuser, As for the rest of the planes level, it was noted that they are less, in general, all levels were within the safety range, which ensure the non-probability of draft occurrence; This ensures the accurately design that happened in terms of the diffuser work, and its fit place within the room. Furthermore, it should be focus on the effect of adding the partition and the gap on the draft effect; Where the percentage of dissatisfaction, (PD) was calculated from equation (3-24), besides checking these values with the draught chart (Ventilation of Building) for sedentary people wearing normal indoor clothing below in subplot (b) of the Fig.(5-16), for these four tests, it was found that the percentage was (6.59) in case of no partition within the room, when the partition had adopted, (PD) started to reaches to (7.14), and then return to fall down and peaks at (4.7) in test(7) of a gap (5%H), while restarted to raise in test(8) of (10%H) gap to (5.6), as shown in subplot (c); Maximum mean air velocity of (0.25) meters per second are specified by both the (ASHRAE 55-1992) Standard and the (ISO 7730) Standard and an design temperature range of between (22-26°C).

The findings found that mixing ventilation might provide occupants with an overall draught sense. It should be noted that this issue is undesirable because it increases energy usage, besides, the temperature of the draught has a considerable influence on the proportion of unsatisfied, known as (Percentage of Dissatisfied, PD). Figure (5-17) illustrate the speed cases in (z-plane) from the moment of air entry and leaving.



a- mean velocity curves corresponding to each level of tests (1, 5, 7, 8).

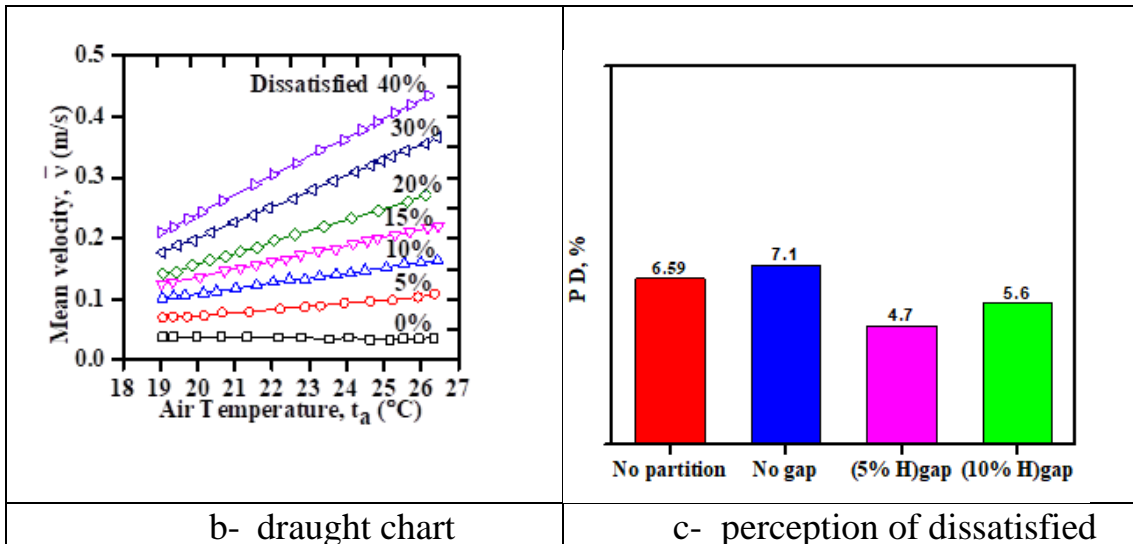
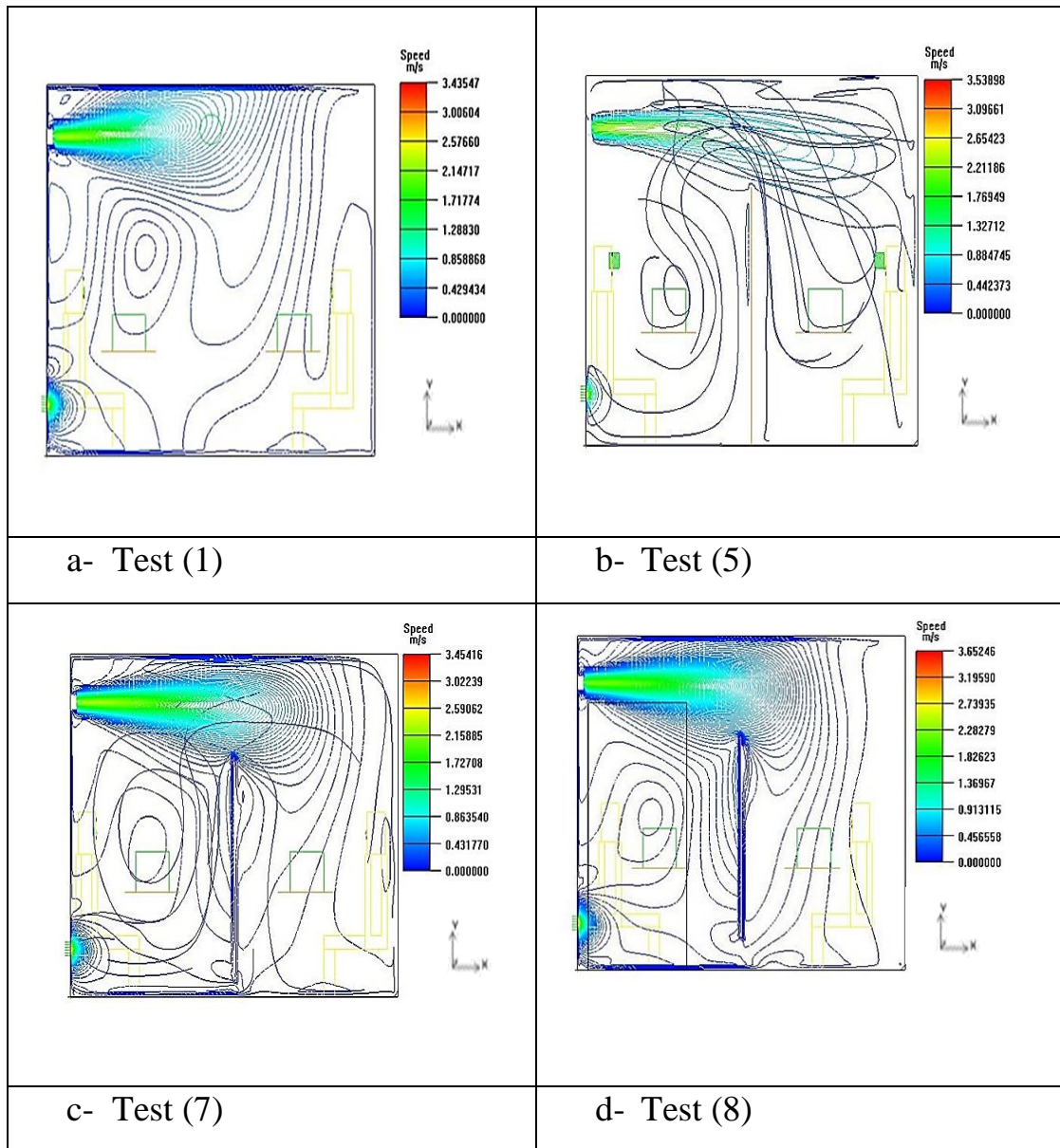


Fig. (5-16) Local thermal comfort charts, and numerical mean velocity curves



**Fig. (5-17)** Illustration of air speed streamlines for the most important tests.

**5.2.4.iii PMV and PPD parameters:**

The internationally recognized (ASHRAE 55) and (ISO 7730) standards for evaluating indoor settings define thermal comfort as "that condition of emotional reaction conveying contentment with the thermal environment." These standards aim to ensure that people have positive experiences when they are inside. As humans, we have an involuntary process that maintains our body temperature. This mechanism causes us to

do things like sweat when the temperature is high or shiver when the temperature is low in order to maintain thermal balance and reduce local discomfort. The human body is capable of adapting to its environment up to a certain limit; but, once that point is reached, the reactions of the body are seen as being unpleasant.

The basic premise of Fanger's notion was that a person's level of thermal comfort could be determined by analyzing their particular metabolic rate, the level of insulation provided by their clothing, and the conditions of their surrounding environment. The (PMV) indicator estimates the median value of a population's votes on a seven-point thermal sensation scale. When the person's internal heat production equals their internal heat loss, thermal equilibrium is reached. (PMV) is affected by different combinations of metabolic rate, insulation, temperature, airspeed. The suggested thermal limits on the (seven points) scale of (PMV) to follow (ASHRAE 55) are between (-0.5) and (0.5).

Once taking into consideration the PMV, one may derive the PPD indicator, in which a numerical estimate of the likely percentage of thermally unsatisfied inhabitants (that is, too warm or too cold), as shown in Fig. (3-22). This can be done after the PMV has been taken into account. (PPD) refers, in its most basic form, to the proportion of people who are likely to meet locally distress. According to (ASHRAE 55), if all indices are utilized.

A thermally comfortable environment can be achieved with an occupant satisfaction level of at least (80%). The remaining percentage of people may experience ten percent discontent owing to local discomfort or partial body discomfort, in addition to ten percent unhappiness due to whole-body discomfort brought on by all of the (PMV) impacting variables listed above. Depending on the PMV that was determined, the PPD might be anywhere from 5 to 100 percent. These levels of comfort will vary from

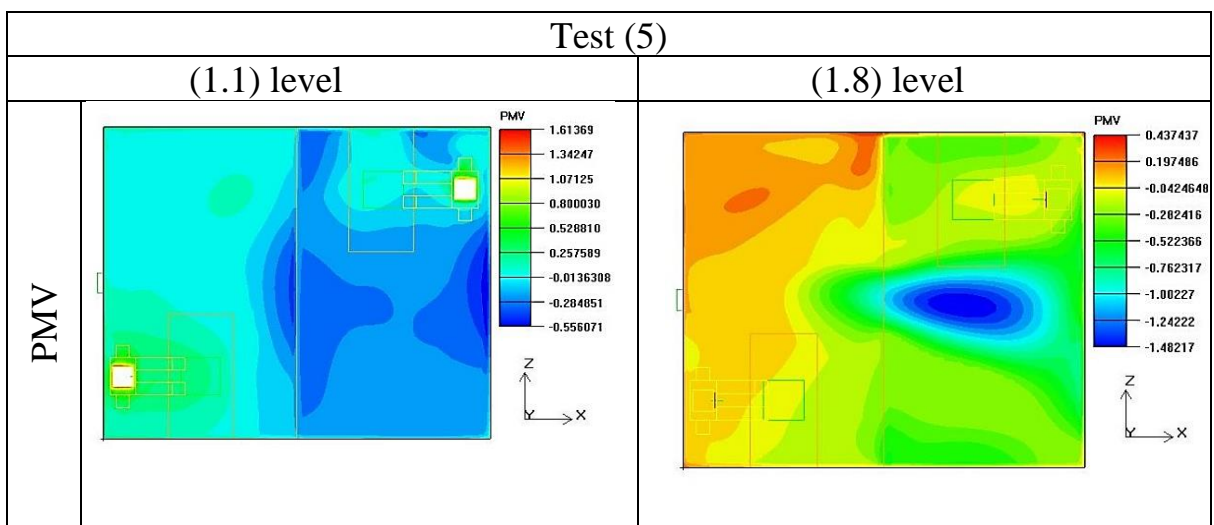
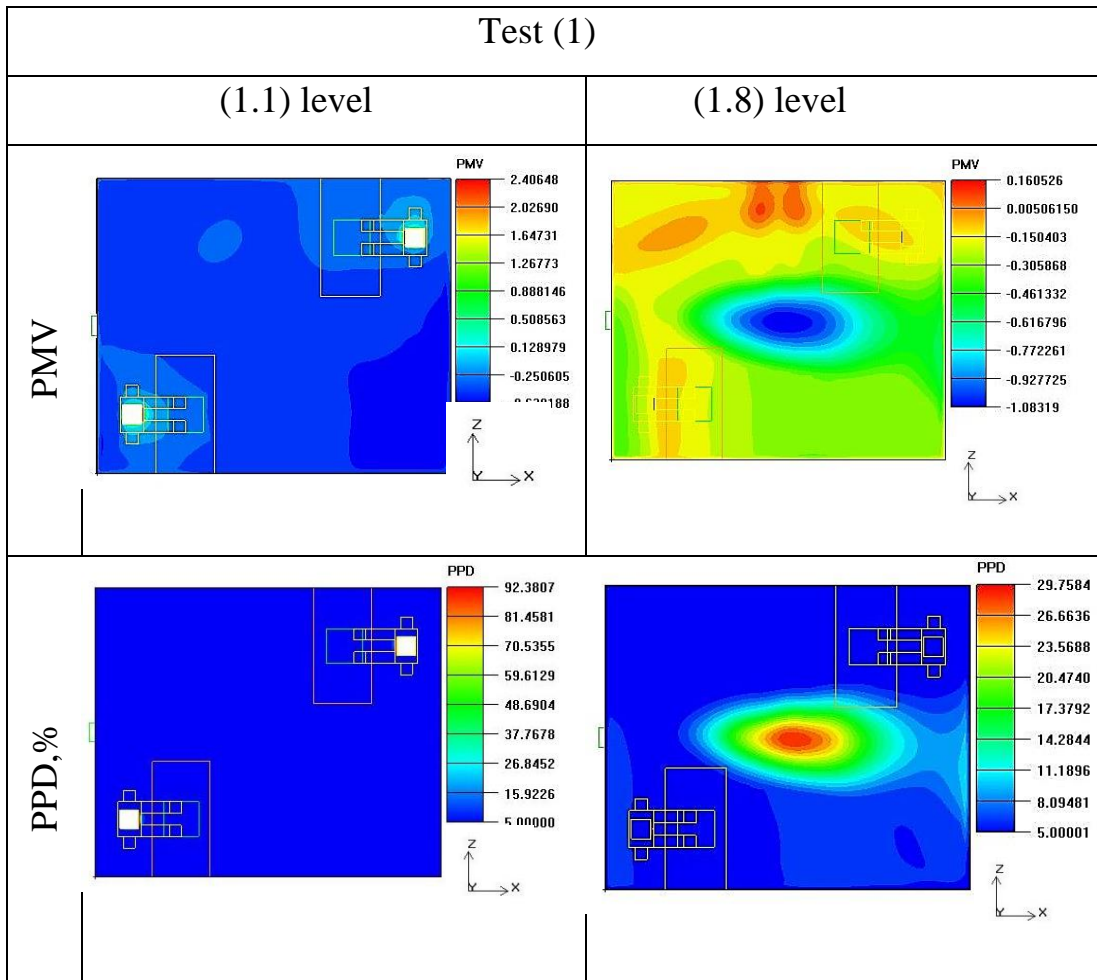
person to person depending on where in the room they are. No occupied spot in the area should be more than (20% PPD) uncomfortable for comfort ranges to meet standards.

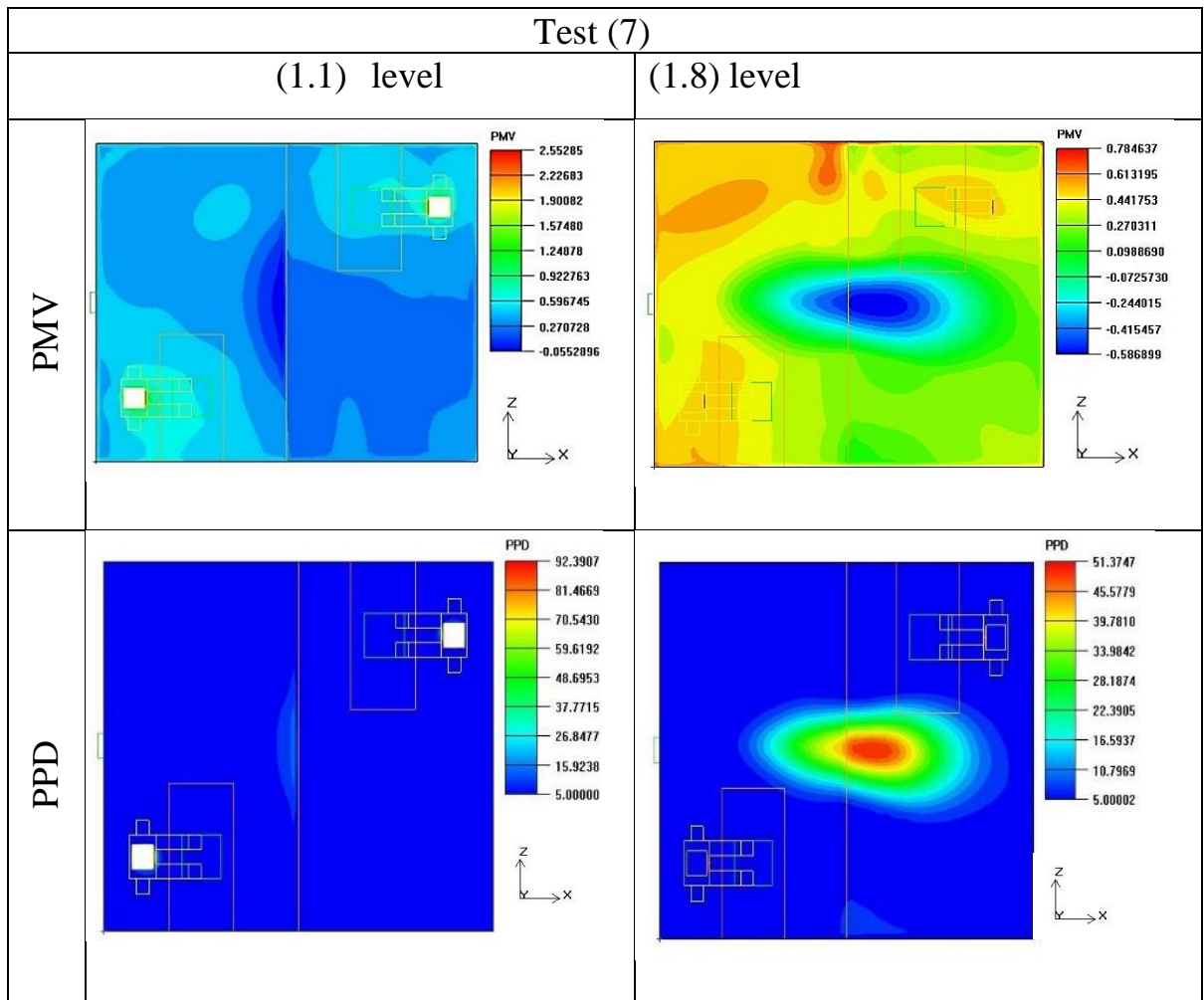
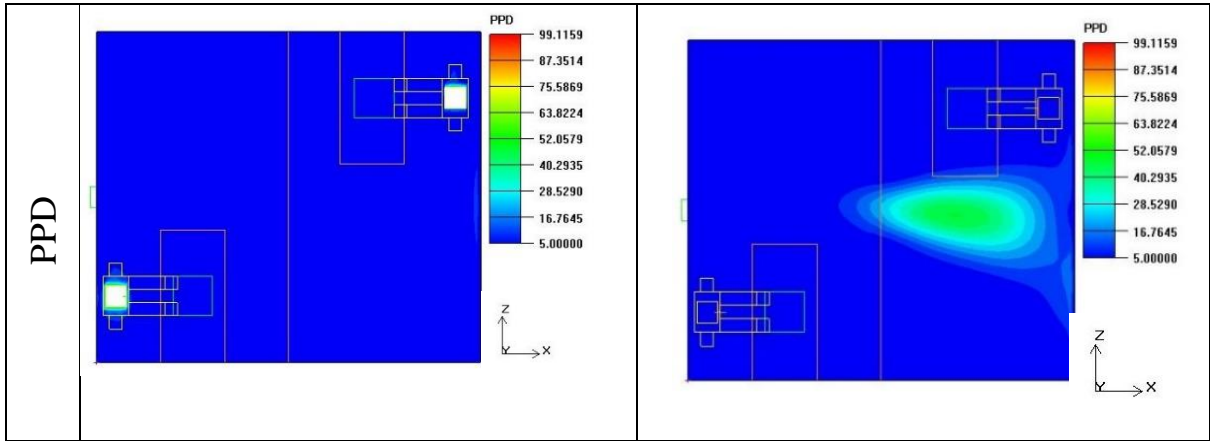
The present study focused on the levels of breathing zones, in the case of sitting and standing person levels to evaluate the (PMV), and (PPD) as illustrated in Fig. (5-18); Table (5-2) listed the (PMV) and (PPD) values for both (1.1 and 1.8) level. By comparing the results obtained with the scheme drawn in chapter (3), it turns out that in case of office room before partitioning, the (PMV) value is about to far away from the accepted range( neutral), and about to reach (slightly cool) range; and when the partition has adopted, the (PMV) value moved closer to the (Neutral) range , especially at (1.1)m at breathing zone, and this acceptability was stabilized at gap of( 0.05 of the room's height) , where an acceptable and reasonable value of (PPD) has obtained in both level of breathing zone (1.1 and1.8).

Fig. (5-19) show the effect of partition gap's height adoption to changing the (PPD) value, the column in pink color represents the test (7) of partition gap's height of (0.05 of the room's height) PPD equals to (5.26) as a more acceptable value, since it begins to reraising in value in test (8) of gap(10%H).

**Table (5-2)** PMV, PPD at breathing zone levels values for each important test.

Test	Levels	PMV	PPD
<b>Test (1)</b>	1.1	-0.275	7.07
	1.8	-0.383	8.76
<b>Test (5)</b>	1.1	-0.018	5.01
	1.8	-0.204	6.21
<b>Test (7)</b>	1.1	0.104	5.36
	1.8	-0.041	5.07
<b>Test (8)</b>	1.1	0.024	5
	1.8	-0.082	5.23





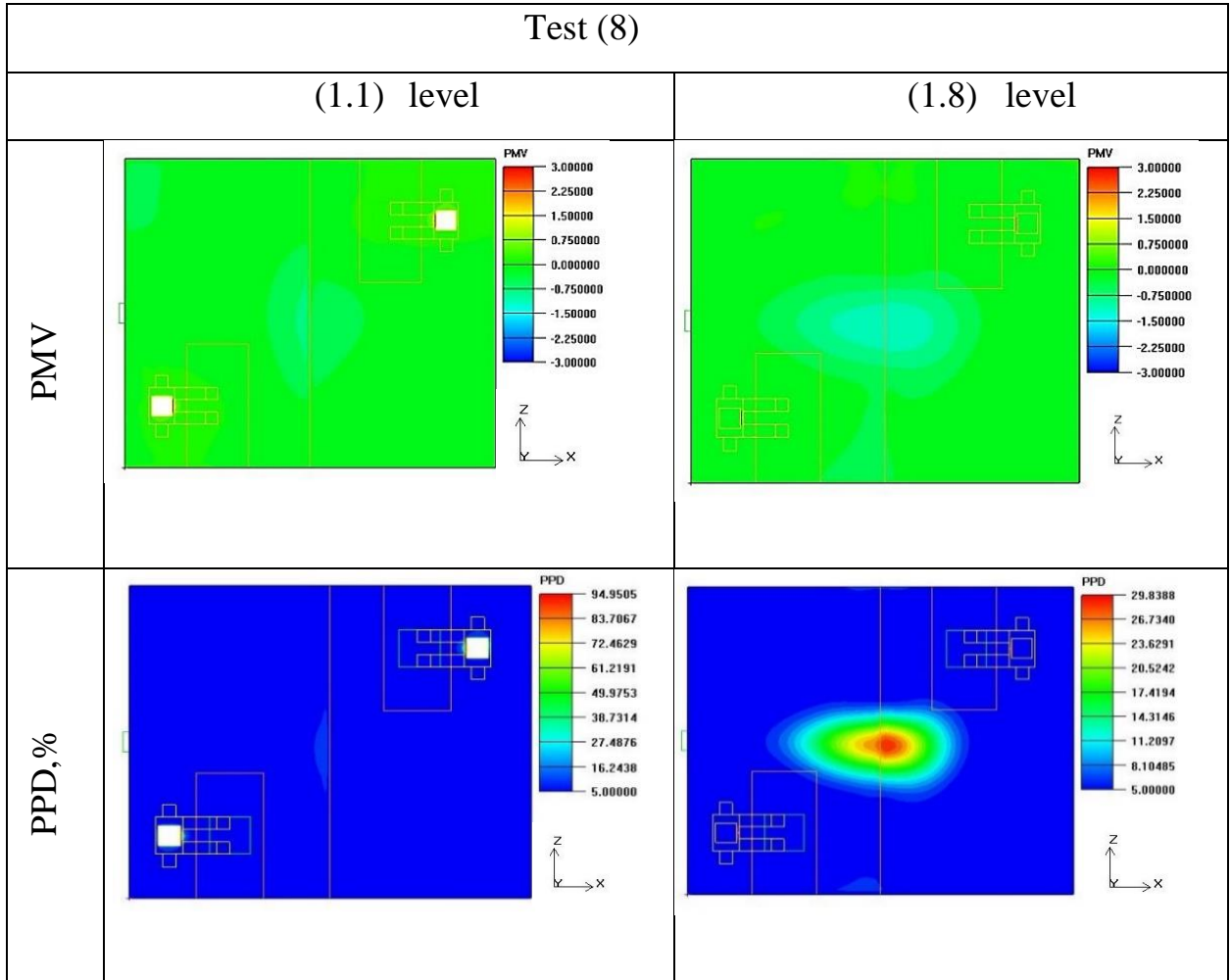
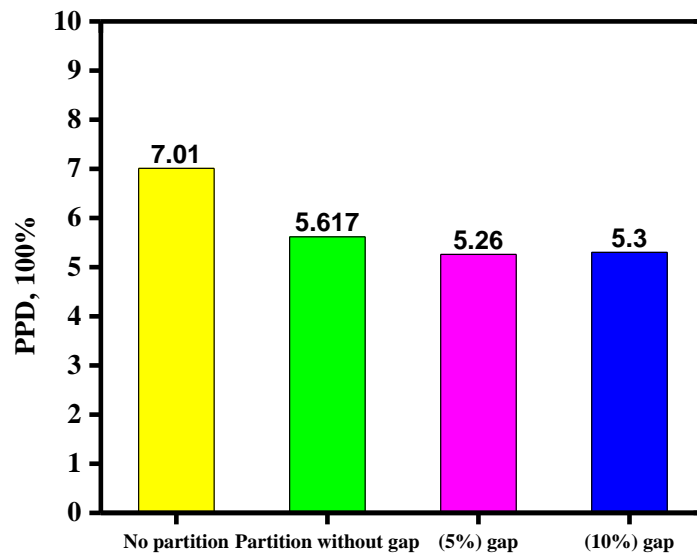


Fig. (5-18) PMV, and PPD contours for case(I) testes



**Fig. (5-19)** (PPD) and partition adoption effect relation.

### 5.3 Experimental Results:

The diffuser which delivers high-speed air, positioned in the middle of the north side wall, as illustrated in Fig. (4-6), where the speed and temperature of the diffuser-supplied air were (2.5 m/s), and (17 °C), correspondingly. Inside the room, three poles were employed, and the temperature was checked at six different heights in each pole ranging from (0 to 1.8) m. Fig. (5-20) illustrates the connection between air temperature and height for three poles, since the average temperature were calculated for three poles in each height level. Because of the cold air supply, the air temperature in the higher floors of the room, is lower. The recorded temperature is somewhat higher at the lower levels due to the heat sources inside the room and then begins to fall as the height from the floor increases due to the presence of an air distributor. According to the results of Fig. (5-20), the temperature increased with the rise in height from (0.4 to 1.1) m, because of heat gains caused by heat sources inside the room, the heat plumes

rose upwards where the hot air is less dense than the cold air. The air temperature continues to fall again because of the preparation of cold air near to the roof of the room, resulting in a uniform temperature distribution. The closest curve to the conditions corresponding to (ASHRAE 2013) standard was the blue one. Both of heat removal efficiency and ventilation efficiency, were calculated experimentally before and after adopting the partition, as well as for each case of gap scenario; as shown in the chart below, Fig. (5-21); and found that both reach their peak values in the case of (5%H) gap which the heat removal efficiency, and the ventilation efficiency increased by (17%,18%) respectively as compared to the case room without partition; and these percentages began in decreasing in case of increasing the height of the gap (10%H) gap.

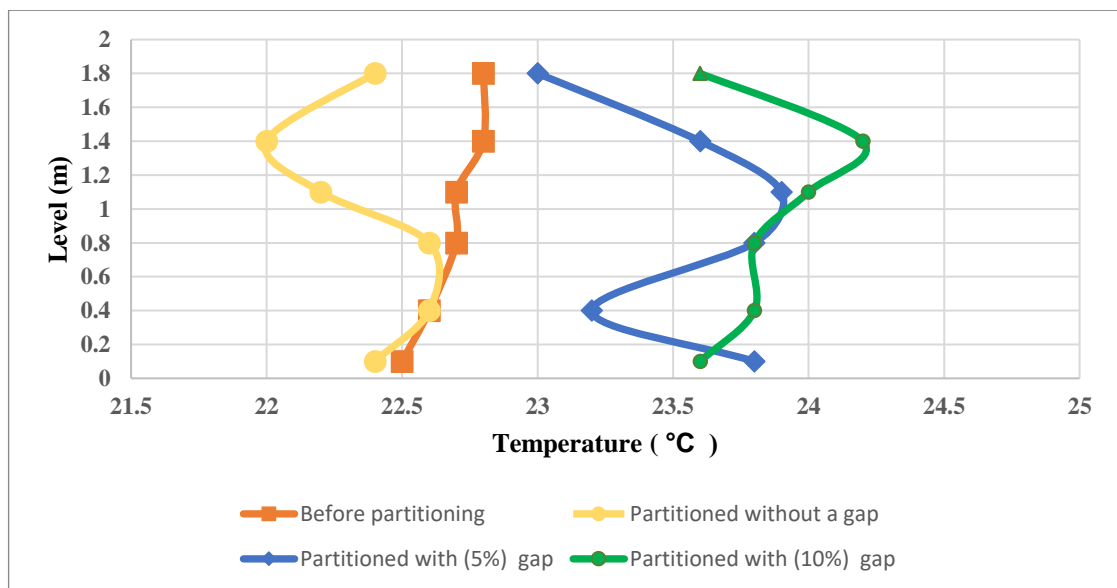


**Fig. (5-20)** Air temperatures curves for each experimental test.

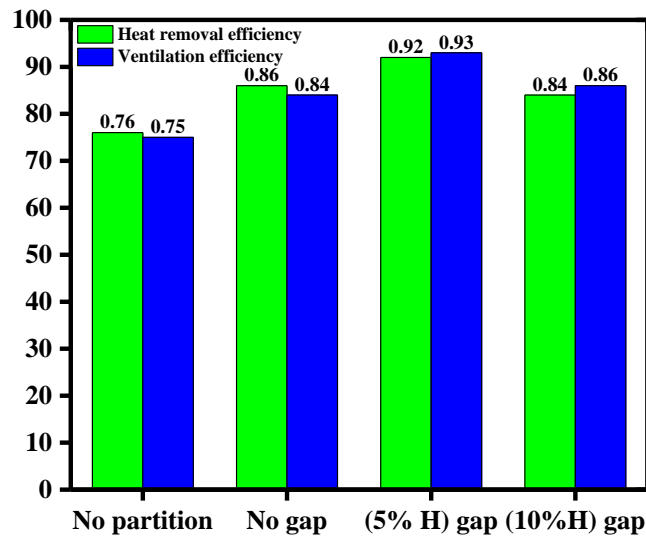


**Fig. (5-21)** Heat removal efficiency ( $\epsilon_t$ ), and ventilation efficiency's ( $\epsilon_c$ ) charts for each experimental test.

### 5.3.1 Average percentage deviation between numerical and experimental results:

The disparity between computational and experimental results might be attributable to a variety of factors, including measuring equipment error, fluctuations in air supply temperature and velocity from the diffuser, and the normal inaccuracy in CFD software running. Using Eq. (3-25), two experimental parameters for the insulated testing room at three measurement poles were used to calculate the percentage average of error between experimental and numerical findings (temperature distribution with height, and CO<sub>2</sub> concentration).

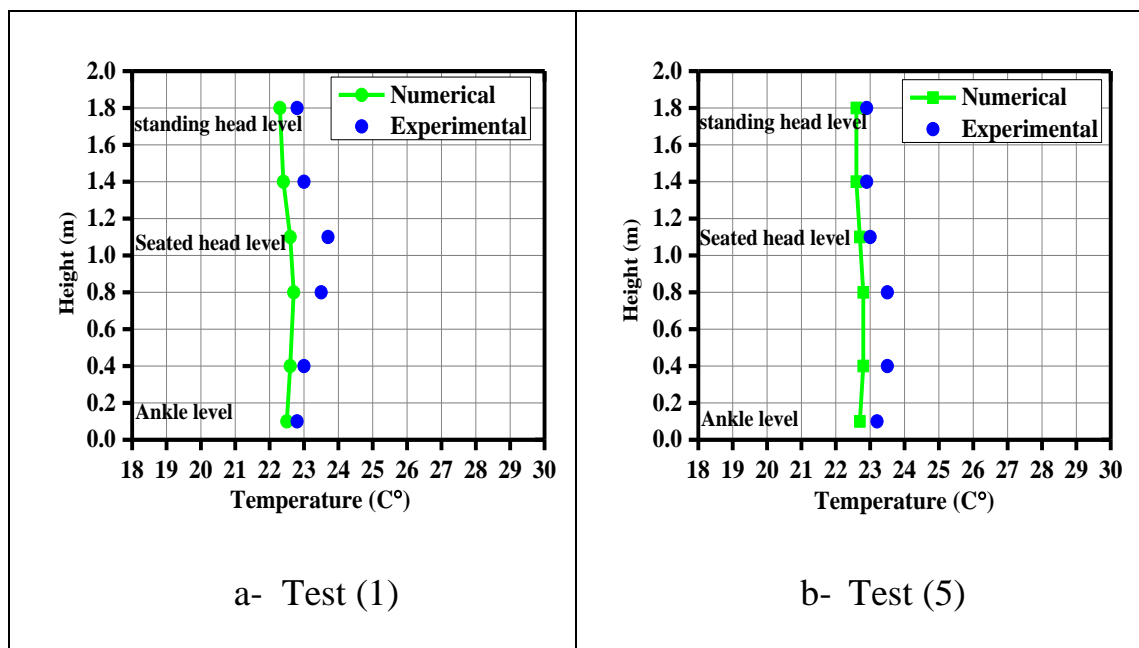
### 5.3.2 Percentage average error for temperature distribution:

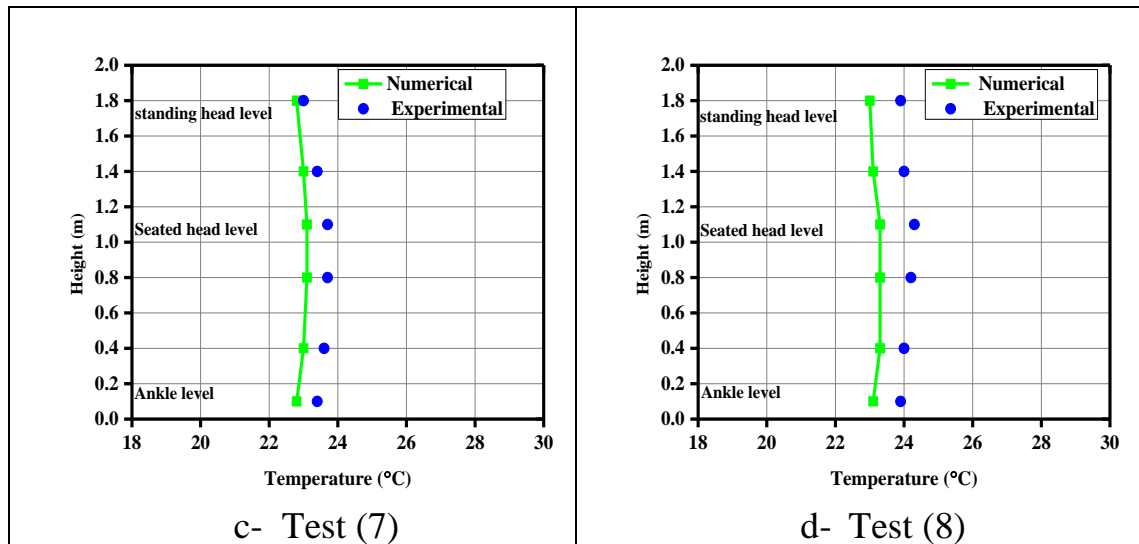
Six points were used to calculate the average error on three measuring poles, with six points at the breathing zone for set and stand person (0.1m to 1.8m) height being the level of breathing zone at each pole, sitting and

standing individuals. The Fig. (5-22) which has four parts (a to d) show the deviation between numerical and experimental findings in every test, at three different measuring stands in the office room.

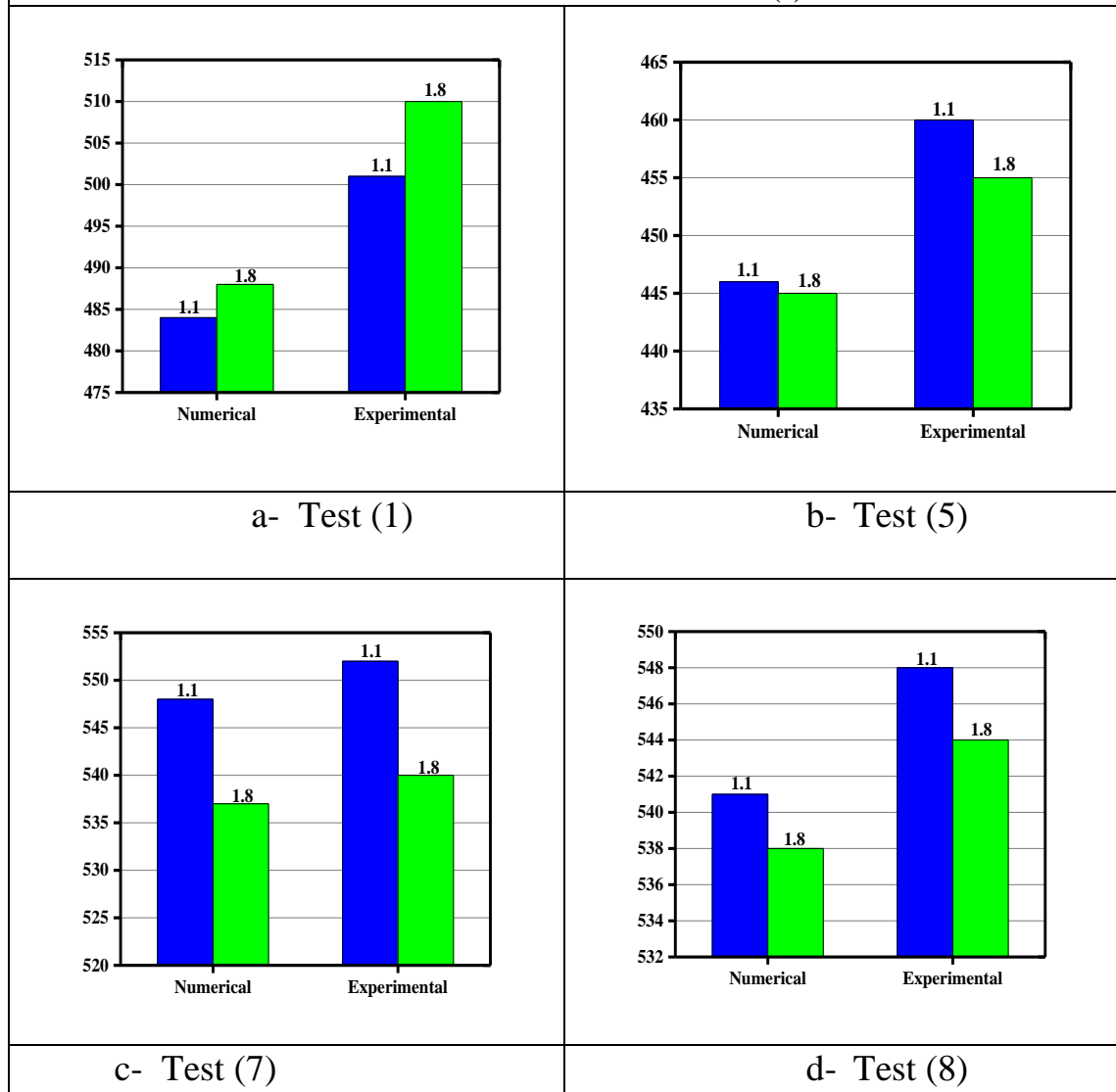
The percentage of error was (2.95%) in case of insulated room before partitioning, then it has been reduced by (0.39) in the test of (5%H) gap; whereas the Fig. (5-23) which contain four parts (a to d) show deviation between the numerical and experimental results for Carbon dioxide concentration of the insulated room. From the diagrams shown below (a to d) it found that the closest numerical test correspond to an experimental reality is the subplot (c) where the average error was (1.46%) in the test of (5%H) gap as a minimum value.

Table (5-3), and (5-4) show the percentage average error for temperature distribution and CO<sub>2</sub> concentration. Because of the irregularities in air supply velocity and supply carbon dioxide that subtracted from the two manikins during the experimental, respectively, these percentage average errors are reasonable.





**Figure (5-22)** Temperature distribution deviation between experimental and numerical results for case (I)



**Fig. (5-23)** CO<sub>2</sub> concentration deviation between experimental and numerical results for case (I)

**Table (5-3)** Percentage average error between experimental and numerical results for temperature distribution for case (I)

Test	$T_m(^{\circ}\text{C})$		Average error, %
	Numerically	Experimentally	
<b>Test (1)</b>	22.7	22.9	2.95
<b>Test (5)</b>	22.46	23.01	2.61
<b>Test (7)</b>	22.98	23.13	2.56
<b>Test (8)</b>	23.18	23.4	3.81

**Table (5-4)** Percentage average error between experimental and numerical results for carbon dioxide concentration for case (I).

Case	$\text{CO}_2$ mean, (PPM)		Average error, %
	Numerically	Experimentally	
<b>Test (1)</b>	486	505.5	3.85
<b>Test (5)</b>	445.5	457.5	2.62
<b>Test (7)</b>	539.5	546	1.46
<b>Test (8)</b>	538	546	2.38

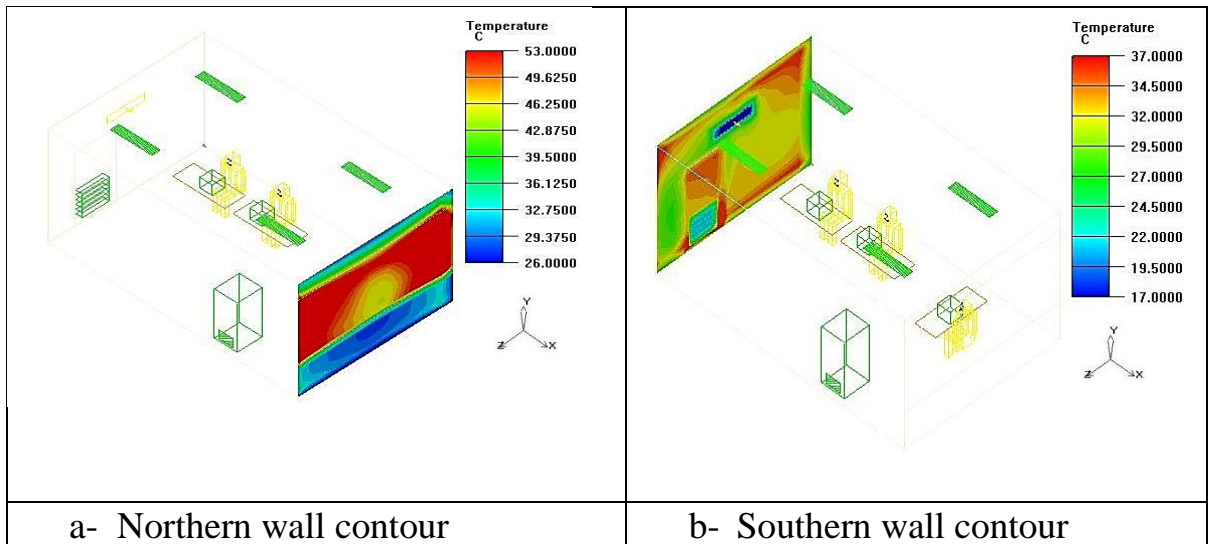
#### 5.4 Numerical Results for Non-insulated Office Rooms (Case II):

Mixing ventilation system, and partition adoption has simulated on two kind of non-thermally insulated office room, that grounded in reality; one of them is a room for a group of professors, inside the building of faculty of engineering, Department of Mechanics, at University of Babylon. And the other is an exchange and financial transfer office room, which locates at the downtown of Hilla city; by using (AIRPAK3.0.16) software program, and (RNG  $k-\epsilon$ ) as a turbulence model.

The goal of the simulation of actual office rooms is to know the impact of the partitions adoption with the presence of the mixing ventilation system on the thermal comfort parameters, also indoor air quality (i.e., PMV, PPD, ADPI, ADI, VP) in addition to calculating the heat removal efficiency( $\epsilon_t$ ), and contaminant removal efficiency( $\epsilon_c$ ).

Fig. (5-24) show the contours of temperatures and speed distribution around the office room for test (9), the subplot(a-b) below shows the chromatic scale of temperatures contour for each of the northern wall, which contain a window exposed to external conditions in which the mean temperature reaches to ( $45^{\circ}\text{C}$ ) inside the room, and the southern wall overlooking to a corridor, and containing a door with exhaust grille in which the mean temperature reach to ( $31.6^{\circ}\text{C}$ ).

After cooling loads had calculated according to Iraqi hot and dry climate. subplot(c,f) represents the (z-plane) contour of temperature, and speed distribution, from the moment the fresh air enters the room through the inlet air diffuser, and outlet exhaust grille respectively. Since the fresh air enters the office room with mean temperature, and speed of ( $18.7^{\circ}\text{C}$ ,  $0.857\text{ m/s}$ ) respectively, each of the air inlet, and exhaust grille contours was illustrated below separately, as they are not on the same plane direction.



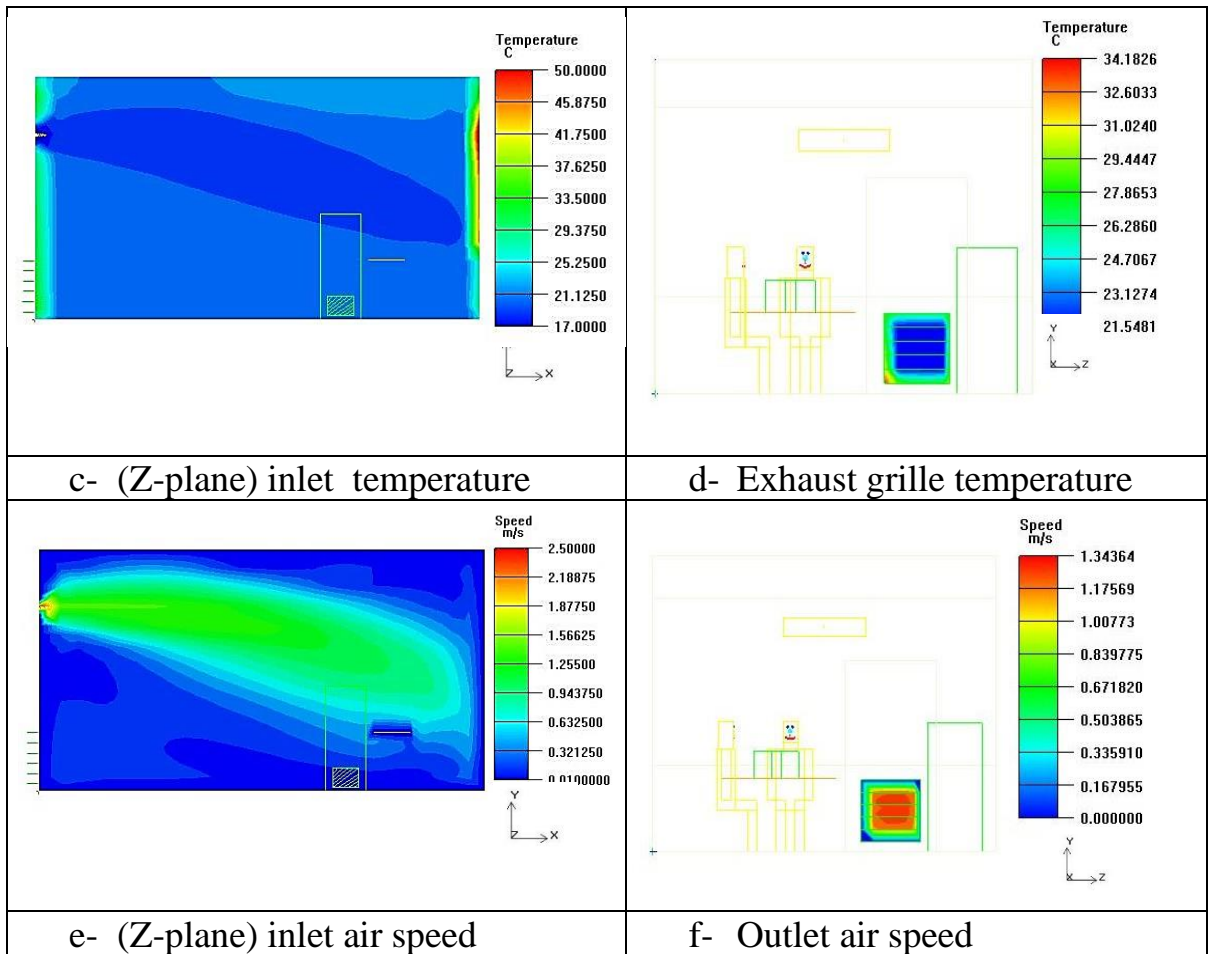


**Fig. (5-24)** temperature distribution, and speed contours around the non-insulated office room.

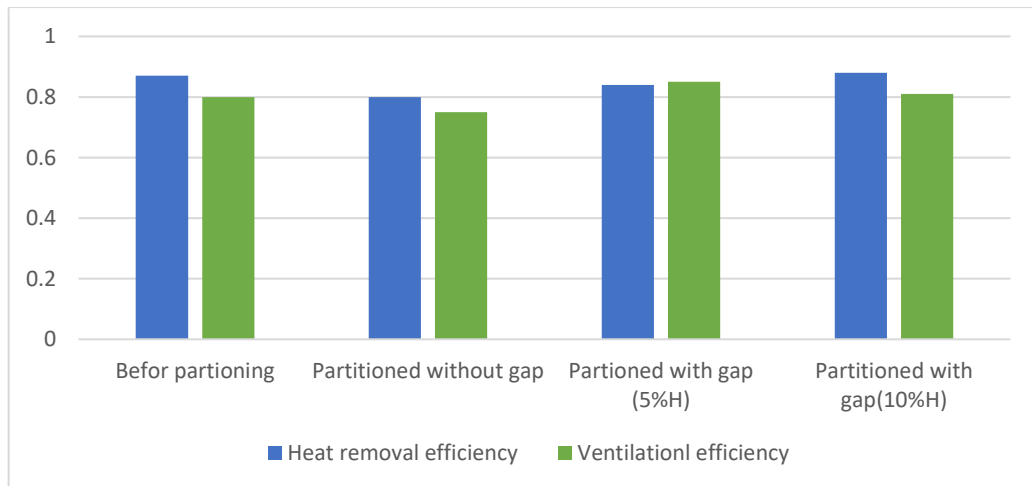


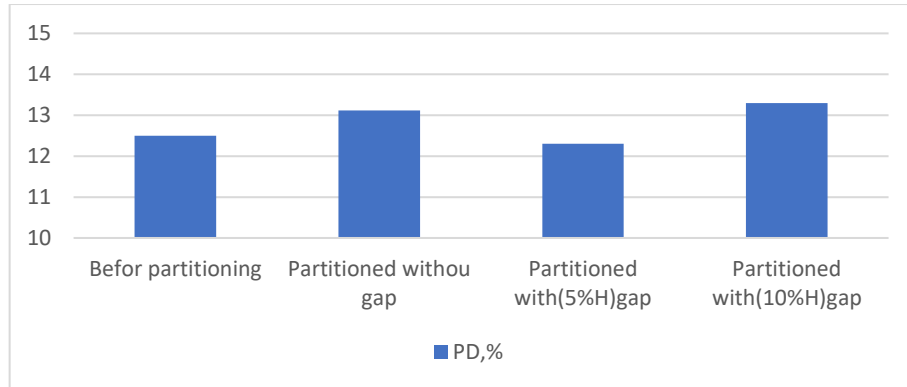
**Fig. (5-25)** Heat removal efficiency, and ventilation efficiency for each test of case (II).

### 5.4.1 Locally draught discomfort:

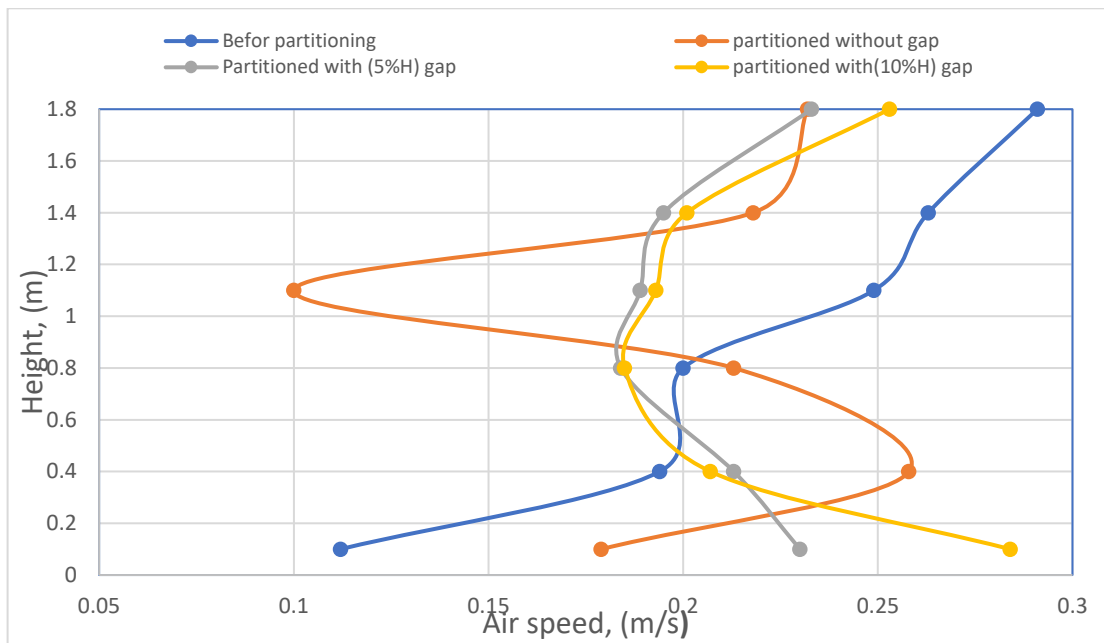
After the results of mean velocity values in every planes of the occupied zone has calculated, and for each tests of non-thermally insulated room; it was found that through the the blue curve in the diagram below Fig. (5-27), there are two high values in case of the office room befor partitioning which are (0.28), (0.291) in the sitting head planes (1.4), and standing head planes (1.8) respectively. Since they are exceeded the acceptable range of (0.25) m/s, according to ASHRAE Standard (55-1992) in addition ISO Standard (7730), both are illustrated in subplots (a,b) of the Fig. (5-28), after the office room has partitioned the highest values began to fall down and be in stable value to (0.218),(0.232), however, in such test, there was found another raising in mean velocity on the legs plane(0.4) as shown in the orange curve of the Fig.(5-28), which is reached from (0.194) to (0.258).

such rising showed the advantage of the gap adoption to the partition , since the latest rising has reduced to (0.213) besides all the remaining planes, as illustrated in the grey curve which is centered the diagram of the Fig. (5-27) , as well as in subplots (c,d) of the Fig.(5-28) showed how the draft has reduced from(0.258) to (0.213) before and after adoption of the gap of (5%H), and when focused on the contours, its noted the reason of such rising is might be the exhaust grille, since more of the consumed air is sucked to the exhaust, that is caused higher air speed in such plane (0.4),exactly at the center of the exhaust grille opening, the more gap height the more chance air to move under the partition, and more uniformly to distribute in more space area as a result to reducing the locally draught discomfort. While the subplots(e,f), and the yellow curve, had shown that in case of further increasing of the gap's height to (10%H), rerising in the mean speed value found for each of the (0.1), (1.8) planes again. That is gave the priority of (5%H) case of a gap adoption on the other scenarios with support from the

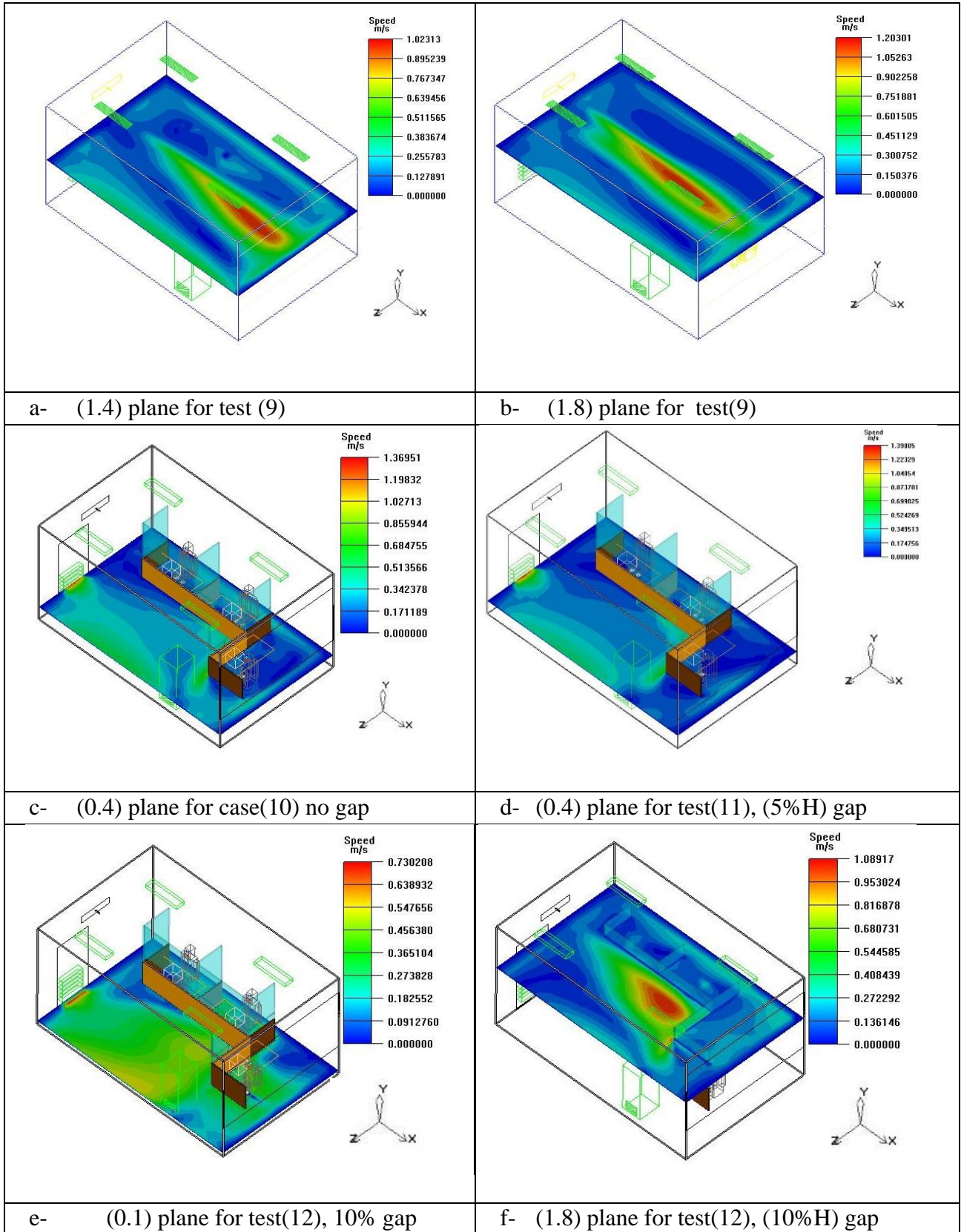
(PD, %) for each case, as has done in the Fig. (5-29), where (12.3%) as a lower acceptable value obtained.

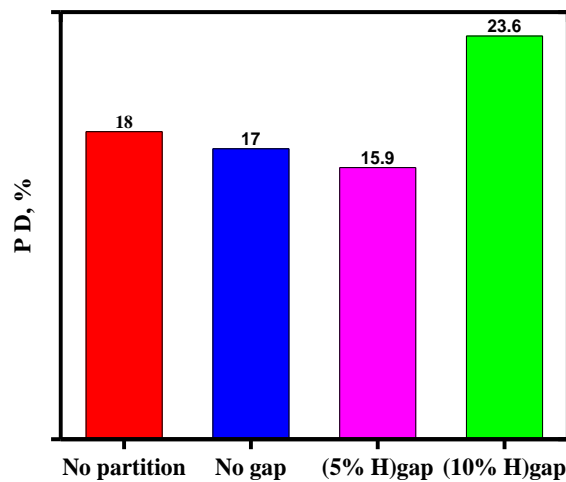


**Fig. (5-26)** Perception of dissatisfied for local thermal discomfort.



**Fig. (5-27)** Curves of mean air speed for each tests of case(II).



**Fig. (5-28)** Draught thermal discomfort for each test of case(II).**Fig. (5-29)** Percentage of dissatisfied, (PD) effect with partitions adoption.

#### 5.4.2 PPD and PMV:

After the results of (PMV, PPD) had obtained numerically, for the non-thermally insulated office room, before and after partitioning. It was found that the value of the thermal comfort parameter representing the (PMV) reached to (-0.7) which is close to the slightly cool range, and began to enter the neutral range (-0.5 to +0.5) according to (ASHRAE 55) in the moment of partition adoption at (-0.3) as a closer value to the acceptable range. Both of the thermal comfort parameters (PMV, PPD) had changed noticeably to (-0.25), (13.3%) respectively as more acceptable values which are closer to the global range of thermal comfort, as listed in Table(5-5)

**Table(5-5)** PMV, PPD values for the non-thermally insulated office room, case(II).

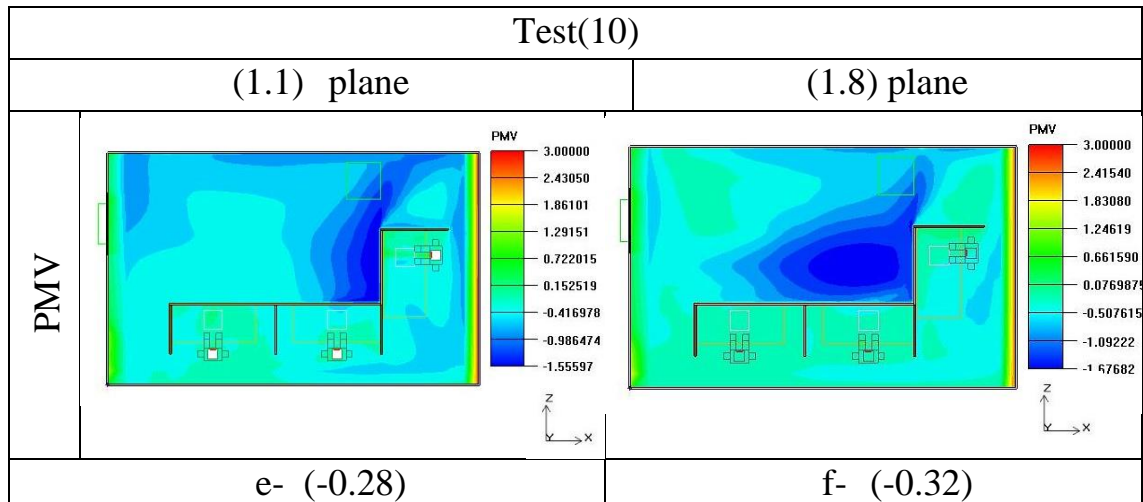
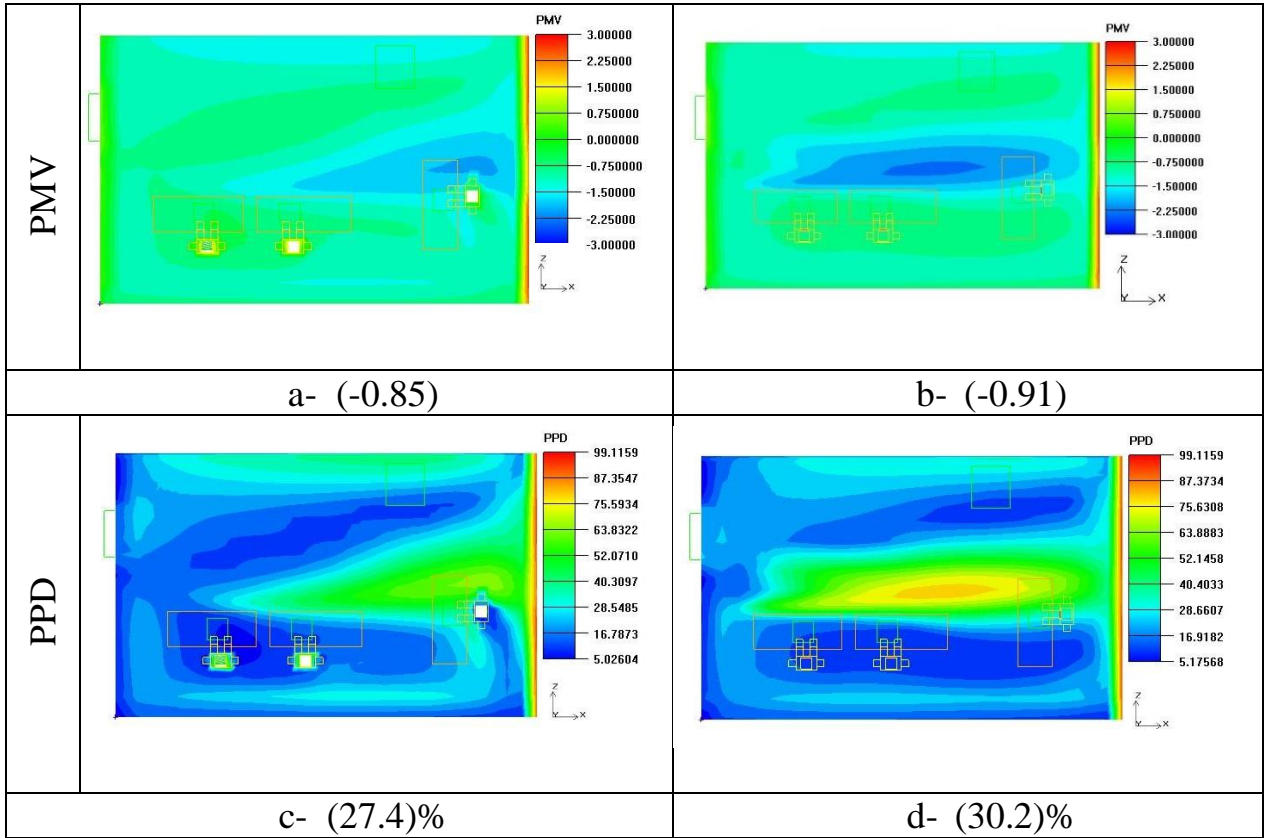
Parameters	Test(9)	Test(10)	Test(11)	Test(12)
PMV	-0.7	-0.30	-0.25	-0.34
PPD, %	26.4	13.9	13.3	13.6
ADPI, %	73	67	75	73

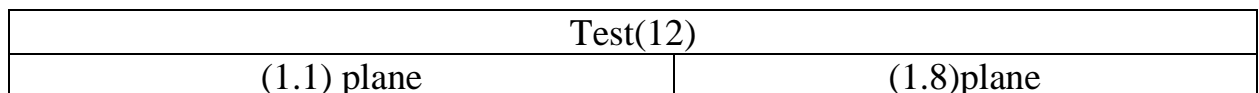
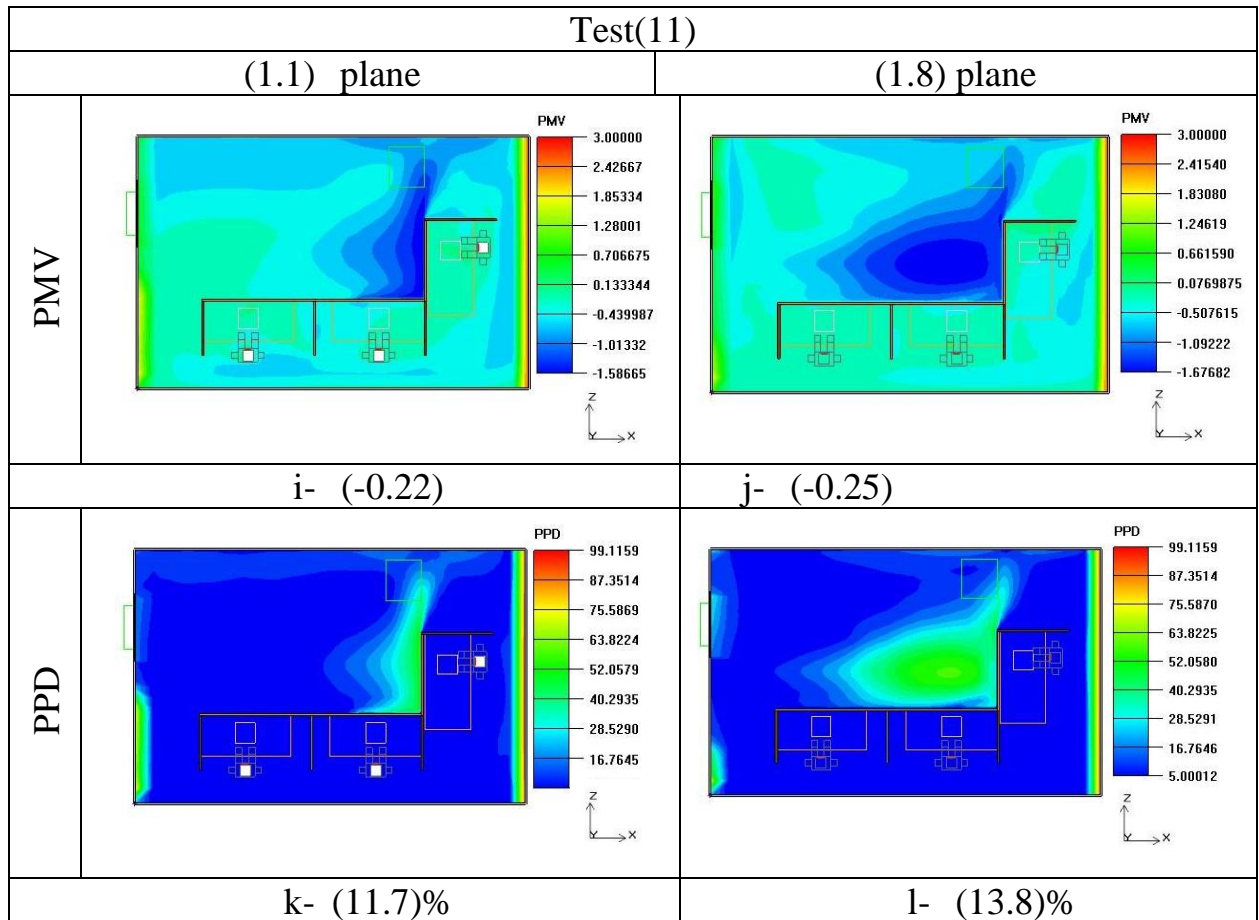
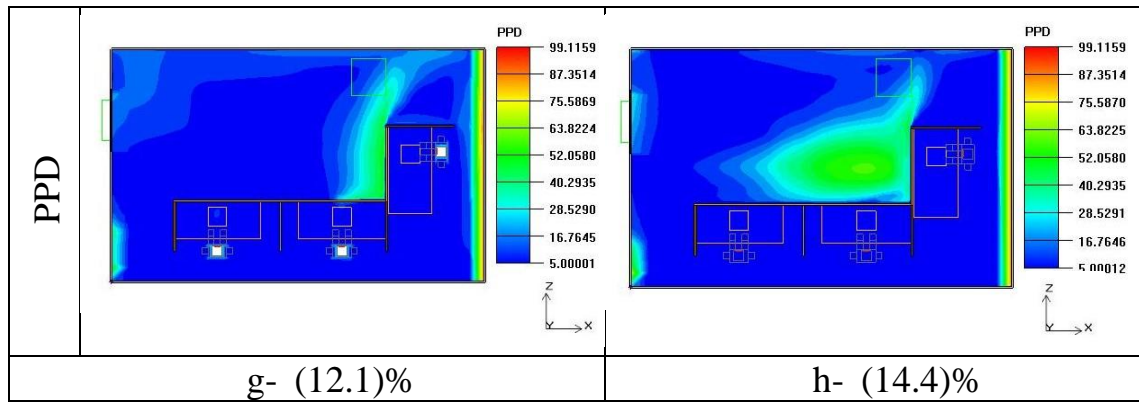
The contours of Fig. (5-30) from (a to p) show thermal comfort criteria for breathing zone levels for (1.1) when the ( plane cut) is positioned on a seated head level and an standing head position. Found that the higher values for both were obtained at (1.8) plane due to the reason of its proximity to the air diffuser inlet, hot air rises to the top, where it's light density. However, the study resorts to choose a study case in which both the (1.8), and (1.1) planes within the acceptable ranges, to assure the thermal comfort of both sitting and standing employees. Highest value to (PPD) were found at (1.8) planes for all the cases as illustrated in subplots(d), and (p) which are not acceptable values.

the study targets to get a percentage less than(20%) closer to (10%) in case of (PPD), and neutral range(-0.5 to +0.5) according to(ASHRAE55, and ISO7730) standards, these findings had obtained as illustrated in subplots (i )to (l), since the (PPD) value reached to (11.7) at breathing plane(1.1) which is closer to (10%), while the (PMV) values reached to (-0.22) to (-0.25) at both breathing plane (sitting head level), and standing head level respectively.

The diagram of the Fig. (5-31) is explaining how the partition adoption with respect to mixing ventilation effect on the predicted of dissatisfied perception. By the desired descent of the value when a gap is adopted to the partition, where it reaches its peak value and then begins to rise as soon as further height of a gap increases.

Test (9)	
(1.1) plane	(1.8) plane





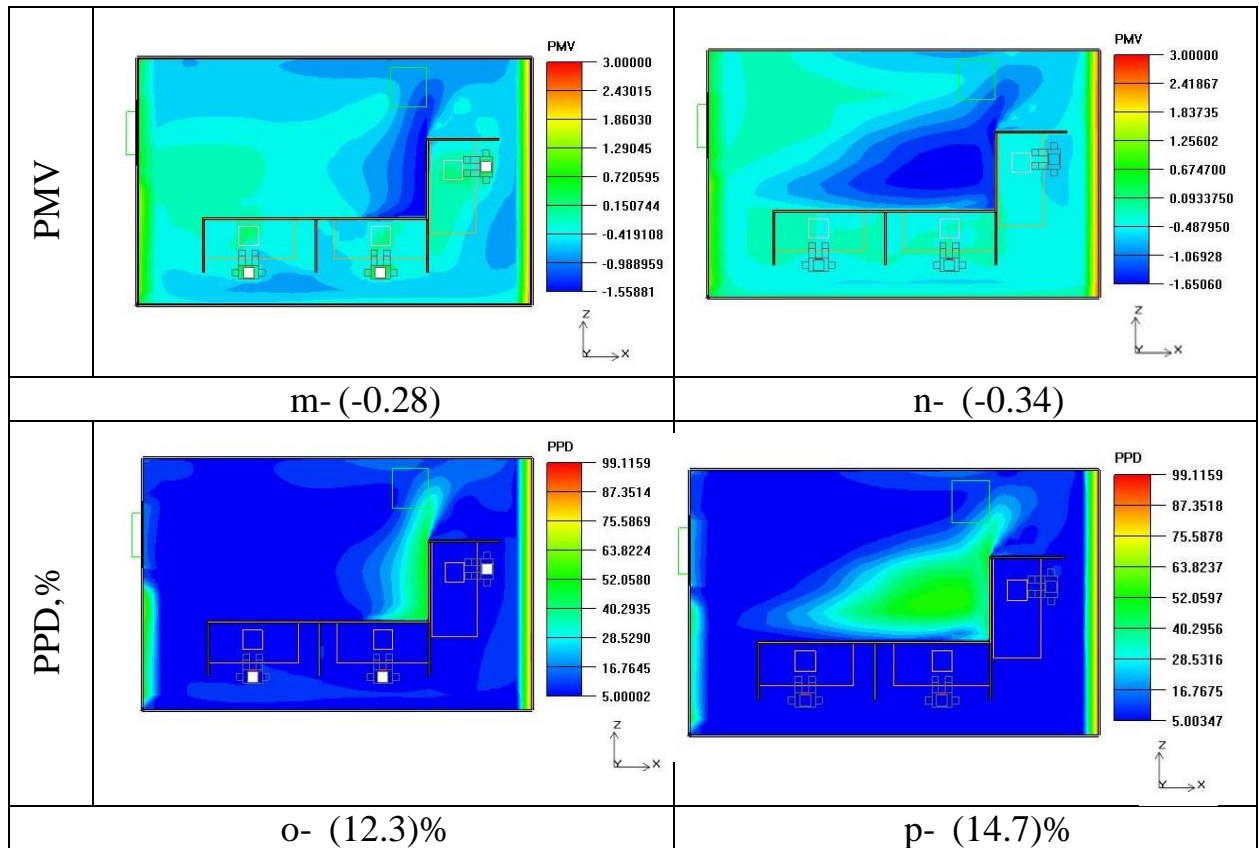


**Fig. (5-30)** PMV, PPD contour for the non-thermally insulated office room

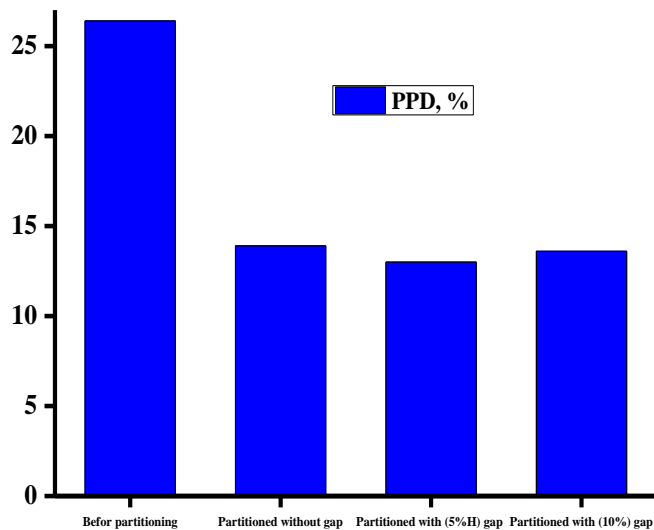


**Fig. (5-31)** PPD, and Partitioning effect relationship corresponding to case(II).

**5.4.3 Air distribution index (ADI), and ventilation performance(VP) :**

Air diffusion index, and ventilation performance has calculated for each cases of the non-thermally insulated room, as listed in Table(5-6), as it known, (ADI) is a metric to calculate uniformity of room air; and that the ventilation system which construct with acceptable (PD) and (PPD) values close to (10%), will have an (ADI) close to (10).

An acceptable value obtained in the test (11) of (4.66) most close to ten from the other cases.

Referring to the (VP) values in the table below, in the case of office room before partitioned the value reaches to (0.96), which close to one , that is refer to the presence of pollutants, and heat distribution balance in the ventilated office room which is reflected in the values of ( $N_t$ ), and ( $N_c$ ).

It's worth noting about the value of (VP) in the case of adoption the room with partition without a gap, which is (0.516), and less than one, indicating that the contaminant efficiency is less than the heat removal efficiency, as in previous explanation, the partition stands as an obstacle for the air moving, as a result increasing the stagnates zone behinds the partitions. The value of (VP) still in decreasing until it reaches its peak point at (0.521), when the gap helped to increasing the value of contaminant efficiency.

Diagrams (a,b) in Fig. (5-32) were drawn for the relationships between indoor air quality indices according to the findings that had obtained, and listed both in Table(5-5), and Table(5-6).

**Table(5-6)** Air distribution index and ventilation parameter, for case(II).

Parameters	Test(9)	Test(10)	Test(11)	Test(12)
<b>VP</b>	0.96	0.516	0.52	0.49

<b>ADI</b>	3.22	4.13	4.66	4.5
$N_t$	3.29	5.75	6.46	6.47
$N_c$	3.17	2.97	3.37	3.213

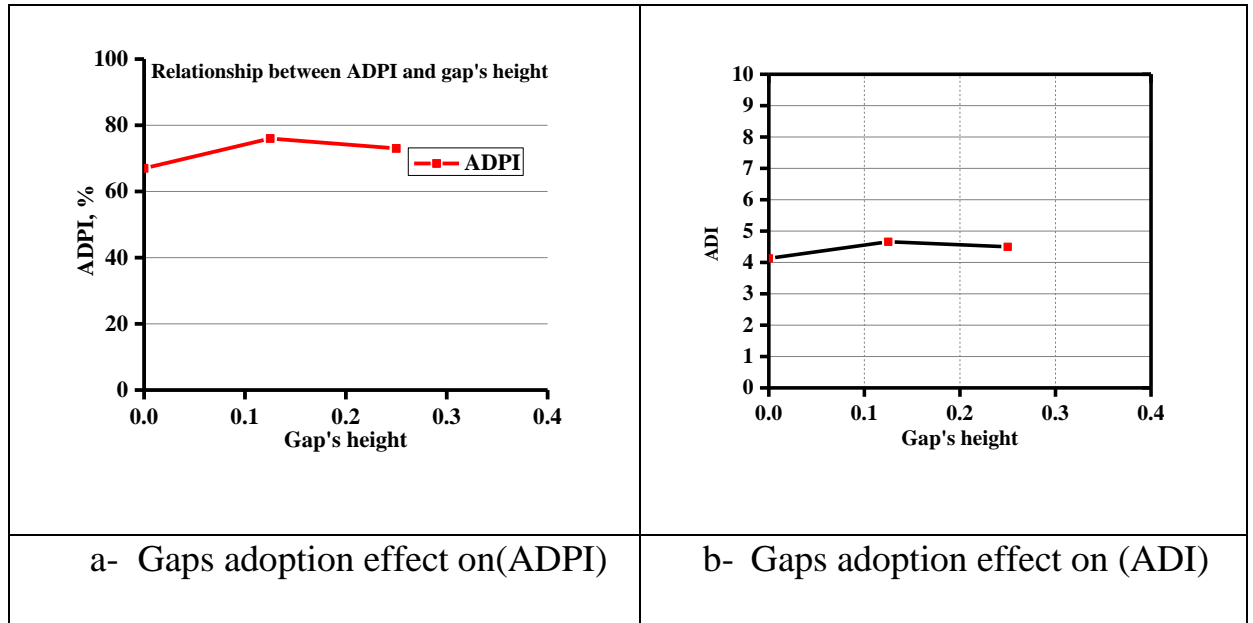


**Fig. (5-32)** Relationship between gap adoption on air distribution indices for case(II)

**5.5 Results for Non- Thermally Insulated Office Room , (Case III):**

The insertion of partitions into non-thermal insulated office rooms, was tested by simulating another actual office room located in the Baghdad center for one of the companies of the financial transfer, by (AIRPAK3.0.16) software simulations, which is a room (9 x 5 x 3), with one window that faces the outside and a door that leads out onto an interior corridor, has ventilation exhaust apertures as showing in the subplots(a to d) in the Fig.(5-33) temperature contours for the northern wall containing a window, besides the southern wall containing a door , as well as the temperature distribution of the exhaust grill. Containing of a group of nine females employee, they work six hours continuously on counting and sorting. Some businesses believe that if it's particularly cool, workers will be more attentive and productive. Scientific evidence, however, refutes this theory.

The effects of chilly workspaces are disproportionately felt by female employees. Current air conditioning systems, according to experts at the University of Maastricht, are a legacy of the (1960s), a time when office occupations were typically held by men. Rooms were therefore maintained at a temperature that a (40-years-old ) man weighing (70) kg would find comfy. For women, who are typically smaller and lighter in weight, the researchers found that this temperature is far from ideal. They become more sensitive to the cold since their metabolic rate is around (35%) lower. According to the most recent research, a pleasant (22)degrees promotes the highest performance on the factory floor.

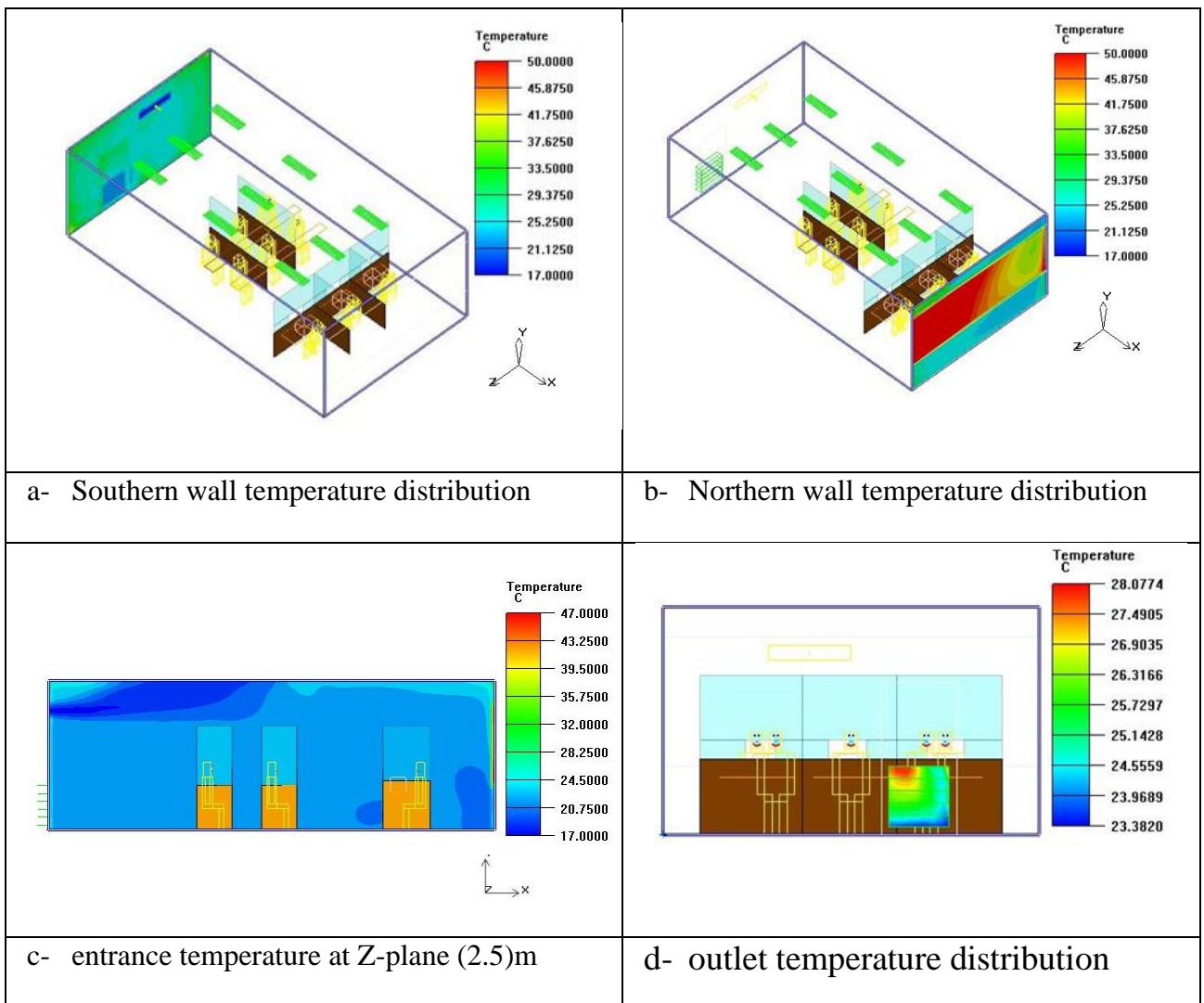
That may reach (24.5) degrees for females. A mixed business should have a room temperature of about (23) degrees, Since everyone is unique, there is no one temperature where everyone feels the most comfortable. However, the Occupational Safety and Health Administration of the United States advises keeping office rooms around (20 to 24.44 )degrees centigrade.

In the current test the same input values will be entered for the previous office unites that is the temperature(17°C), air velocity (2.5 m/s)leaving the diffuser of the ventilation sysytem, only change person's input, which is the thermal insulation from clothes, where the type of clothes used for the simulated emplyees are entered in the (AIRPAK3.0.16) software, according to Table(3-10), and with sedentary activity(office),(clo.) of (0.55) with respect to (ASHRAE -55), and (ISO 7730) reccomendations (0 to 15) and (0 to 2) respectively, and (1.2) metabolic rate(met) according to the same standards of (1 to 2) met. For actively sitting occupants(e.g. office work).

in order to predicts about the conditioning of women's ventilation system by calulating thermal comfort parameters (PMV, and PPD).The subplots (e), and (f) showing the air speed contours at the inlet and outlet. The heat removal efficiency and ventilation efficiency were both calculated

for the studied cases of the office room represented by the case of before partitioned, partitioned without agap, partitioned with (0.05H)gap, and partitioned with (0.1H)gap, that are tests(13 to 16) respectively.

According to the chart drawn below in Fig.(5-34), the addition of the gaps to the partitions enhanced both efficiencies, the higher the gap's height the better the two efficiencies, however, based on the current room's height efficiencies had reached to their peak results in test (15).



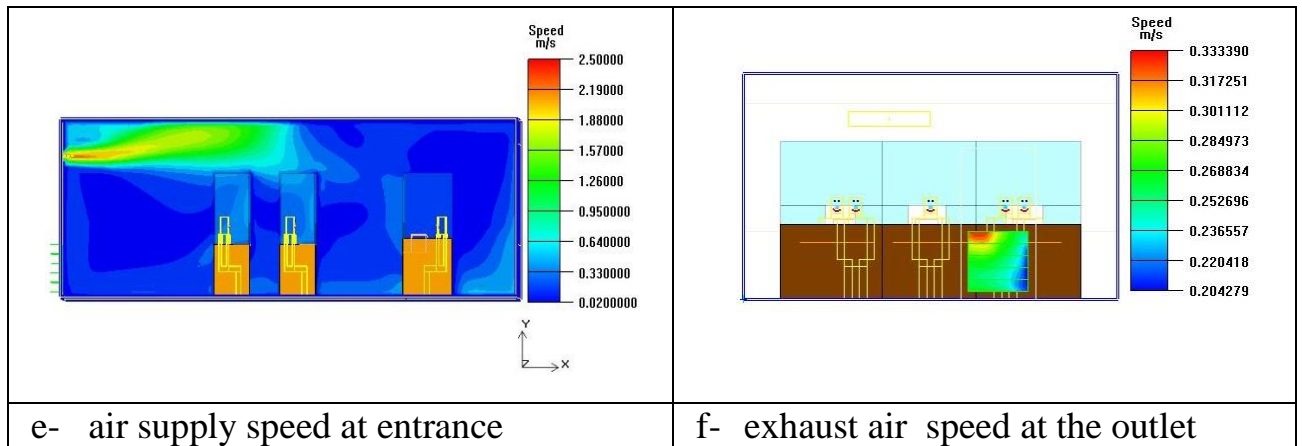


**Fig. (5-33)** Temperature, and speed contours for case(III).

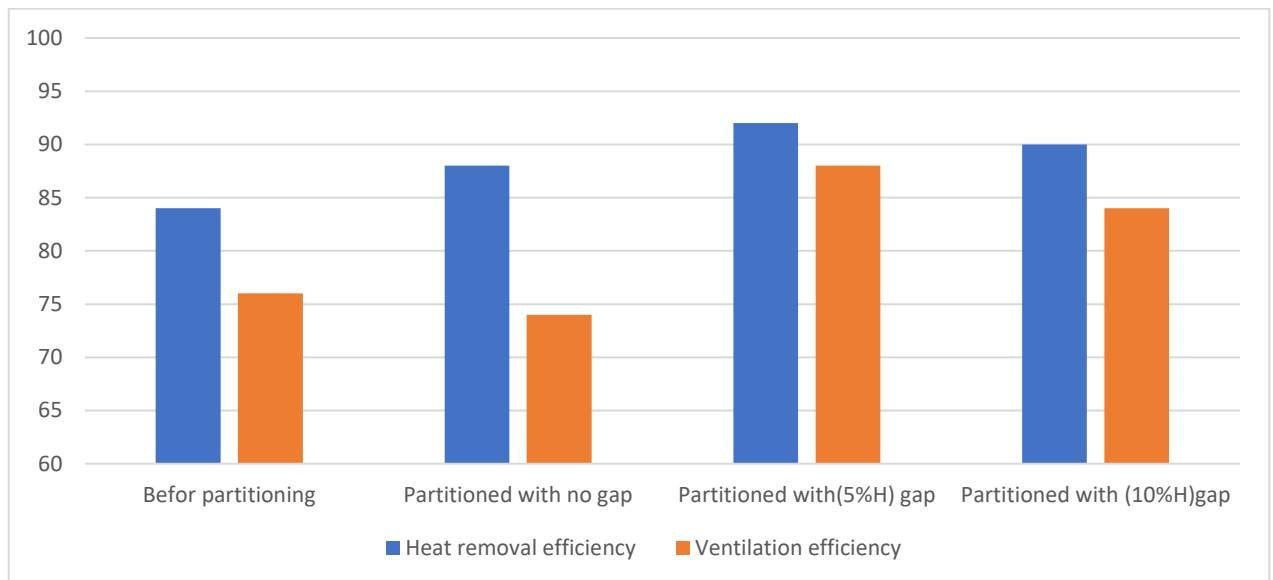


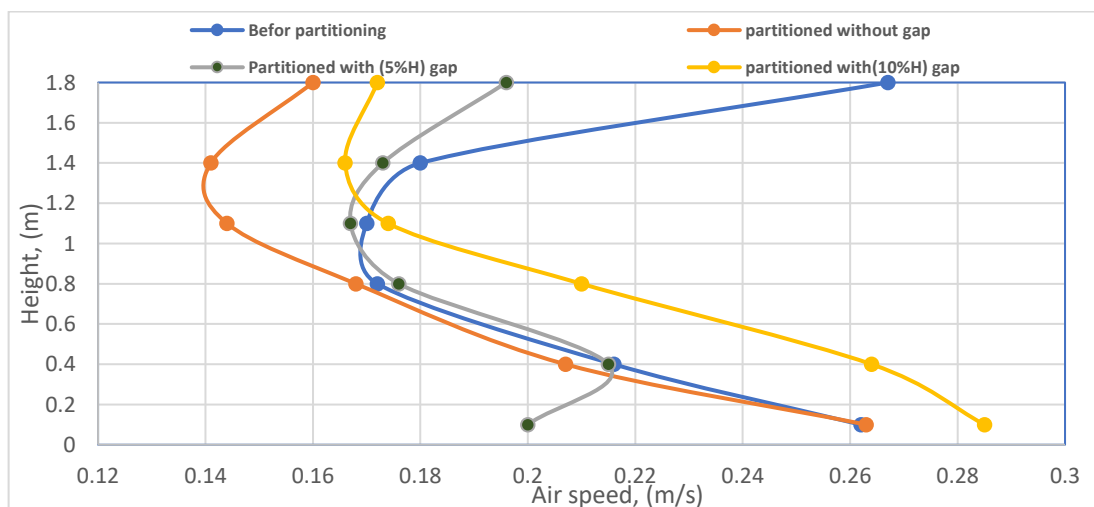
**Fig. (5-34)** Heat removal, and ventilation efficiencies for case(III).

**5.5.1 Local thermal discomfort(Draft):**

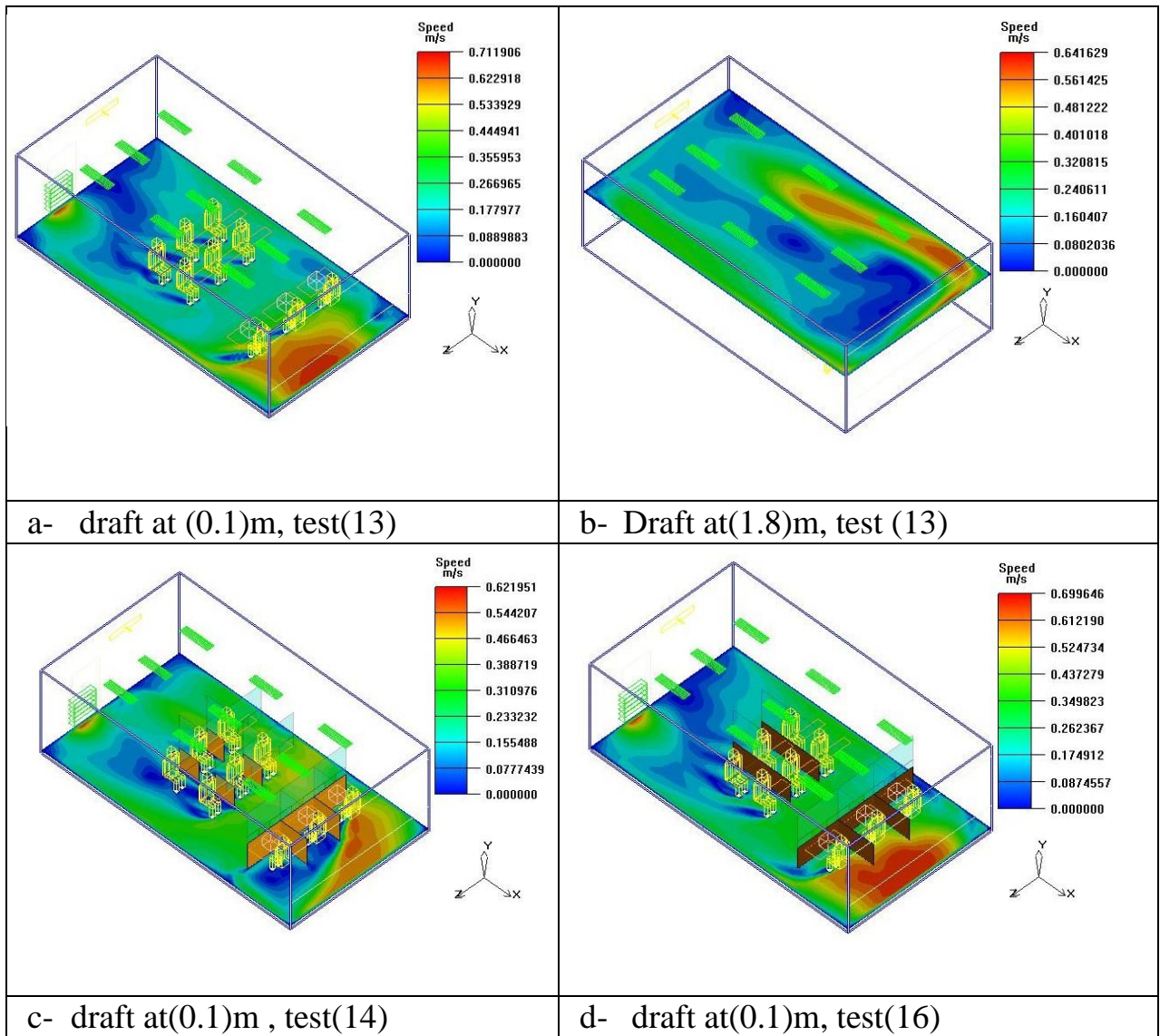
After calculating the the air speed inside the occupants zone of the office room, for six important levels represnting by ankle(0.1),legges(0.4), chest(0.8), breathing (1.1),sitting head level(1.4). and standing dead level(1.8) meters. Findings found that the office room befor partitioning, test (13) had two undesirable draft values, exactly in (0.1), and (1.8) meters as (0.262), (0.267)m/s respectively, as illustrated on the blue coloured curve in the Fig. (5-35), as well as shown in the countous in the subplots(a,b) of the

Fig. (5-36). Such undesirable drafts, has reduced to (0.16)m/s at (1.8) level, but still remain undesired at (0.1) level in test (18) when the partition has adopted without a gap, represented by the orange curve in the Fig. (5-35), and shown the contour (c) in the Fig. (5-36). However, while adopting gaps to the partitions, such locally undesirable draught has removed, reached to (0.24)m/s in case of (1.8)level, and (0.16)m/s in case of (0.1)level, such occurrence has denoted by the grey colour curve; Further increasing in the gap's height led the air speed return to undesirable value, in the yellow curve the air speed reached to (0.285)m/s at (1.8)level, the rest of levels were starting to increase again, subplot (d) showing the draft air on the(0.1)level at test (16). After mean air velocity values for all levels inside the room has found numerically by the (AIRPAK3.0.16) software, the percentage of dissatisfied has calculated for each case by the equ.(3-10), all the cases were less the (20%) according to the subplot (c), chart(5-37).

Partitioned aroom had a significant effect on recucing the percentage of dissatisfied close to (10%), in the tests of (15), and(16) the (PD) had reached its minimum value to (12.98)%,(13.3)%. The closer this ratio is to ten, the more it gurantees that the office room is air-conditioned, and ventilated for those sitting within it.



**Fig. (5-35) Local drought discomfort curves**



**Fig. (5-36)** Locally draft comtours.

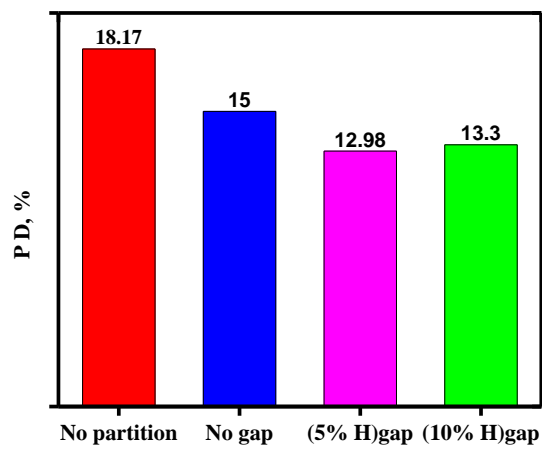


**Fig. (5-37)** Percentage dissatisfied,% chart for the case(III).

### 5.5.2 Thermal comfort parameters, PMV, and PPD:

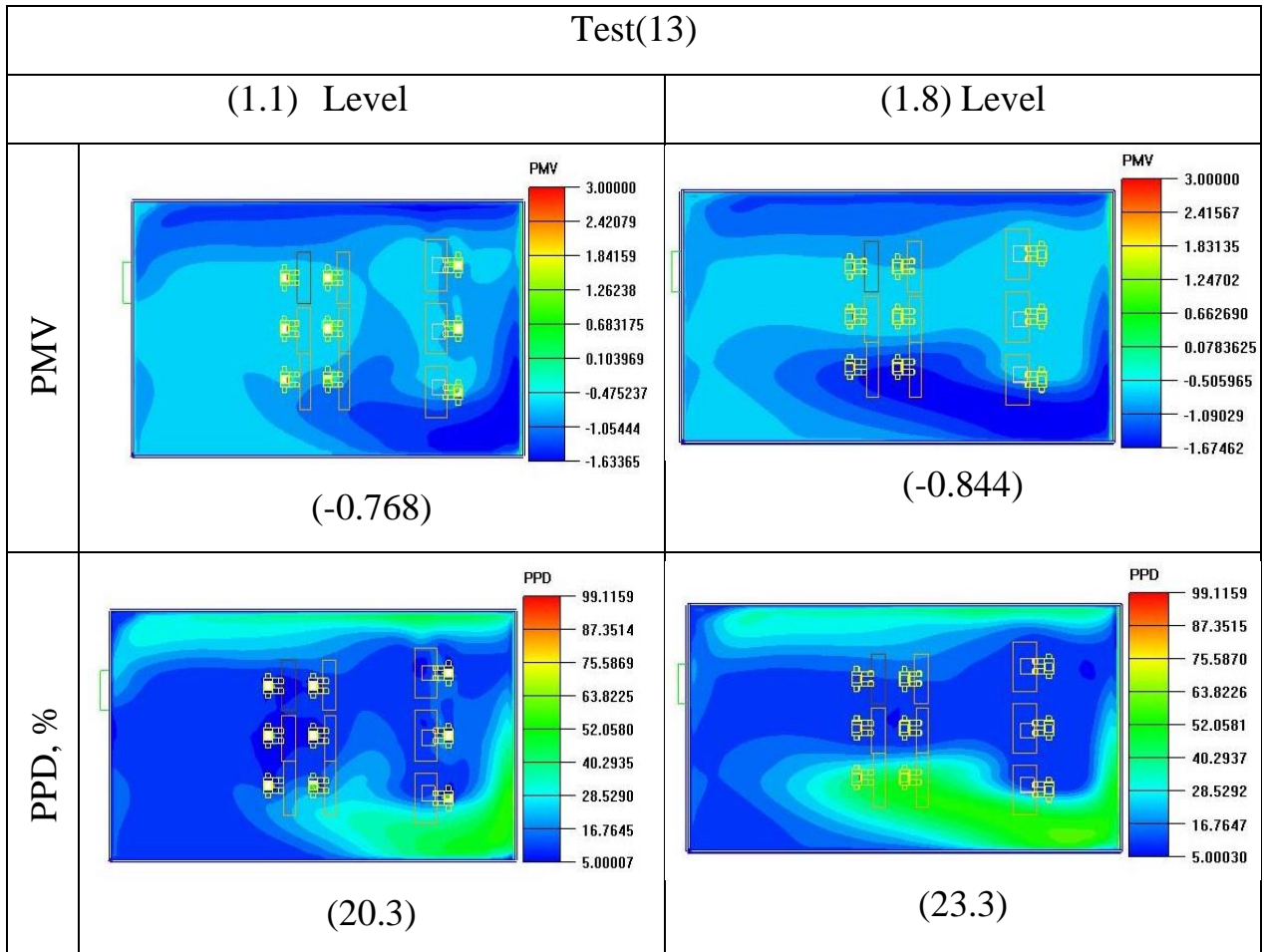
Table (5-6), listed thermal comfort parameters, that were found numerically, after the thermal insulation of clothes, and metabolic rate were determined. The mean value overall the office room before and after partitioning has listed. In the test (13), a (-0.8) is far away from the acceptable range to (ASHRAE-55) in which recommended ( $\pm 0.5$ ) as a comfortable range. As a result to the value of (PPD) which related to the PMV value in calculations, (23.74) was higher than (20%) as a maximum allowable range. After partitions have been adopted, it was noticed a clear change in (PMV, PPD, and also the ADPI) predictions. (PMV) has slightly lowered to (-0.73) which does not apply to (ASHRAE-55) nor with the (ISO -7730) which expanded the acceptable range to ( $\pm 0.7$ ), in case of modern buildings. So as the value of (PPD) remains higher than (20%), but it is worth noting about adding gaps impacts to the parameters values a very noticeable descending fall down for each parameter as listed in the table below, in the test (15) minor value for (PPD), and a closer value to the neutral had been obtained, as well as the value of (ADPI), where most of the ventilation systems specialize in offices recommended in design to achieve (ADPI) of (80%) or greater, according to (ASHRAE-2001) fundamentals.

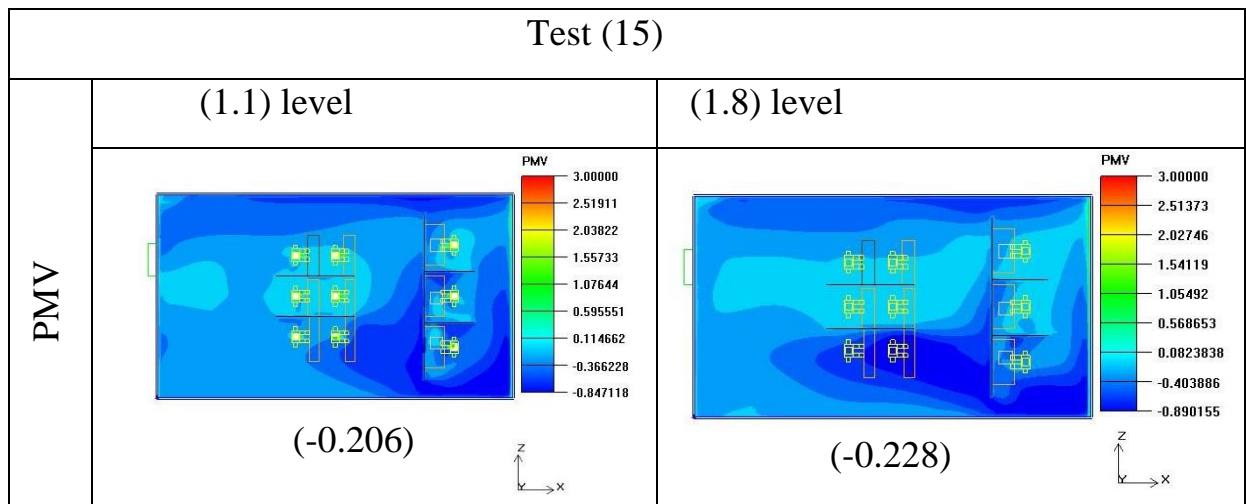
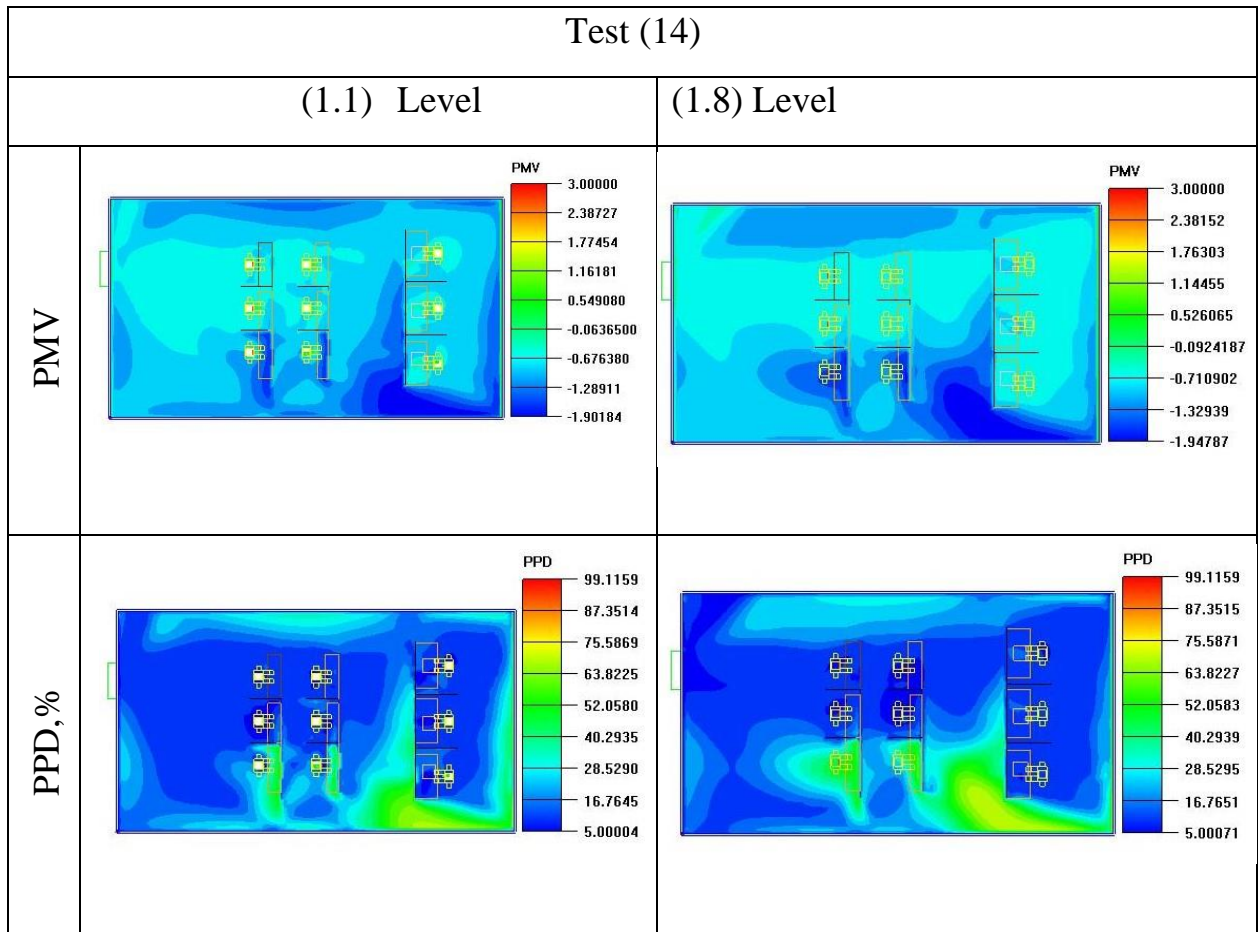
Returning the parameters to undesirable values in case of (16), such case concerning with females, ensures that women employees are more affected than men by cold offices, in the same condition that applies to the past office. The contours in Fig. (5-38), show the thermal comfort regions corresponding to (1.1), (1.8) most important levels of breathing zones for each particularly tests from (13 to 16), each level mentioned its values of (PMV, and PPD), the color wheel of the (PPD) counter has been reduced to (20%) as the highest percentage, which is the maximum acceptable limit, to know more clearly which part of the office room facing high percentage of

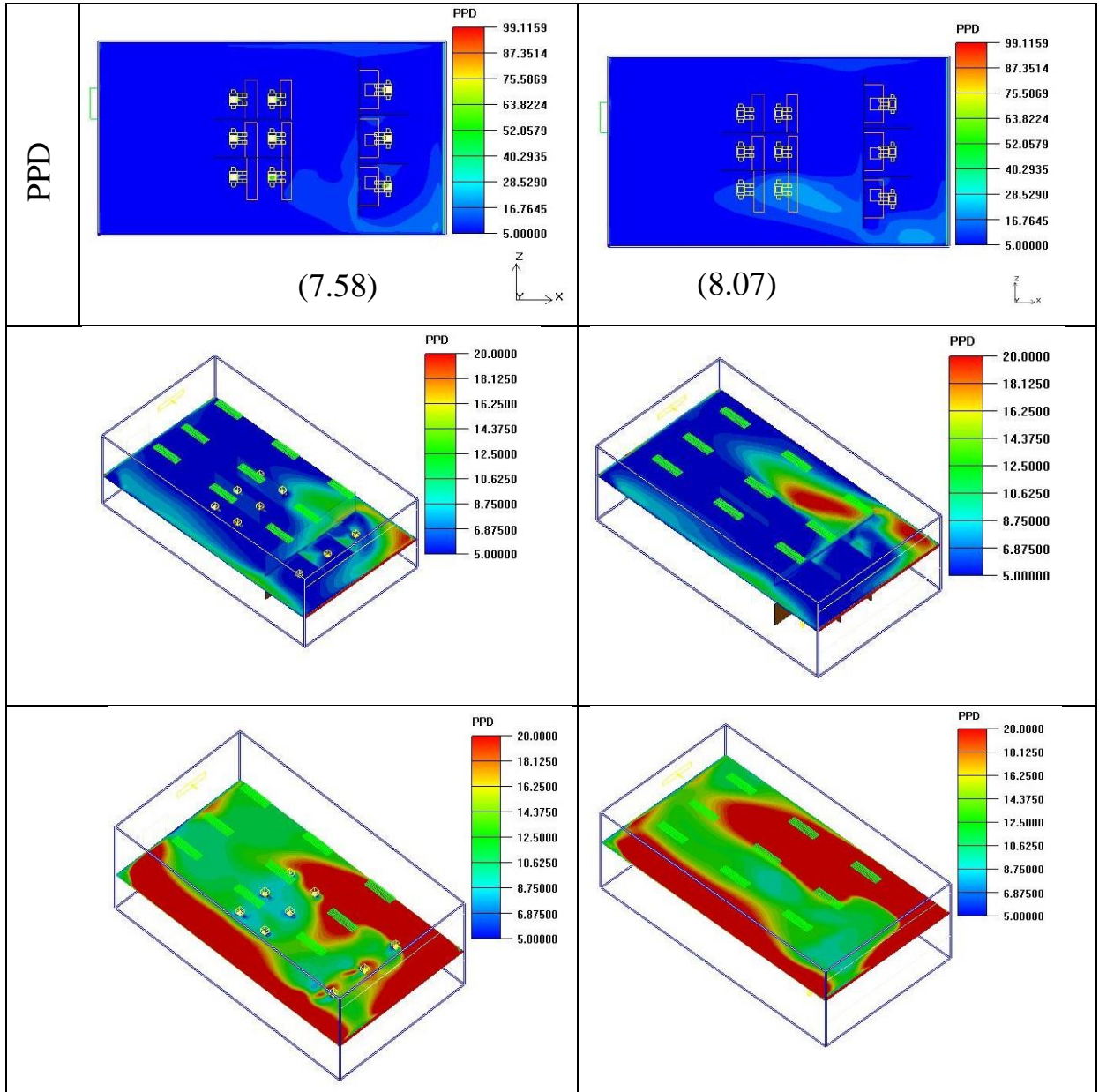
dissatisfied, in case of partition adptions, as shown in countors related to tests (14,15, and 16) , by putting the planes of (1.1), and (1.8) level in isometric view in order to make more sense. A diagram in Fig. (5-39)was drawn summerizing the relationship between partition adoption besides gaps to the value of (PPD).

**Table(5-7)** thermal comfort parameters for case(III).

Parameters	Test(13)	Test(14)	Test(15)	Test(16)
<b>PMV</b>	-0.8	-0.73	-0.2	-0.48
<b>PPD,%</b>	23.74	23.71	10.67	16.53
<b>ADPI,%</b>	72	73	79	76







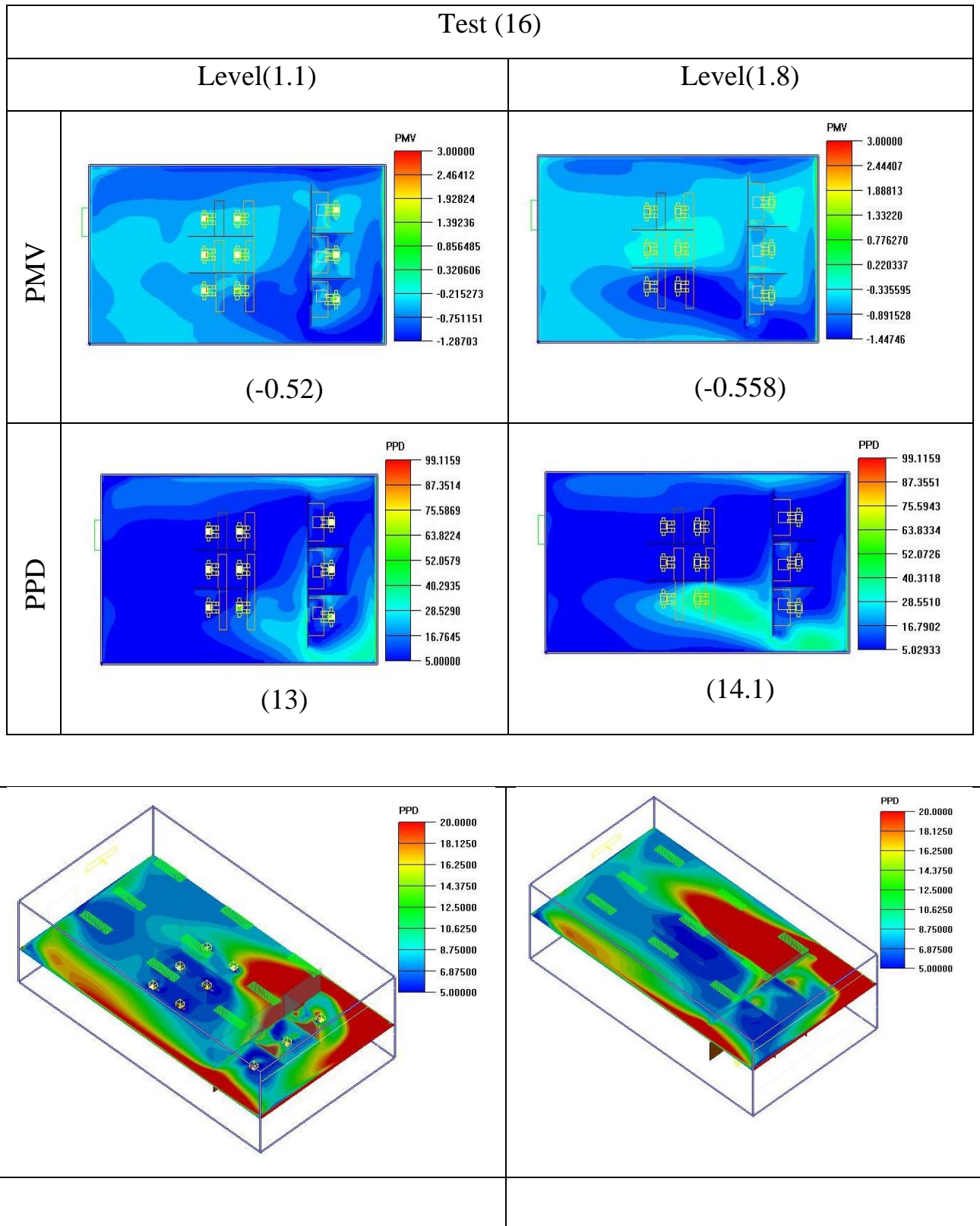


**Fig. (5-38)** thermal comfoert parameters contours.

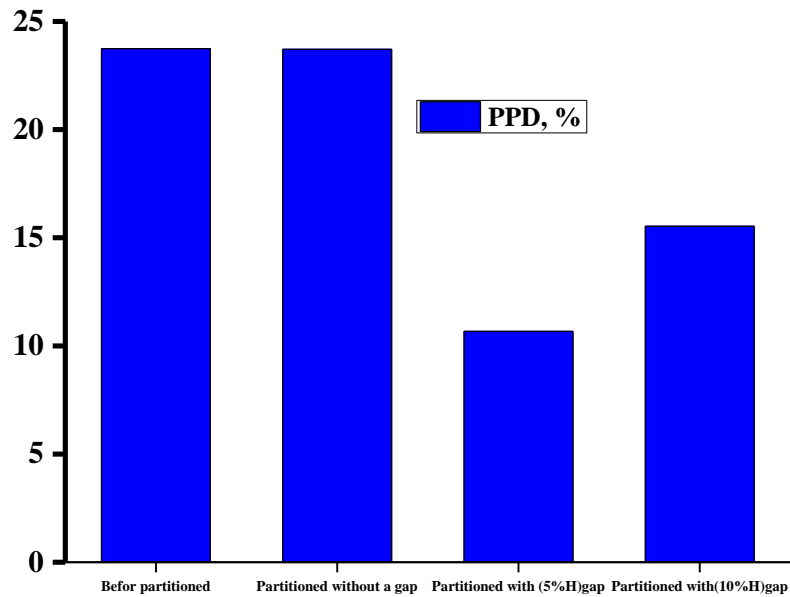


**Fig. (5-39)** PPD variation for each case in the non-thermally insulated room.

### 5.5.3 Ventilation parameter, and air diffusion index:

There is a basic, and important goal in calculating the previous parameters of thermal comfort, that is (PPD), and (VD) which is calculated based on the equ.(3-15), that is the (ADI), and (VP), as listed in the table (5-7) for each case before and after partitioning, according to what was previously mentioned the importance of the results of both factors; it was found that (VP) values are inversely proportional to the (ADI), the more (ADI) close to (10) the less the (VP) to unity.

**Table (5-8)** Air distribution index, and ventilation performance findings.

Parameters	Test(13)	Test(14)	Test(15)	Test(16)
<b>VP</b>	0.711	0.76	0.39	0.58
<b>ADI</b>	3.36	3.30	5.44	4.17
<b>N<sub>t</sub></b>	3.96	3.77	8.62	5.44
<b>N<sub>c</sub></b>	2.816	2.89	3.44	3.208

**Chapter six**  
**CONCLUSIONS AND**  
**SUGGESTIONS FOR FUTURE**  
**WORKS**

## Chapter six

### CONCLUSIONS AND SUGGESTIONS FOR FUTURE WORKS

#### 6.1 Conclusions

In view of the recent conditions related to the conditions of social distancing, especially in the Corona crisis, the current study focused on the impact of adding partition into office units on thermal comfort, and indoor air quality by mixing ventilation adoption under Iraqi climate. Through the most important conclusions are included in the points below:

1- An efficient ventilation indicator needs to be sufficient to account for the effectiveness of ventilation as well as the distribution of temperature inside the ventilated room.

2- Gap adoption beside a partition has a significant effect on enhancing the indoor air quality, and thermal comfort, since the ventilation efficiency increased from (0.84) to (0.93) in case of (0.5 of the room's length) with(0.7 of the room's height) for the insulated office room, and in case of non- insulated office room heat removal efficiency has effected significantly by gap adoption with the partition, since it increased from (0.80) to(0.85).

3- Increasing the gap height raises the (ADPI) value until it peaks at (5%) of the room height, at which point it decreases to (10%) of the room height.

4- The mixing ventilation system has the advantage that it provides the occupants with an overall draught sense, due to the slightly gradient of temperature along the occupants' zone.

5- Placing a gap below a partition, had a clear role in reducing draft in the region of standing head level, and legs level.

6-The findings related to (PMV) had not reached the positive side of the acceptable range (+0.5) after the neutral according to the input data corresponding to the current design conditions.

7- Partition adoption has a significant effect on (PPD) value, it helped to reduce the (PPD) value from (7.01%) to (5.26%) in case of partition gap's height of (5%) of the room's height.

8- Although there are visible effects of the partition on the air movement, the influence of the partition on the airflow in the room lacks a distinct trend. For instance, the outcomes with (50 percent) demonstrate that increasing the gap height enhances the air distribution index.

9- Ventilation parameter (VP) results were inversely proportional to (ADI) results, where the higher value of a particular case, the lower the (ADI), and vice versa.

## **6.2 Suggestions for Future Works:**

1- Studying age of air for a non-thermally insulated partitioned office unit, numerically and experimentally.

2- Using personal ventilation system in addition to mixing ventilation in the same field of the current study and investigate the most functional scenarios.

3- Studying the effect of office partitioning on the age of air for large halls providing more than one air supply, ceiling supply for example.

4- Studying the advantage of placing plants inside an office unit to enhance the mixing ventilation system on indoor air quality.

# REFERENCES

---

## References

- [1] Jia, L. R., Han, J., Chen, X., Li, Q. Y., Lee, C. C., and Fung, Y. H., 2021. Interaction between Thermal Comfort, Indoor Air Quality and Ventilation Energy Consumption of Educational Buildings: A Comprehensive Review. *Buildings*, vol. 11, no. 12, 591, 2021.
- [2] Sun, D., and Jia, C. “Study on joint management of indoor natural ventilation environment by coupling ceiling fan with air conditioner”. *Journal of Asian Architecture and Building Engineering*, pp. 1–13, (2021).
- [3] Abbas Mahdi, A., and Hassan, Z. Experimental and Numerical Study of Air Flow Diffusion and Contaminants Circulation in Room Ventilation Related with Iraqi Climate. *International Journal of Mechanical Engineering and Applications*, vol. 4, no. 2, 24, (2016). <https://doi.org/10.11648/j.ijmea.20160402.11>
- [4] Tolga, U. “Effect of Different Ventilation Types on Office Buildings”. A SED Architectural Association School of Architecture, (2015).
- [5] Saraga, D. E. Special issue on indoor air quality. *Applied Sciences*, vol. 10, no. 4, 1501, (2020).
- [6] World Health Organization (WHO). Household Air Pollution. Available online: <https://www.who.int/data/gho/data/themes/topics/topic-details/GHO/household-air-pollution> (accessed on 6 September 2021).
- [7] Gao, S., Wang, Y. A., Zhang, S. M., Zhao, M., Meng, X. Z., Zhang, L. Y., and Jin, L. W. Numerical investigation on the relationship between human thermal comfort and thermal balance under radiant cooling system. *Energy Procedia*, vol.105, pp. 2879-2884, (2017).
- [8] Hopfe, C., Mcleod, R., 2015 *The passive house designer’s manual*. Routledge.
- [9] Jia, L. R., Han, J., Chen, X., Li, Q.-Y., Lee, C. C., and Fung, Y. H. “Interaction between thermal comfort, indoor air quality and ventilation energy consumption of educational buildings”, A comprehensive review. *Buildings*, vol. 11, no.12, 591, (2021). <https://doi.org/10.3390/buildings11120591>
- [10] Awbi, H. B. 2008. *Ventilation of buildings*. Taylor and Francis. Second edition. (2008)
- [11] Fanger, P. O. Moderate thermal environments Determination of the PMV and PPD indices and specification of the conditions for thermal comfort. ISO 7730, (1984).

- [12] Schiller, G., Arens, E. A., Bauman, F., Benton, C., Fountain, M., and Doherty, T. 1988. "A field study of thermal environments and comfort in office buildings". Escholarship.org. Retrieved from <https://escholarship.org/uc/item/4km240x7>
- [13] Borowski, M., Zwolińska, K., and Czerwiński, M. An Experimental Study of Thermal Comfort and Indoor Air Quality—A Case Study of a Hotel Building. *Energies*, vol. 15, no. 6, (2022) <https://doi.org/10.3390/en15062026>
- [14] ISO Standard 7730, Ergonomics of the Thermal Environment—Analytical Determination and Interpretation of Thermal Comfort Using Calculation of the PMV and PPD Indices and Local Thermal Comfort. International Organization for Standardization: Geneva, Switzerland, (2005).
- [15] ASHRAE Standard 55. Thermal environmental conditions for human occupancy. Atlanta, (2010).
- [16] Aryal, P., and Leephakpreeda, T. "Effects of Partition on Thermal Comfort, Indoor Air Quality, Energy Consumption, and Perception in Air-Conditioned Buildings". *Journal of Solar Energy Engineering*, vol 138, no. 5, (2016). <https://doi.org/10.1115/1.4034072>
- [17] Mani, V., Abhilasha, G., and Lavanya, S. "IoT based smart energy management system". *International Journal of Applied Engineering Research*, vol. 12, no.16, pp: 5455-5462, 2017.
- [18] Lee, H., and Awbi, H. B. Effect of internal partitioning on indoor air quality of rooms with mixing ventilation - Basic study. *Building and Environment*, vol. 39, no.2, pp:127–141, (2004).
- [19] Roasaei, Amin, and Omid Rahaei. Improvement of Indoor Air Flow Quality under the Influence of Internal Partition Walls in Air-Conditioned Office Spaces Using CFD Method. *Armanshahr Architecture and Urban Development*13, no.30, (May21,2020), pp: 69-81, 2020.
- [20] Yi, Y., Xu, W., Gupta, J.K., Guity, A., Marmion, P., Manning, A., Gulick, B., Zhang, X., and Chen, Q. "Experimental study on displacement and mixing ventilation systems for a patient ward," *HVAC&R Research*, vol. 15, no.6, pp. 1175-1191, (2009).
- [21] Karava, P., Athienitis, A. K., Stathopoulos, T., & Mouriki, E. "Experimental study of the thermal performance of a large institutional building with mixed-mode cooling and hybrid ventilation". *Building and Environment*, 57, 313–326, (2012). <https://doi.org/10.1016/j.buildenv.2012.06.003>
- [22] Tomasi, R., Krajčák, M., Simone, A., & Olesen, B. W. "Experimental evaluation of air distribution in mechanically

- ventilated residential rooms: Thermal comfort and ventilation effectiveness”. *Energy and Buildings*, vol. 60, pp. 28-37, (2013).
- [23] Yin, H., Li, A., Liu, Z., Sun, Y., & Chen, T. “Experimental study on airflow characteristics of a square column attached ventilation mode”. *Building and Environment*, vol.109, pp. 112-120, (2016).
- [24] Borowski, Marek, Klaudia Zwolińska, and Marcin Czerwiński. “An Experimental Study of Thermal Comfort and Indoor Air Quality—a Case Study of a Hotel Building.” *Energies* 15, no. 6 March 10, 2022
- [25] Cheong, K.W., Djunaedy, E.E., Chua, Y.L., Tham, K.W., Sekhar, S.C., Wong, N.H., & Ullah, M.B. Thermal comfort study of an air-conditioned lecture theatre in the tropics. *Building and Environment*, vol. 38, pp. 63-73, (2003).
- [26] Cao, G. Y., Jorma Heikkinen, and Helena Järnström. "Protection of office workers from exposure to respiratory diseases by a novel ventilation system." *Proceedings of indoor air*, 2013.
- [27] AbouZeid, Ahmed, and Essam E. Khalil. “Effect of Internal Partitions on Thermal Comfort and IAQ Level Provided by Underfloor Air Distribution System in a Typical Office Space.” 14th International Energy Conversion Engineering Conference, July 22, 2016.
- [28] Aryal, P., & Leephakpreeda, T. CFD Analysis on Thermal Comfort and Indoor Air Quality Affected by Partitions in Air-Conditioned Building. *Applie Mechanics and Materials*, vol. 836, pp. 121–126, (2016)
- [29] Ahn, Hyeunguk, Donghyun Rim, and L. James Lo. "Ventilation and energy performance of partitioned indoor spaces under mixing and displacement ventilation." *Building Simulation*. vol. 11. no. 3. Springer Berlin Heidelberg, (2018).
- [30] Awbi, H. B. (2017). Ventilation for Good Indoor Air Quality and Energy Efficiency. *Energy Procedia*, vol. 112, pp. 277–286
- [31] Al-Assaad, Douaa, Nesreen Ghaddar, and Kamel Ghali., "Performance of Mixing Ventilation System Coupled With Dynamic Personalized Ventilator for Thermal Comfort." *ASME 2017 Heat Transfer Summer Conference*. American Society of Mechanical Engineers Digital Collection, (2017).
- [32] Liu, X., Wu, X., Chen, L., & Zhou, R. Effects of internal partitions on flow field and air contaminant distribution under different ventilation modes. *International Journal of Environmental Research and Public Health*, vol. 15, no.11, (2018) .
- [33] Villafruela, J. M., Olmedo, I., Berlanga, F. A., & Ruiz de Adana, M. Assessment of displacement ventilation systems in airborne

- infection risk in hospital rooms. PLOS ONE, vol.14, no.1, 0211390, (2019).
- [34] Roasaei, Amin, and Omid Rahaei. "Improvement of Indoor Air Flow Quality under the Influence of Internal Partition Walls in Air-Conditioned Office Spaces Using CFD Method." *Armanshahr Architecture and Urban Development*, vol. 13, no.30 (May21,2020), pp. 69-81.
- [35] Prajapati, S., Mehta, N., Chharia, A., & Upadhyay, Y. Computational fluid dynamics-based disease transmission modeling of SARS-CoV-2 Intensive Care Unit. *Materials Today: Proceedings*, (2021).
- [36] Lee, H., and Awbi, H. B. Effect of internal partitioning on indoor air quality of rooms with mixing ventilation—basic study. *Building and Environment*, 39(2), 127–141, (2004).
- [37] Abbas Mahdi, Alaa. "Experimental and Numerical Study of Air Flow Diffusion and Contaminants Circulation in Room Ventilation Related with Iraqi Climate." *International Journal of Mechanical Engineering and Applications*, vol. 4, no. 2, pp. 24, 2016.
- [38] Hameed, M., experimental and numerical investigation on air flow and temperature distribution under different geometries of displacement ventilation devices in an office room, M.Sc. Thesis, University of Babylon, (2017).
- [39] Hassan, A. A. M., Mahdi, A. A., Khadim. M. W., "A computational and Experimental Investigation of Air Flow and Contaminant Concentration in a Laboratory with Mixing Ventilation System" M.Sc. Thesis, University of Karbala, Iraq, (2018).
- [40] Liu, M., Liu, J., Cao, Q., Li, X., & Liu, S. Corrigendum to "Evaluation of different air distribution systems in a commercial airliner cabin in terms of comfort and COVID-19 infection risk" *Build. Environ.*, Volume 208, January 2022, 108590. *Building and Environment*, 214, 108939, (2022).
- [41] Contrada, F., Causone, F., Allab, Y., & Kindinis, A. A new method for air exchange efficiency assessment including natural and mixed mode ventilation. *Energy and Buildings*, vol. 254, 111553, (2022).
- [42] Chi, F., Pan, J., Liu, Y., & Guo, Y. Improvement of thermal comfort by hydraulic-driven ventilation device and space partition arrangement towards building energy saving. *Applied Energy*, vol. 299, 117292, (2021).
- [43] Airpak, 3.0.16. User's Guide. 2007<sup>th</sup> edition.
- [44] Chen, Q. COMPARISON of DIFFERENTk- $\epsilon$  MODELS for INDOOR AIR FLOW COMPUTATIONS. *Numerical Heat*

- Transfer, Part B: Fundamentals 28, no.3(October 1995): pp.353–69, (1995).
- [45] Yakhot, V., S. A. Orszag, S. Thangam, T. B. Gatski, and C. G. Speziale. Development of Turbulence Models for Shear Flows by a Double Expansion Technique. *Physics of Fluids A: Fluid Dynamics* 4, no. 7 (July 1992): pp. 1510–20, (1992).
- [46] Versteeg, H. K., and Malalasekera, W. An introduction to computational fluid dynamics: the finite volume method. Pearson education, (1996).
- [47] PDF Room. ASHRAE Handbook - Fundamentals (SI Edition), (2009).
- [48] P. Holman. Heat transfer. Tenth Edition, (2010).
- [49] Khaled, .A.J. Air condition and refrigeration engineering, first edition, p.216, (1984).
- [50] ASHRAE handbook. Heating, HVAC Systems and Equipment (SI). Panel heating and cooling, (2012).
- [51] Fanger, P. O. Introduction of the olf and decipol units to quantify air pollution perceived by humans indoors and outdoors. *Energy Build*, vol.12, pp. 1–6, (1988).
- [52] Fanger, P. O. A comfort equation for indoor air quality and ventilation, *Proc. Healthy Buildings '88*, B. Berglund and T. Lindvall (eds), Stockholm, vol. 1, pp. 39–51, (1988).
- [53] Fanger, P. O. and Pederson, C. J. K. Discomfort due to air velocities in spaces, *Proc. Meet. of Commission B1, B2 and E1 of the International Institute of Refrigeration*, Belgrade, pp. 271–8, (1977).
- [54] Fanger, P. O. Provide good air quality for people and improve their productivity, in *Air Distribution in Rooms (Proc. of ROOMVENT 2000)*, H. B. Awbi (ed.), vol. 1, pp. 1–5, (2000) .
- [55] Ahn, H., Rim, D., and Lo, L. J. Ventilation and energy performance of partitioned indoor spaces under mixing and displacement ventilation. *Building Simulation*, vol. 11, no. 3, pp. 561–574, (2017). <https://doi.org/10.1007/s12273-017-0410-z>.
- [56] Fanger, P. O. and Christensen, N. K. Perception of draught in ventilated spaces. *Ergonomics*, vol. 29, no. 2, pp. 215–35, (1986).
- [57] Liu, S., and Novoselac, A. 2015. Air Diffusion Performance Index (ADPI) of diffusers for heating mode. *Building and Environment*, 87, pp. 215–223. <https://doi.org/10.1016/j.buildenv.2015.01.021>.
- [58] Fanger, P.O. Thermal comfort - Analysis and applications in environmental engineering, McGraw-Hill Book Company, New York, USA, (1970).

- 
- [59] Fanger P.O.. Introduction of the Olf and Decipol units to quantify air pollution perceived by humans indoors and outdoors. *Energy and Buildings*, vol.12, pp.1-6, (1988).
- [60] [http://ashraemeteo.info/v2.0/index.php?lat=33.267&lng=44.233&place=%27%27&wmo=406500&ashrae\\_version=2017](http://ashraemeteo.info/v2.0/index.php?lat=33.267&lng=44.233&place=%27%27&wmo=406500&ashrae_version=2017)
- [61] ASHRAE, Inc. 2009 ASHRAE handbook: Fundamentals. American Society of Heating, Refrigeration and Air-Conditioning Engineers, (2009).
- [62] Rabani, M., Madessa, H. B., Nord, N., and Schild, P. Performance analysis of an active diffuser in mixing ventilation for cell office by using numerical approach. *E3S Web of Conferences*, 111, 04033, (2019). <https://doi.org/10.1051/e3sconf/201911104033>
- [63] Mahdi A. A. and Hassan, Z. Experimental and Numerical Study of Air Flow Diffusion and Contaminants Circulation in Room Ventilation Related with Iraqi Climate. *International Journal of Mechanical Engineering and Applications*, 4(2), 24. (2016). <https://doi.org/10.11648/j.ijmea.20160402.11>

# APPENDICES

## Appendix (A-1)

**Calculation of total cooling loads, and the flowrate (Q) for the insulated office room, (Case I):**

$$Q_T = 2Q_p + 2Q_{pc} + Q_{lamp} + Q_{inf}$$
$$= (2 \times 75) + (2 \times 60) + (100) + \left( \frac{7 \times (3 \times 2.5 \times 2.5)}{3600} \right)$$

$$= 150 + 120 + 100 + 0.036$$

$$= 370.03 \text{ WATT}$$

$$Q = \dot{m} C_p \Delta T$$

$$370.03 = \dot{m} \times (1.005) \times (24 - 17)$$

$$\dot{m} = \frac{370.03}{7.035} \rightarrow \dot{m} = 52.598 \left( \frac{g}{s} \right)$$

$$\dot{m} = 0.0525 \left( \frac{kg}{s} \right)$$

$$\dot{m} = \rho Q$$

$$Q = \left( \frac{0.0525}{1.2} \right) \rightarrow Q = 0.0437 \left( \frac{m^3}{s} \right) \text{ or } 43.75 \left( \frac{L}{s} \right).$$

$$ACH = \left( \frac{Q_s}{V_{room}} \times 3600 \right) = \frac{0.0437}{(3 \times 2.5 \times 2.5)} \rightarrow 8.39$$

## Appendix (A-2)

### Air System Design Load Summary for Non-Thermally Insulated Office Room.

Table (A-2) cooling loads data in July, at (3 PM), for (Case II) .

Computed by (HAP 4.9)

<b>Zone load</b>	<b>Sensible heat flux (W/m<sup>2</sup>)</b>	<b>Surface area(m<sup>2</sup>)</b>
Northern wall	26.03	11.5625
Window	200	5.5625
Southern wall	21.36	11.625
Door	73.29	2
Eastern wall	0	18.6
Western wall	0	18.6
Ceiling	0	22.5
Infiltration	4.25 WATT	

### Appendix (A-3)

#### Air System Design Load Summary for Non-Thermally Insulated Office Room.

Table (A-3) cooling loads data in July, at (3 PM), for (Case III).

Computed by (HAP 4.9)

<b>Zone load</b>	<b>Sensible heat flux (W/m<sup>2</sup>)</b>	<b>Surface area(m<sup>2</sup>)</b>
<b>Northern wall</b>	13.03	15
<b>Window</b>	170	5.5625
<b>Southern wall</b>	18.60	15
<b>Door</b>	73.29	2
<b>Eastern wall</b>	0	27
<b>Western wall</b>	0	27
<b>Ceiling</b>	0	45
<b>Infiltration</b>	7.3 WATT	

## Appendix (B)

### Heat removal, and ventilation efficiencies calculations

#### Heat removal efficiency calculation

Test (1)	
$\varepsilon_T = \frac{T_{out} - T_{in}}{T_{mean} - T_{in}} = \frac{21.332 - 17}{22.9 - 17} \longrightarrow$	0.73
Test (5)	
$\varepsilon_T = \frac{T_{out} - T_{in}}{T_{mean} - T_{in}} = \frac{22.626 - 17}{22.3 - 17} \longrightarrow$	0.93
Test (7)	
$\varepsilon_T = \frac{T_{out} - T_{in}}{T_{mean} - T_{in}} = \frac{22.68 - 17}{22.98 - 17} \longrightarrow$	0.97
Test (8)	
$\varepsilon_T = \frac{T_{out} - T_{in}}{T_{mean} - T_{in}} = \frac{22.3 - 17}{23.18 - 17} \longrightarrow$	0.85

#### Ventilation efficiency calculation

Test (1)	
$\varepsilon_c = \frac{C_{out} - C_{in}}{C_{mean} - C_{in}} = \frac{464.5 - 400}{486 - 400} \longrightarrow$	0.75
Test (5)	
$\varepsilon_c = \frac{C_{out} - C_{in}}{T_{mean} - T_{in}} = \frac{438.22 - 400}{445.5 - 400} \longrightarrow$	0.84
Test (7)	
$\varepsilon_c = \frac{C_{out} - C_{in}}{T_{mean} - T_{in}} = \frac{529.7 - 400}{539.5 - 400} \longrightarrow$	0.93
Test (8)	
$\varepsilon_c = \frac{C_{out} - C_{in}}{C_{mean} - C_{in}} = \frac{518 - 400}{538 - 400} \longrightarrow$	0.86

## **Laptop device and Windows specifications**

Device name sherin Filamerz  
Processor Intel(R) Core (TM) i7-8650U CPU @ 1.90GHz 2.11 GHz  
Installed RAM 16.00 GB  
Product ID 00330-62945-31537-AAOEM  
System type 64-bit operating system, x64-based processor  
Pen and touch Pen and touch support with 10 touch points  
Edition Windows 11 Pro  
Version 21H2  
Installed on 11/24/2021  
OS build 22000.978  
Serial number 019693775157  
Experience Windows Feature Experience Pack 1000.22000.978.0

**Local Thermal Discomfort Parameter (Percentage dissatisfied) Calculation**

$$PD = 13800 \left[ \left( \frac{\bar{V} - 0.04}{t_a - 13.7} + 0.0293 \right)^2 - 8.57 \times 10^{-4} \right]$$

<b>Test (1)</b>
<b>PD</b> = 13800 $\left[ \left( \frac{0.105 - 0.04}{22.7 - 13.7} + 0.0293 \right)^2 - 8.57 \times 10^{-4} \right] = 6.59\%$
<b>Test (5)</b>
<b>PD</b> = 13800 $\left[ \left( \frac{0.108 - 0.04}{22.55 - 13.7} + 0.0293 \right)^2 - 8.57 \times 10^{-4} \right] = 7.102\%$
<b>Test (7)</b>
<b>PD</b> = 13800 $\left[ \left( \frac{0.091 - 0.04}{23.18 - 13.7} + 0.0293 \right)^2 - 8.57 \times 10^{-4} \right] = 4.7\%$
<b>Test (8)</b>
<b>PD</b> = 13800 $\left[ \left( \frac{0.0899 - 0.04}{22.98 - 13.7} + 0.0293 \right)^2 - 8.57 \times 10^{-4} \right] = 5.6\%$

**Percentage dissatisfied parameter for each case study**

$$PD = 395 e^{-1.8(\dot{v}^{0.25})} \quad , \quad \dot{v} = \frac{L}{s} \times \frac{1}{olf}$$

<b>( Case I)</b>
$\dot{v} = 43.7 \times \frac{1}{2} = 3.47 \quad , \quad PD = 395 e^{(-1.8(21.85)^{0.25})} = 8.06$
<b>( Case II)</b>
$\dot{v} = (16.4 \times \frac{1}{3}) = 5.46 \quad , \quad PD = 395 e^{(-1.8(5.46)^{0.25})} = 25.21\%$
<b>(Case III)</b>
$\dot{v} = 48.17 \times \frac{1}{9} = 5.352 \quad , \quad PD = 395 e^{(-1.8(5.352)^{0.25})} = 25.56$

## Appendix (C)

### Calibration of Instruments



a- anemometer certificate



b- Data logger certificate

## الخلاصة

أصبحت المباني المزودة بأنظمة تهوية من الضروريات الأساسية للشركات التي تتطلع إلى توفير الراحة الحرارية وجودة الهواء من أجل تعزيز مستوى الإنتاجية لأداء الموظفين، خاصة بعد جائحة كورونا. المباني في القطاعين العام والخاص على حد سواء بعد الدول الاسكندنافية التي كانت الأولى في تصاميم التهوية، أصبح العمل في ظل ظروف التباعد الاجتماعي، عاد الباحثون حول العالم لإعادة النظر في دراستهم لمفهوم التهوية في زمن وباء كورونا لمعرفة تأثيره على الراحة الحرارية وجودة الهواء.

لذلك سيتم في هذا البحث دراسة أثر وضع الفواصل بين موظفي مكتب معين من أجل التنبؤ بجودة الهواء و الراحة الحرارية من خلال اعتماد نظام تهوية المختلط الذي يحتوي على مصدر هواء جانبي للجدار، و عادم للهواء في نفس جانب الجدار، في ظل المناخ العراقي، حيث منطقتي الفرات الاوسط، والمنطقة الجنوبية مناطق حارة وجافة في فصل الصيف.

تمت دراسة هذا البحث عدديا باستخدام برنامج محاكاة دقيق وسريع متخصص في أنظمة التهوية. تم اختيار غرفة مكتب معزولة حراريا كحالة دراسية عدديا وتجريبيا وإجراء مقارنة بين كلتا النتيجتين. إلى جانب ذلك، هناك غرفتان مكتبيتان غير معزولتان حراريا كحالات واقعية، لكل حالة واقعية موقع وأبعاد وجنس مختلف للموظفين، وقد تم تنفيذ هذا الأخير وفقا لأنواع الملابس التي تم استخدامها في عملية المحاكاة.

تم حساب كفاءة إزالة الحرارة، وكفاءة التهوية قبل وبعد وضع الفواصل في كل حالة، بالإضافة إلى مؤشر توزيع الهواء (ADI)، و(ADI)، علاوة على ذلك، الراحة الحرارية (PPD، PMV)، وعدم الراحة المحلية، وتأثير تعزيز وظيفة الفواصل من خلال الفجوة الموجودة أسفل الفاصل، وكيف غيرت الكفاءة، وكيف قللت عدم الراحة المحلية أيضا.

ووفقا للنتائج فإن نظام التهوية المختلطة يتميز بأنه يوفر للشاغلين حاسة التقليل من عدم الراحة المحلية، نظرا للتدرج الطفيف في درجة الحرارة على طول منطقة الشاغلين، بالإضافة إلى أن اعتماد الفجوات بجانب الفاصل له تأثير كبير على تعزيز جودة الهواء الداخلي، والراحة الحرارية، حيث زادت كفاءة التهوية من (0.84) إلى (0.93) في حالة (0.5 من طول الغرفة) مع (0.7 من ارتفاع الغرفة) لغرفة المكتب المعزولة، وفي حالة عدم عزل غرفة المكتب تكون كفاءة إزالة الحرارة قد تأثرت بشكل كبير باعتماد الفجوة مع القسم، حيث ارتفعت من (0.80) إلى (0.85). كما انخفضت قيم (PPD) إلى

هذه القيمة المقبولة من (23.74% إلى 10.67%) في حالة غرفة المكتب التي تشغلها الإناث ، ومن (26.4% إلى 13.3%) في حالة غرفة المكتب التي يشغلها الذكور.

وخلصت الدراسة إلى وضع فجوة أسفل الفاصل، كان له دور واضح في تقليل عدم الراحة المحليه في منطقة الوقوف على مستوى الرأس، ومستوى الساقين. كما أن مزايا استخدام برنامج (AIRPAK3.0.16) إلى جانب نموذج الاضطراب (RNG K-ε) يرجع إلى النتائج الأقرب بين المقارنتين العددية والتجريبية، حيث أن الخطأ الأعلى الذي تم الوصول إليه كان (3.81%) في حالة ارتفاع فجوة القاطع (H %10) من ارتفاع الغرفة.



جمهورية العراق  
وزارة التعليم العالي و البحث العلمي  
جامعة بابل/ كلية الهندسة  
قسم الهندسة الميكانيكية

## التفسير العددي والعملي لمعيار توزيع الهواء في غرفه مقسمة ضمن ظروف العراق الجوية

رسالة مقدمة إلى كلية الهندسة بجامعة بابل كجزء من متطلبات نيل شهاده الماجستير  
في الهندسة / الهندسة الميكانيكية / القدرة

أعدت من قبل الباحثه :  
شرين صباح جاسم فلامرز

بإشراف :  
الأستاذ الدكتور علاء عباس مهدي

